MIXING IN GRANULAR SYSTEMS AND APPLIED COATING TECHNOLOGY

by

Brian Gerome Warshawsky

B.S.
Brown University, 1995

Submitted to the Department of Materials Science and Engineering in
Partial Fulfillment of the Requirements for the Degree of
Master of Science in Materials Science and Engineering

at the

MASSACHUSETTS INSTITUTE OF TECHNOLOGY

June 1998

Signature of Author: _____
Department of Materials Science and Engineering
May 8, 1998

Certified by: _____
Professor Michael J. Cima
Sumitomo Electric Industries Professor of Engineering
Thesis Supervisor

Accepted by: _____
Linn W. Hobbs
John F. Elliott Professor of Materials
Chairman, Departmental Committee on Graduate Students

Science

MIXING IN GRANULAR SYSTEMS AND APPLIED COATING TECHNOLOGY

By

Brian Gerome Warshawsky

Submitted to the Department of Materials Science and Engineering

on May 8, 1998 in partial fulfillment of the requirements for the

Degree of Master of Science in Materials Science and Engineering

ABSTRACT

The purpose of this thesis was to augment the research conducted by Dr. William Rowe, providing further understanding of the process parameters involved in bulk coatings utilizing sodium silicate slurries, and a basic understanding of the behavior of granular materials in rotary drum mixers. Rotary mixers are prime means for creating such coatings. Continuous mixers are preferred over batch models, in order to obtain high production volumes. The mixing time is difficult to predict in a continuous process, whereas in a batch system it is easily controlled. The particle flow behavior must be characterized, as the amount of time a given particle spends in the coating zone will affect its coating thickness and quality. Factors influencing residence time in the coating zone include granule particle size, amount of slurry added and its viscosity, and mixer flight arrangement. The effect of varying process conditions on residence time distribution will be examined, as well as coating transfer. The results of the experiments can be used to develop a more thorough understanding of granule behavior in continuous mixers, and will be of significance for agricultural seed coating, minerals processing, and pharmaceutical manufacture.

X-ray Fluorescence Spectroscopy and copper tracer granules were used to study the residence time distribution of granules in a rotary drum mixer. The mean residence time is inversely related to granule particle size. Mean residence time (MRT) decreases with increasing particle size. Thus, the time spent in the coating zone will be greater for granules of smaller particle size. Separate tracer measurements were used to study the effect of slurry yield stress on granule flow behavior. Two regimes were found. The MRT increases with increasing viscosity, exhibits a maximum, and then begins to decrease.

Visual analysis and copper tracer granules were used to study the effect of applied moisture on flow behavior. Increasing moisture had little effect until a threshold value, at which point, mean residence time increased significantly. The threshold is predicted to coincide with the emergence of capillary forces between particles.

Inductively Coupled Plasma Atomic Emission Spectroscopy and copper tracer granules were used to examine the bulk flow behavior of granules in an industrial scale coating process. The bulk flow behavior was found to be much more plug-like than that of the laboratory mixer. The

residence time distribution was narrower and the mean residence time was significantly shorter than that of the laboratory mixer.

The coating process under investigation was found to have inadequate dispersion of the pigment particles, and to produce non-uniform coatings. An optical and a scanning electron microscope and an electrokinetic sonic amplitude measurement device were used to study to slurry formulation and coating quality. The ESA experiments demonstrated that the surfactants currently in use have little to no effect on the dispersion of titanium dioxide or kaolin clay.

A study of the temperature distribution throughout the length of a laboratory mixer was conducted in order to test the accuracy of the heat and moisture model developed by Dr. Rowe. The predicted mixer temperature profile was found to not quite agree with that of the actual laboratory mixer.

A coating transfer study was used to examine the transfer of coating slurry between granules throughout the length of the mixer. The results corroborate Dr. Rowe's conclusion that the majority of slurry coating occurs very soon after slurry application.

Thesis Supervisor: Michael J. Cima
Title: Sumitomo Electric Industries Professor of Engineering

TABLE OF CONTENTS

LIST OF FIGURES

LIST OF TABLES

ACKNOWLEDGEMENTS

I would like to thank a fine group of people, without whom, this thesis would not have been possible. First, I would like to thank my advisor, Professor Michael Cima, for his advice and direction on this research project. Thank you Dr. Cima, for also providing insight into materials processing over the past two years. Special thanks go to John Centorino, Lenny Rigione, and Barbara Layne for answering my endless stream of questions and requests without a sign of frustration. Thanks also to the graduate students of the CPRL for making the lab an amusing place to work.

I would like to thank the manufacturing company, which will go unnamed, for sponsoring this research. Dr. D. Reed in particular spent a great deal of time answering questions, shipping material, transporting rock granules, and working in the pilot plant, and for that I want to express my deepest appreciation. Thanks to everyone else at the company who provided assistance over the past year.

Finally, a mighty thanks to all of my friends and family who helped me procrastinate and otherwise kept me sane over the past two years. I couldn't have done it without you.

CHAPTER 1
INTRODUCTION TO GRANULAR MATERIALS AND SURFACE COATING FORMULATIONS

Granular materials are pervasive in both the built and natural environments. Vast amounts of granular materials are involved in the manufacture of cement and plastics, and in grain and ore processing. The dynamics of granular materials are demonstrated in nature by avalanche and earthquake behavior. Granular materials are particularly interesting because they exhibit unusual physical characteristics. A mass of particles can at times flow like a liquid, as in avalanches, while it can also sustain internal stresses like a solid.[1] The following section will outline some of the unique characteristics of granular materials. The second section will then describe surface coating formulations.

1.1 GRANULAR MATERIALS

1.1.1 PROPERTIES

Granular materials exhibit a number of unique properties that makes them distinct from standard liquids or solids. Granular materials exhibit heaping, thixotropy, arching effects, non-Newtonian shearing, segregation, and stick-slip motion.[2] The most familiar property of granular materials is their tendency to form piles, or "heap", with a "self selecting" angle of repose, θ_r. The angle of repose is the angle of the pile surface from horizontal. The angle of repose can be considered a material property, as a pile of uniform granules will have a specific θ_r. The angle of repose has been found to increase with decreasing particle size. The shape of the particles will also effect θ_r. Round particles, for example, have a lower angle of repose than pyramidal particles.[3]

Adding particulate material to the top of a pile will cause a temporary increase in the surface angle. At an angle, θ_m, avalanches occur which return the angle of the surface to θ_r. The angle of repose θ_r, must be exceeded by an additional amount δ, before avalanches will occur. This is due to the need for clearance of the upper sliding layer over the profile of the underlying layer.[4,5] The angle θ_m, where $\theta_m = \theta_r + \delta$, is termed the maximum angle of stability.[6] During an avalanche material only flows in the surface layer, with the bulk remaining stable. This is unlike standard liquid flow. For a review of research on granular materials, see references [7], [8], & [9]. The

characteristics outlined here have a significant effect on the behavior of flowing granular materials, and make the processing of granular materials non-trivial.

1.1.2 PROCESSING: MIXING

Rotary drums and cylinders are used for batch and continuous processing of granular materials. These devices are used for mixing, humidification, dehumidification, and convective heat transfer.[10] Rotary drums and cylinders may be smooth walled or have flights (baffles) to break up the material flow. The motion of particles in smooth walled rotary mixers has been found to take on six separate patterns, dependent upon rotational speed, cylinder diameter, percent fill, bed/wall friction, and specific particle characteristics.[11] The six patterns include slipping, slumping, rolling, cascading, cataracting, and centrifuging.[11,12] The flow patterns are illustrated in Figure 1.1. In general, the processing of granular materials occurs in the rolling or cascading flow regimes.

Mixing in the rolling and cascading regimes can be separated into two types, radial and axial, and occurs primarily in the active surface region. The active region consists of only the granules in motion, rolling down the slope made up of stationary granules. Radial mixing occurs in planes perpendicular to the axis of the mixer, and is caused by the percolation of particles into voids below the active layer. The velocity of the particles will significantly affect the amount of radial mixing. Higher particle velocities reduce the probability of a particle dropping into the non-active region. Thus radial mixing is a function of mixer rotational speed.[13] Axial mixing describes the movement of particles between radial mixing planes.[13] Axial mixing is diffusional in nature, and has been attributed to random collisions[10], velocity gradients[13], and angle of repose based segregation. Gravitational force also affects material flow if the axis of the mixer is not horizontal.

Material in the mixer must be well mixed and the components should be uniformly distributed, for effective bulk materials processing. Non-uniformity, such as material segregated by particle size, can reduce the effectiveness of the process, or result in product with varying materials properties. The mechanisms of segregation have been, and continue to be studied by a number of researchers, due to its significance in the processing of granular materials.

1.1.3 SEGREGATION

Segregation can occur during pouring, shaking, vibration, shear, freeze-thaw cycling and fluidization of granular materials.[14] Segregation has been attributed to differences in particle size, shape, density, and resilience, but particle size has been found to be most influential.[15] Two types of segregation have been found in rotary mixers. The first, termed radial segregation, occurs soon after rotation begins. Radial segregation involves the development of a buried core of smaller particles along the axis of rotation.[13,16,17] Radial segregation is illustrated in Figure 1.2. Segregation in this manner has been attributed to the percolation of smaller particles into the central bed of material, from which it never escapes.[13] The second type of segregation occurs in the axial direction and only following radial segregation.[17] The cause of axial segregation is not well understood. Researchers have attributed axial segregation to fluctuations in particle concentration and end effects.[18] An increase in small particle concentration due to radial segregation may increase the dynamic angle of repose in the region of heightened concentration. The material will then segregate further as large particles, which have lower characteristic angles of repose, separate out of the regions of high θ_r.[10,13] Axial segregation was found to be readily apparent in experiments on colored particles in closed-end mixers. Bands of concentrated particles separated by particle size were formed by axial segregation.[18] An illustration of axial segregation is shown in Figure 1.3. Additionally, segregation bands were found to travel down the length of the mixer until a stable configuration was achieved.[17] Segregation can only effectively be reduced by eliminating the stable central bed. One mechanism for breaking up the bed is to add flights to the walls of the mixer. Little work has been published regarding the various flight designs and their effectiveness due to their proprietary nature.

1.2 COATINGS FOR COLOR MODIFICATION

1.2.1 PROPERTIES/FORMULATION

The bulk coating process under examination involves the alteration of surface color of granular particles through the application of a colored coating. Coating opacity is necessary in order to conceal the color of the base material. Opacity is provided by sub-micron particles, which diffract and scatter light such that no transmission of the base material color can occur. Titanium dioxide particles perform this role in most paint formulations. The coating thickness

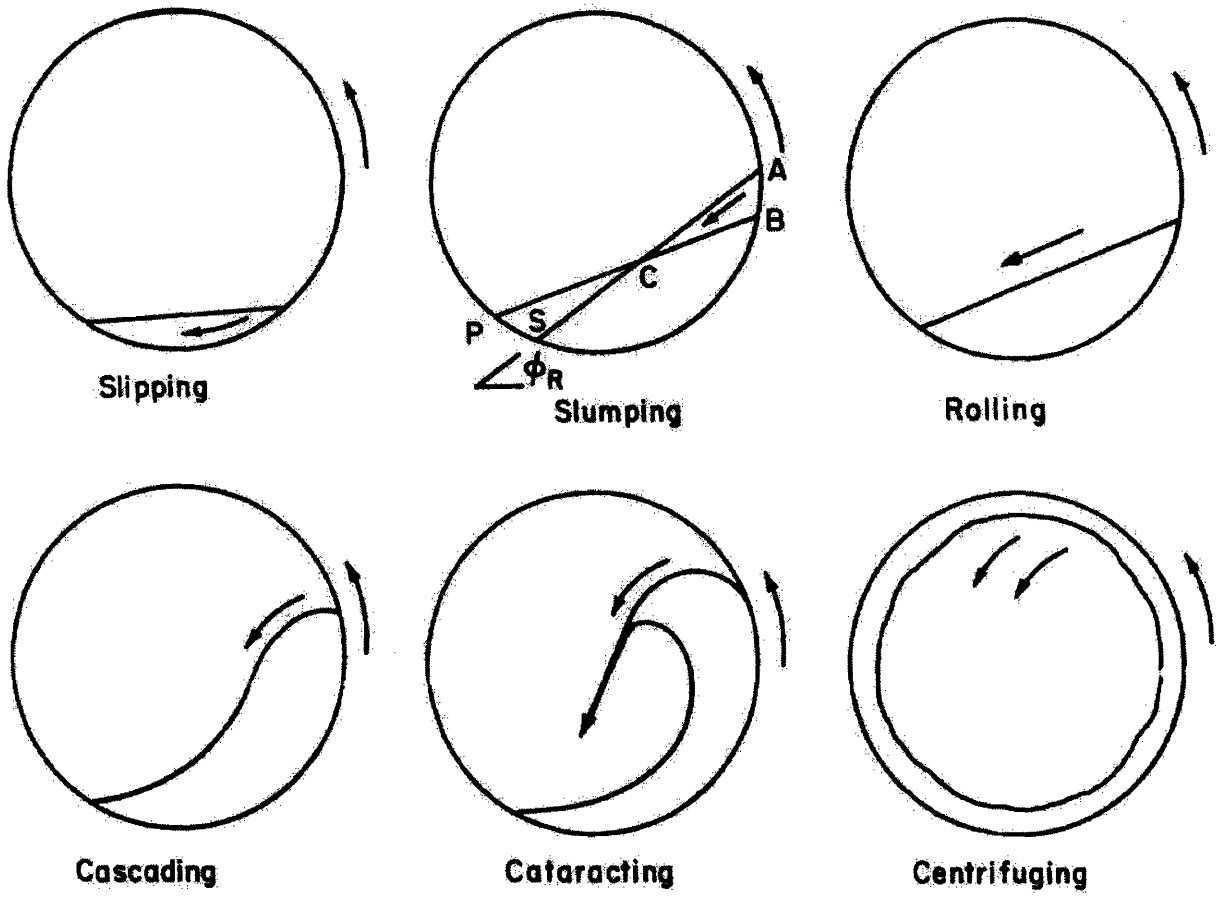

Figure 1.1 The Six Flow Configurations of Granular Materials in a Smooth Walled Rotary Cylinder

Taken from H. Henein et al. See reference [11].

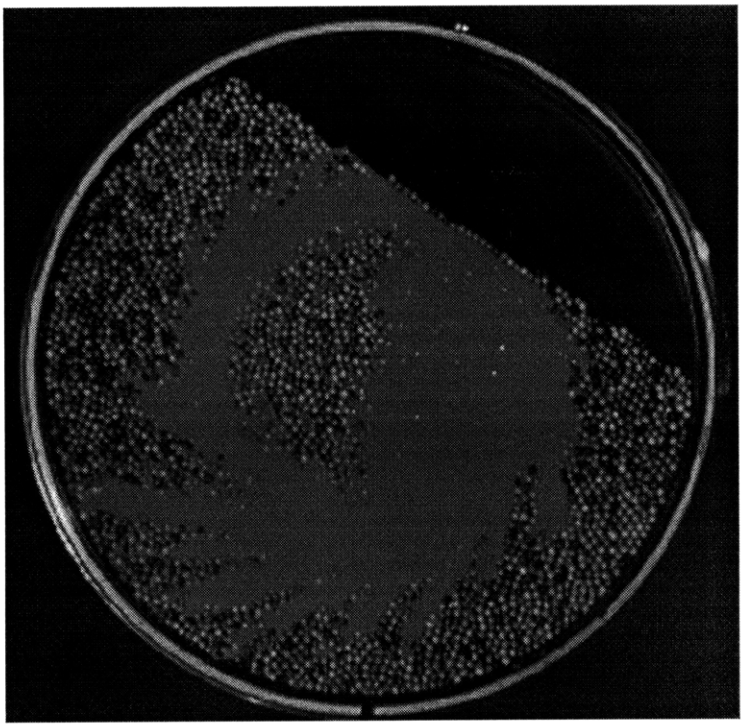

Figure 1.2 Radial Segregation in Rotary Drum Mixers

This is a 2-D drum mixer, initially filled with smaller particles on the right and larger on the left. The smaller particles tend to segregate in the center of the mixer. The size ratio is about 3:1. Taken from J.J McCarthy et al. [9]

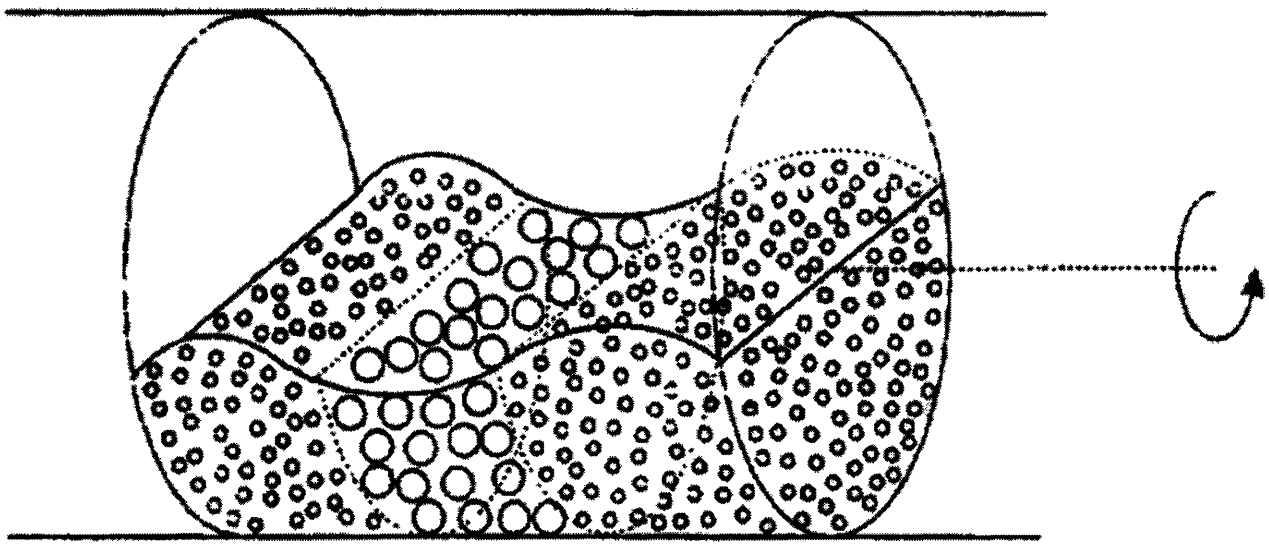

Figure 1.3 Axial Segregation in Rotary Drum Mixers

Taken from Nakagawa et al. [21]

and concentration of titanium dioxide particles in the coating must be maintained above a minimum threshold in order to maintain opacity.[20] A coating formulation is then made up of the following: 1) A liquid, which initially provides ease of spreading, yet will later evaporate to leave a solid coating. 2) Opacifiers, such as titanium dioxide. 3) Clay is used to create a matte finish, modify the slurry rheology, and provide a mechanism for taking up space between the pigment particles.[21] The pigment particles are best utilized when they are evenly spread through the slurry, with space between each. The clay extends the space between the pigment particles, thereby improving pigment utilization. Other ingredients may include additional color pigments, binders, surfactants (for modifying slurry rheology), dispersants, and defoamers. Titanium dioxide is a significant cost factor in the coating formulation. Optimization of the titanium dioxide utilization is thus important.

1.2.2 FLOCCULATION/MIXING

Initial mixing of a coating slurry is crucial to break up any agglomerated pigment or extender particles. A variety of mixers exist for the purpose of creating good dispersions, including ball and roll mills, and ultrasonic cavitators. Mixers use impact and shearing forces to break up agglomerates. Doroszkowski [21], provides a detailed description.[21]

Even the most effective mixing process, however, will not guarantee a proper dispersion of particles. Formulations containing sub-micron particles are termed colloidal solutions. The particles move about via Brownian motion due to their small size. Interactions will inevitably occur as the particle trajectories cross. These interactions can potentially lead to flocculation (aggregation).

The stability of the dispersion is determined by the "collision efficiency" of these particle interactions.[22] High collision efficiency is the case when most collisions result in agglomeration. Flocculation of particles is dependent upon the repulsion forces between the particles. Forces between particles are due to a combination of surface charge, Van der Waals, and hydration effects and are specific to each material.[22] The pH of the solution can also affect the repulsion forces.

The inter-particle repulsion forces must be strong enough to prevent collisions, in order to produce a stable solution. One mechanism for increasing the repulsion forces is to add dispersing agents. Dispersants adsorb onto the particle surfaces and maintain their separation

(steric-stabilization).[22] The effects of dispersing agents vary depending upon the particulate material. An appropriate dispersing agent or combination of agents must thus be identified for a given formulation. Flocculation will rapidly occur, and the solution will return to a non-uniform state, without repulsive forces between particles.

CHAPTER 2
RESIDENCE TIME IN ROTARY DRUM MIXERS

The processing of granular materials occurs in a number of industries such as concrete, activated carbon, plastics, and roofing granules. The unique flow and storage properties of granular materials, distinct from that of standard solids and liquids, increase the complexity of their processing and provide a number of avenues for research.

Past researchers have examined the flow and stability characteristics of granules in piles[23], hopper storage, and mixing processes in order to determine the mechanisms of avalanches, proper storage methods, and the probability of particle size segregation during movement and storage.[26] In general, adequate mixing is crucial for process uniformity. A number of studies have been conducted, using a variety of materials systems and measurement techniques, which clearly demonstrated that segregation by particle size occurs in rotating drum mixers and vibrating beds.[16,26] Segregation of particles results from a combination of causes, including particle size distribution, particle density disparities, and mixer characteristics. It is crucial that the mechanism of segregation and the effects of changing processing variables be characterized, in order to optimize the processing of granular materials. This chapter will study the effect of changing process variables on segregation and material flow in a rotary drum mixer used for industrial coatings.

The amount of time a particle spends in a given process is termed its *residence time*. Movement of granules relative to one another occurs inside the mixer due to random collisions between granules and with container walls. Granular material thus normally does not move in a linear fashion, termed *plug flow*. Granular material moving through a mixer will have a distribution of residence times centered around a mean value, due to the nonlinear flow patterns. This is defined as the *Residence Time Distribution* (RTD). The mean value is the *Mean Residence Time* (MRT). See Figure 2.1.

It is important to control the mean residence time and the breadth of the distribution in coating processes, in order to produce uniform coatings. Great disparity in residence times would indicate that some particles spend significantly more time in the coating region, and likely

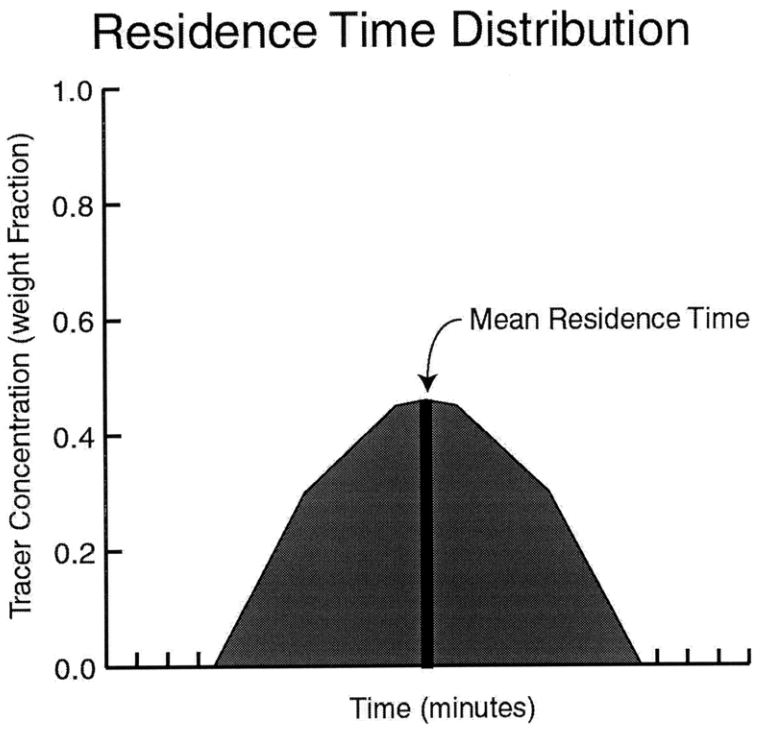

Figure 2.1 Example of a Residence Time Distribution

result in non-uniform coating thicknesses. Variation in process conditions, such as input particle size distribution, coating slurry yield stress, and granule bed moisture can modify residence time. Experiments were conducted on a large laboratory scale inclined rotary drum mixer equipped with two distinct types of flights. An illustration of the mixer is provided in Figure 2.2. The media used were rock granules with a range in particle size. Figure 2.3 provides a graphical description of the average distribution of particle sizes. The coatings were made with sodium silicate, clay, and pigment dispersions. The next section of this chapter demonstrates the effect of varying particle size on the residence time, and suggests that control of input material properties is crucial to coating uniformity. The third section examines the effect of increasing the coating slurry yield stress on the RTD. Finally, the fourth section outlines the relationship between moisture in the input material and RTD.

2.1 THE EFFECT OF PARTICLE SIZE ON RESIDENCE TIME DISTRIBUTION

2.1.1 EXPERIMENTAL PROCEDURES

Developing a measurement technique was the first step necessary for the examination of the RTD of particles flowing through the mixer. A requirement, beyond obtaining an accurate measure of the residence time, was that the method of detection not affect the mixing process. Previous researchers have used sampling thieves[27], visual analysis[16,26,19], ferromagnetic tracer[28], digital subtraction radiography[24], and positron emission tomography[29] for analysis of mixing behavior. An attempt was made to minimize the tracer required so as not to disrupt the standard material flow. In general, as tracer flows through a mixer and is mixed with standard material, the initial input peak spreads out, and the concentration of tracer is reduced. This effect is illustrated in Figure 2.4. The measurement technique must provide low level detection of the tracer granules, for this reason. Granules bearing a copper coating were used as the tracer material, in an approach similar to that used by Dr. William Rowe.[20] The RTD was determined by measuring the copper concentration in samples of output flow taken over time. A Metorex X-Met 880 Energy Dispersive X-ray Fluorescence elemental analysis system with a SAPS 2152 probe was used to detect the concentration of copper in each sample.[30]

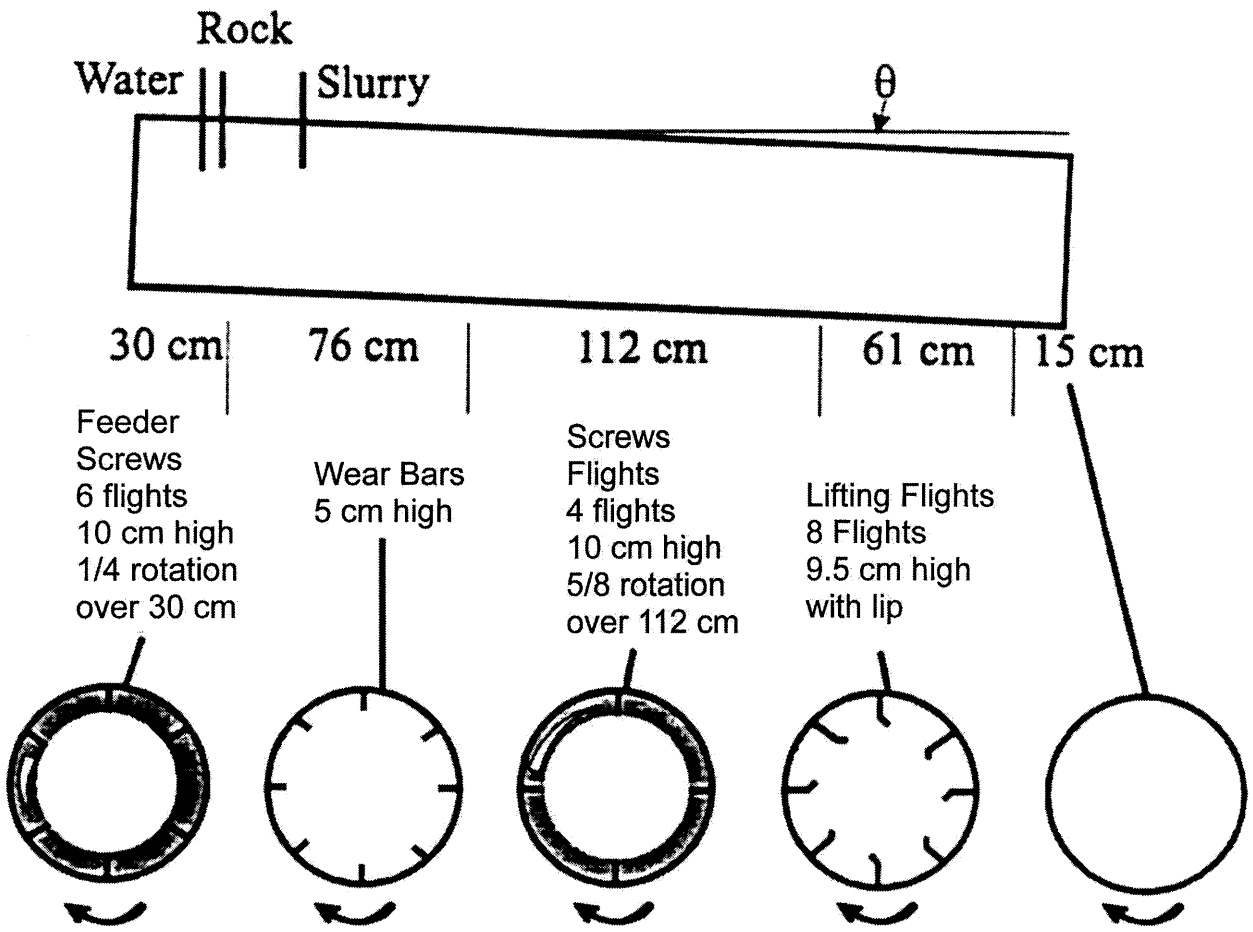

Figure 2.2 Diagram of Laboratory Mixer

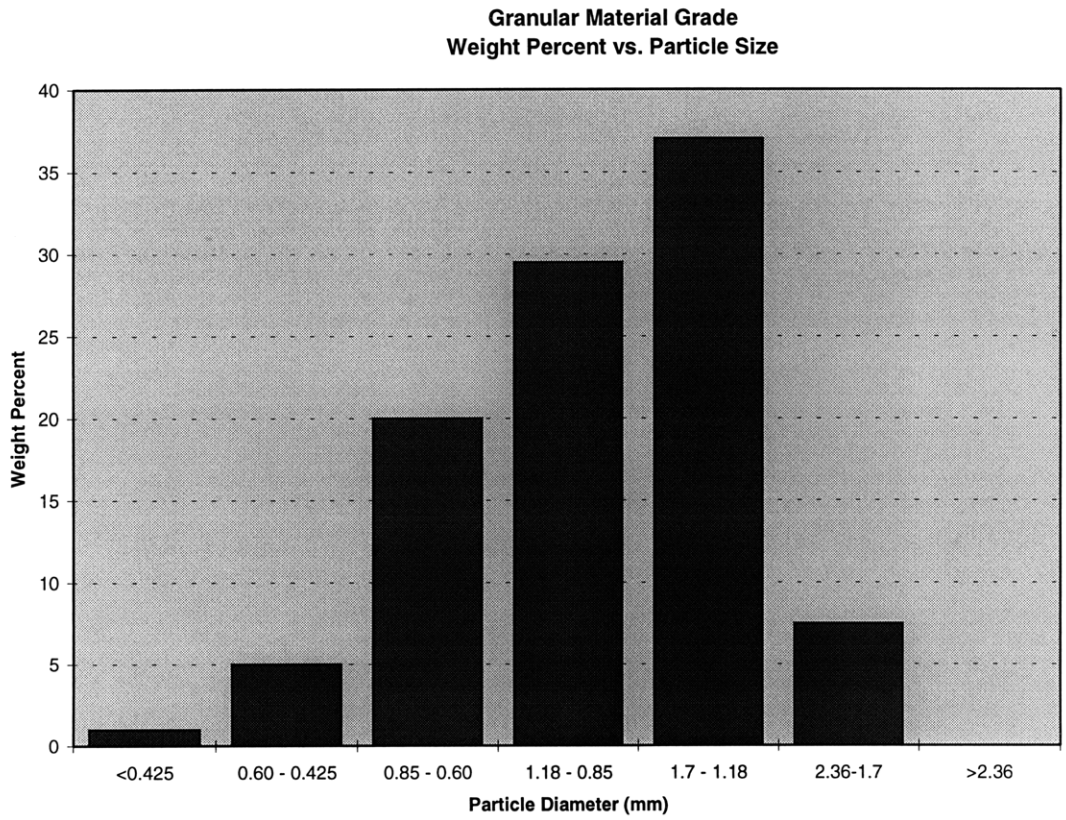

Figure 2.3 Graph of the Particle Size Distribution (Average Values)

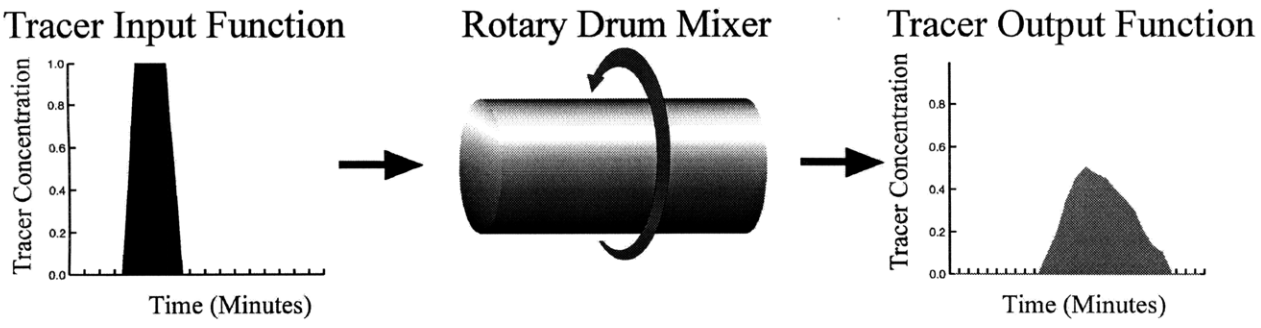

Figure 2.4 Spreading of Concentration Peak

The tracer material was separated into three distinct particle size ranges using metal sieves of varying pore diameter. The three sieve cuts generated had diameters: greater then 1.18 mm, between 1.18 mm and 0.85 mm, and below 0.85 mm. These segments were termed *Coarse*, *Midgrade*, and *Fine*.

The XRF measurement technique is based on the assumption that the copper intensity, or the amount of copper measured, is directly related to the concentration of tracer in a sample. The ratio of the mass of copper in a granule's coating to that granule's mass should decrease with increasing particle size, assuming that all particles have equivalent coating thicknesses. A visual analysis of cross-sectioned granules demonstrated that coating thickness does not vary significantly with increasing particle size. Due to the limited particle size range created with each tracer sieve cut, the copper mass to granule mass ratio variation between particles in a specific sieve cut should not be significant. The copper concentration of the coating may vary between granules, due to inconstancies in the coating process. Variation in the copper coating between granules would result in tracer concentration measurement error. The variation in copper concentration between granules was assumed, however, to be negligible.

The mixer was allowed to run until it reached a steady state before starting each experiment. The standard input flow was then diverted, and the flow was replaced with tracer for a 30-second period. The standard input material flow was returned after 30 seconds. Samples were then taken every fifteen seconds after an initial interval of 2 minutes. Experiments were conducted dry or with the application of a sodium silicate slurry. The slurry was based on a typical slurry formula[31], but thinned with additional water to aid tracer identification.

Procedures for using the X-MET XRF analysis system were as follows: Four 7 mL test cups were filled with material from each run. Each cup was covered with a SPEX polypropylene film. Four cups were used in order to obtain an average value representative of the sample, as the volume of material tested in each cup was fairly small. Each test cup was then measured four times for copper concentration using the X-MET. The measurements were given in counts per second, and were averaged over a 25-second measurement period. The sample cup was rotated after each measurement, in order to change the orientation of the cup on the XRF probe. The cup was rotated in order to reduce the associated error, since the measured intensity varied somewhat according to the sample cup orientation.[32] The sixteen measurements per sample were then averaged to give an approximate copper concentration.

The XRF measurement technique provides a fairly accurate picture of the concentration of tracer particles in the output flow. The XRF results closely matched those from a visual RTD measurement technique, in which samples were taken and individual tracer particles were counted. The visual counting method will be explained in more detail in Section 2.3.1. Unfortunately, the level of detection provided by the XRF technique was not as low as that of the visual method. Non-uniformity of copper coating between granules, differences between copper readings for small versus large tracer particles, the small volume of particles measured by the XRF probe, and the variation in XRF readings for the same sample cup may have introduced error into these experiments.

2.1.2 OBSERVATIONS

Table 2.1 provides a summary of the parameters and results of the particle size experiments.

Table 2.1 Particle Size Variation RTD Experiment Parameters

Run	Particle size range (mm)	Slurry applied	Water rate (L/second)	Initial tracer observed (seconds)	Peak copper Concentration (seconds)	Estimated mean residence time (seconds)
C	> 1.18	no	0	270	330	348
CS	> 1.18	yes	0	330	555	486
MS	1.18 > x > 0.85	yes	0	405	510	544
FS	< 0.85	yes	0	375*	510	541

* First sample measured.

Figure 2.5 is a graph of the RTD for coarse tracer granules with and without slurry applied. The measured results were normalized in order to simplify comparison of the two runs. The RTD for run C, without slurry, is approximately half as broad as that of run CS. The peak measured copper concentration for run C is approximately double that of run CS, which corresponds with the broadening of the peak in run CS. The results from runs C and CS exhibit oscillations with a period of 45 seconds. The source of the oscillations is unclear, although it is hypothesized that they may be a function of the mixer rotation rate and flight arrangement. Oscillatory behavior was less evident in the subsequent experiments. The peak value measured for run CS occurred well after the center of the pulse, as a result of the oscillations, and thus appears anomalous in Table 2.1.

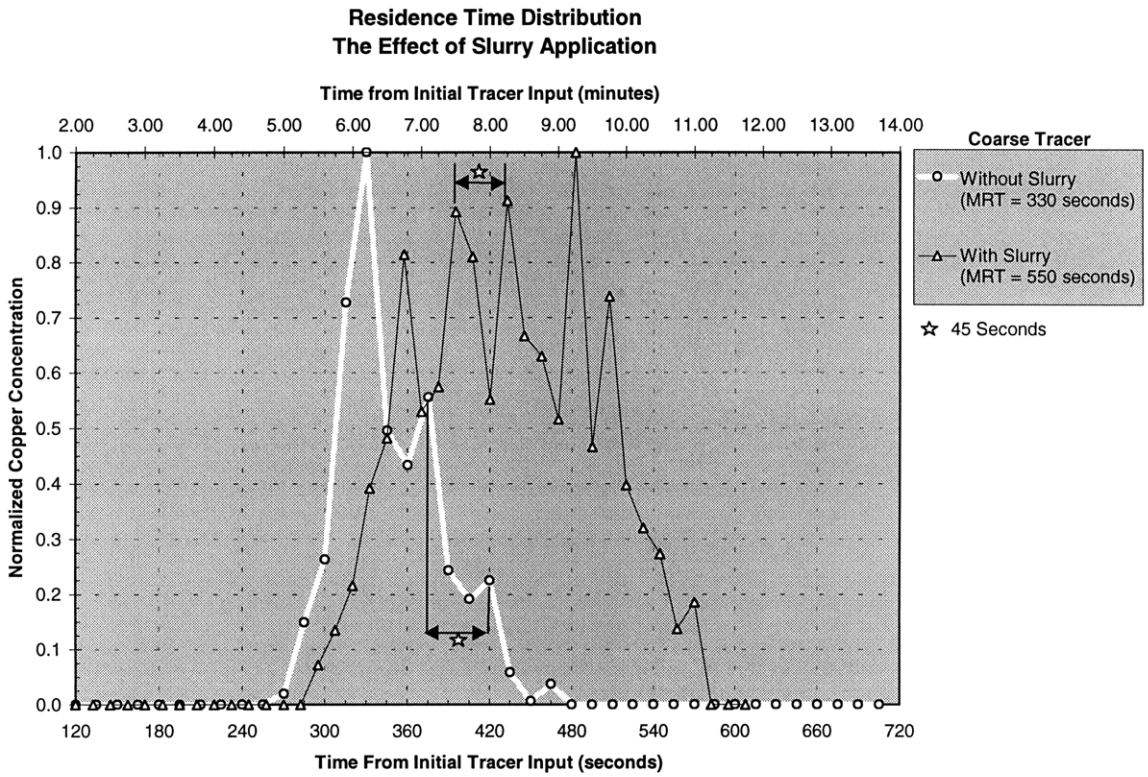

Figure 2.5 Graph of Coarse Tracer Granule RTD with and without Slurry Application

Figure 2.6 is a graph of the three particle size RTD runs which involved the application of slurry. It is clear that the mean residence time for the coarse granules is significantly shorter than those of the midgrade (MS), and fine (FS) runs. This separation is on the order of one minute. The separation between the MS and FS runs, however, is not appreciable.

A series of XRF measurements were made on samples of increasing copper tracer concentration, in order to relate the measured XRF intensities with actual copper tracer concentration. The results are shown in Figure 2.7.

Each sample bag from the RTD experiments was screened for the particle size range of the tracer, in order to increase the signal to noise ratio for these samples. The signal was the copper tracer and noise was the amount of non-copper coated granules. For example, the sample bags for the midgrade tracer run were screened and only the midgrade material was measured for copper concentration. Removing the coarse and fine grades from each sample increased the overall copper concentration 300 percent, without affecting the relative level of copper between sample bags. Prior to screening, the maximum concentration at the tracer peak would have been approximately 6 percent copper tracer material. With screening, the sample was found to have approximately 17 percent copper coated granules. Magnification of the tracer peak in this manner allowed us to use the XRF to measure smaller tracer concentrations than originally expected.

Figure 2.8 demonstrates the variation in results associated with the XRF measurement technique. The error bars illustrate 95% confidence limits for measurements on each sample bag. The limits were calculated with the following formula:

$$\text{limits} = \pm\frac{ts}{\sqrt{N}}$$

The standard deviation, s, was calculated for each bag using the sixteen measurements per bag. The student's modifier, t, was taken to be 2.13, and N was 16 because there were sixteen measurements.[33]

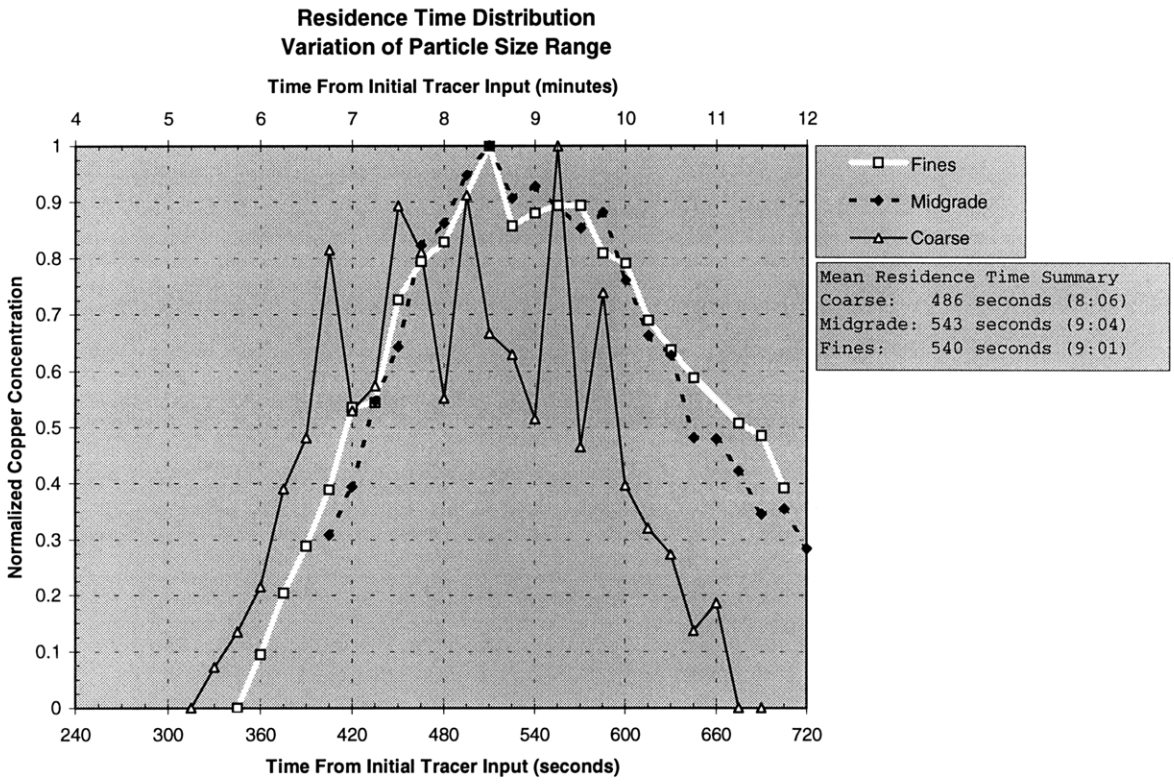

Figure 2.6 Graph of the Three RTD Runs with Slurry Application

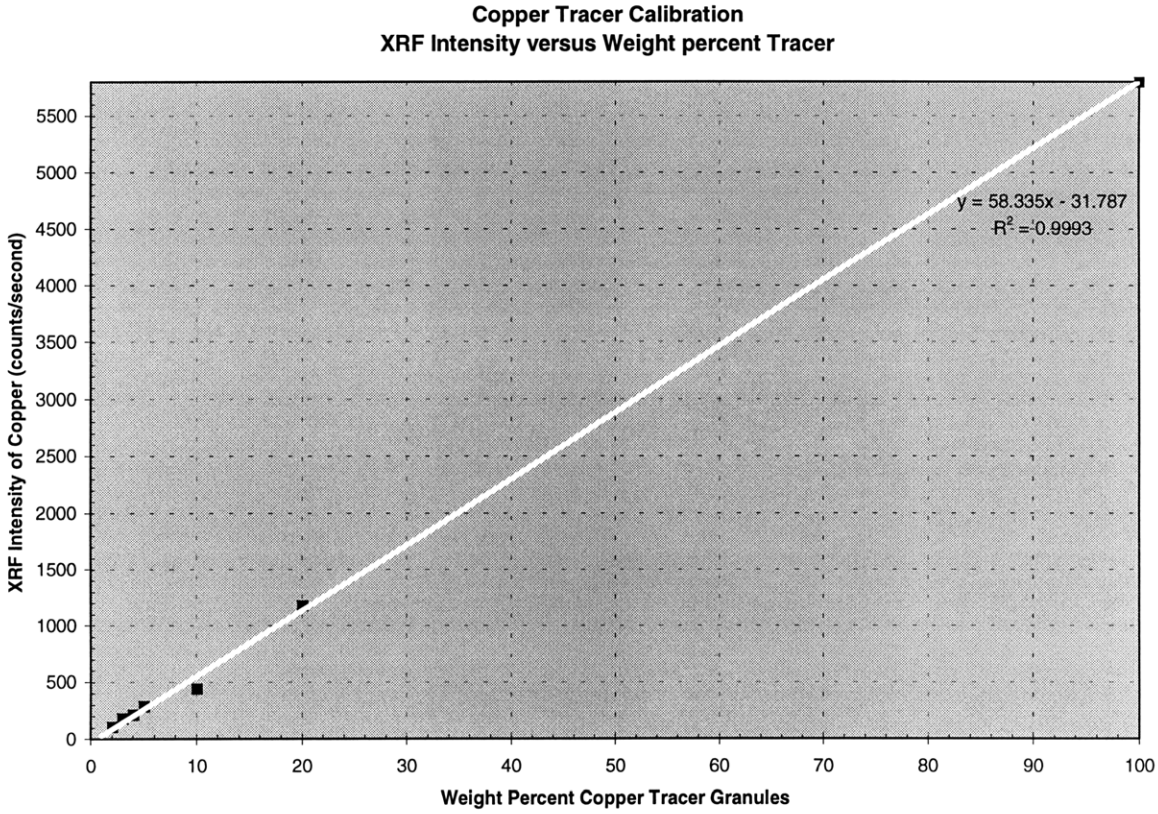

Figure 2.7 XRF Calibration Study: Measured Copper Intensity versus Copper Concentration

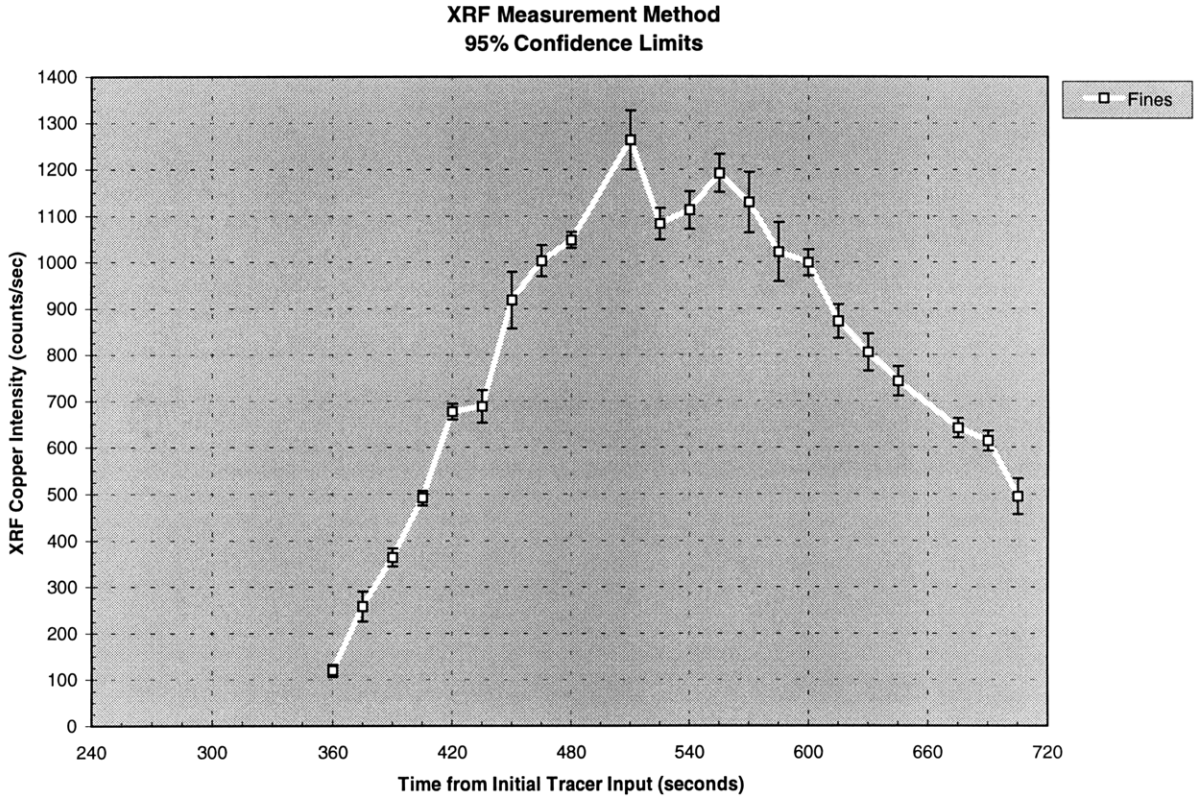

Figure 2.8 95% Confidence limits for an RTD Measured with XRF

In Figure 2.9 the same graph is shown with the error bars calculated using a method recommended by Metorex, the X-Met manufacturer. Statistical error associated with counting X-ray quanta over time provides the majority of experimental error, according to the manufacturer.[34] The measured intensity values are actually a function of the quanta count (P) less a background count (B). The measurement error is thus a function of statistical deviations for both the quanta count and the background count. The statistical deviation for P and B are $\sqrt{P}$ and $\sqrt{B}$ respectively. The function of the error is then given as the sum of the squares of these errors:

$$\text{Error per measurement} = \sqrt{(P + B)}$$

The error of each sample was taken to be the quadratic sum of the individual measurement errors, since each data point was the average of 16 measurements.[33] The error values calculated in this manner were very significant.

Figure 2.10 presents a comparison of the results of the XRF RTD measurement technique with those from the optical counting method. For this run the tracer material was made up of all grades of material, coarse, midgrade and fines. The optical method offered detection of significantly lower concentrations of tracer, e.g. 1 particle in 5 grams of material, rather than the higher detection limit of the XRF method. The results of the two measurement techniques have a correlation coefficient of 0.90 for the region in which the X-MET was able to measure the copper tracer content. We believe XRF is a valid RTD measurement technique, due to the high correlation between visual and XRF measurement techniques.

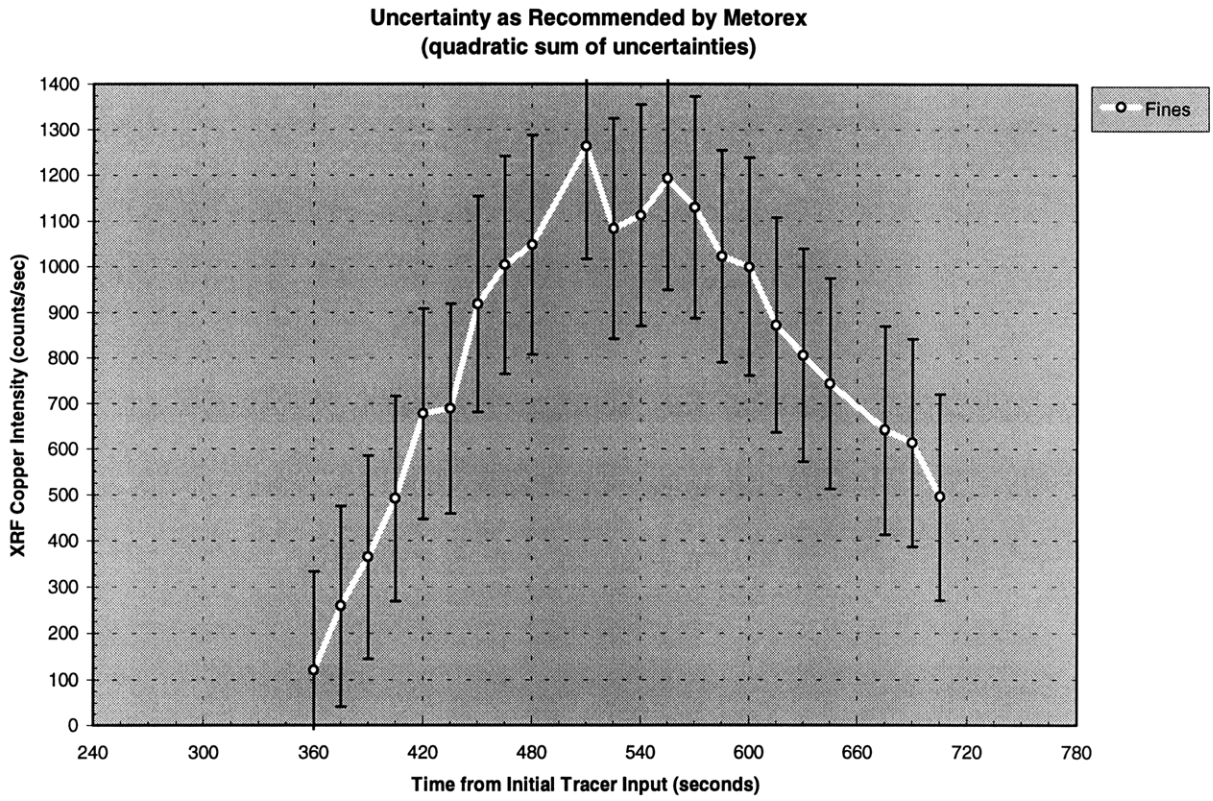

Figure 2.9 Error Bars for a RTD Measured with the XRF Method, as Recommended by Metorex (the X-MET Manufacturer)

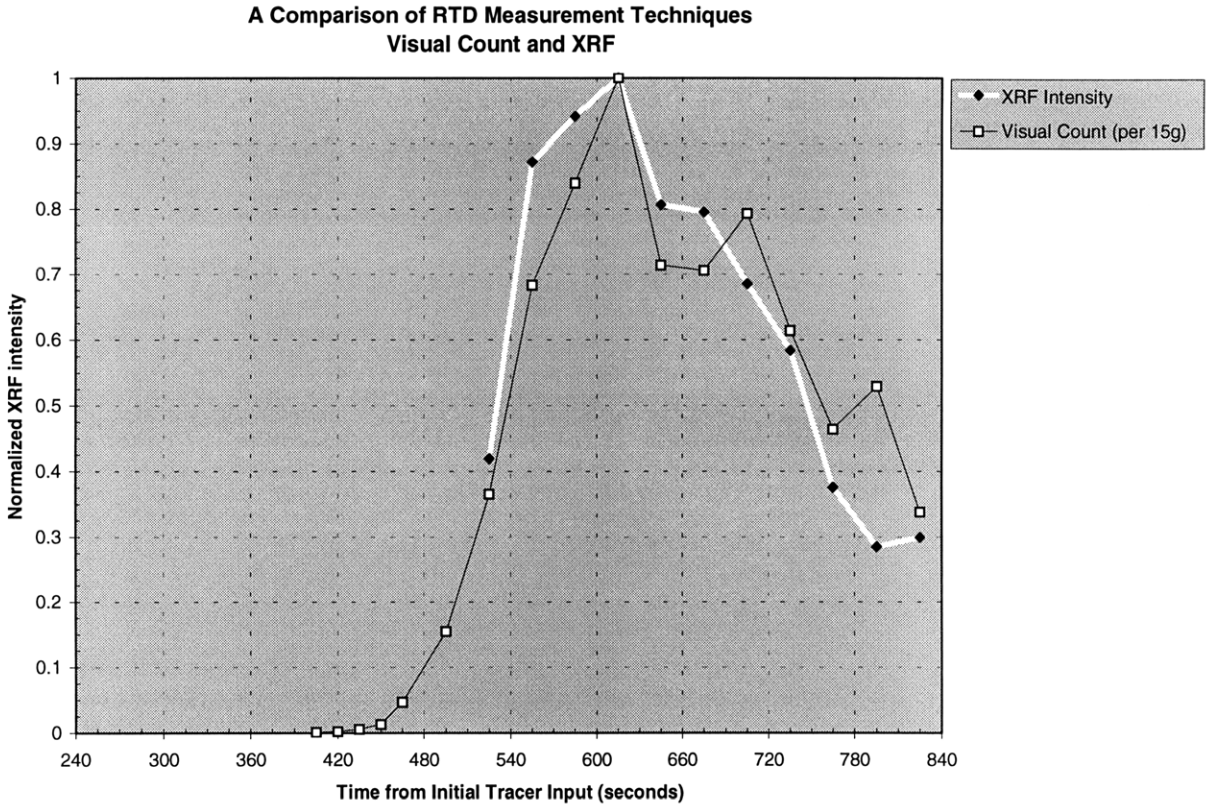

Figure 2.10 Comparison of Optical Counting and XRF RTD Measurement Techniques

2.1.3 DISCUSSION

The addition of slurry to the granular material mixing process broadened the tracer pulse peak, as shown in Figure 2.5. The viscosity of the liquid-granule mass increased due to the viscosity and surface tension of the liquid. The application of liquid also imparted interaction forces between individual particles and the walls, flights, and other granules due to the cohesive capillary forces.[35,36] The addition of interaction forces caused an increase in diffusion, as evidenced by the broadening of the tracer peak. The addition of slurry also resulted in an increase in the volumetric hold-up, or the amount of material held in the mixer. An increase in hold-up indicates that the rate of material flow in the mixer was reduced. The addition of slurry may also lead to agglomeration of the smaller particles onto larger ones. It is unclear what affect agglomeration would have on the flow rate for these agglomerated particles. Increasing particle size results in increased flow rate, as was demonstrated above. The potential flow rate increase due to increase size may be countered to some extent with an increase in surface roughness and a decrease in density.

The initial mix of particles will tend to segregate during avalanches in rotating drum mixers.[13] Segregation occurs when the general mix of material has a higher dynamic angle of repose than that of one or many of the constituents. The angle of repose is a function of particle shape, density, size, surface roughness, and elasticity.[15] In the experiments by Zik et al., the mixers consisted of closed containers, and segregation led to bands of single phase material. In our experiments, the coarse granules flowed through the mixer at a faster rate than smaller granules. It is not clear whether segregation led to this behavior. The relationship between MRT and particle size did not appear to be linear in these preliminary experiments. We predict that the MRT would decrease exponentially with particle size for the distribution in particle sizes utilized in these experiments. A graph of the trend we predict along with our preliminary data points is provided in Figure 2.11. The data points were calculated using the mean residence time results from the three particle size RTD experiments, and an approximate mean particle size for each respective run. Future experiments should be conducted to more thoroughly analyze this relationship.

The results of this series of experiments point to the following conclusions. Coarse granules with higher flow rates will be exposed to the process environment for less time than smaller granules. This potential difference in flow rates may be significant for processes that involve

heat transfer to or from the granules. For example, in the case of a kiln baking process where granules must be raised to a given temperature, larger particles with lower surface to volume ratios will heat more slowly then smaller particles. Thus the process conditions experienced in the interior of larger granules could possibly be different than that experienced by smaller granules. Conversely, when granules lose heat in order to evaporate a coating binder, they will also be affected by this difference in flow rates. Smaller granules would rapidly lose heat and possibly leave the mixer wet, while the larger granules would exit the kiln dry and at a higher temperature. A secondary affect of the difference in flow rates for continuous mixers is that the volumetric hold up will be more concentrated in fine grained material than the material in the input and output flow.

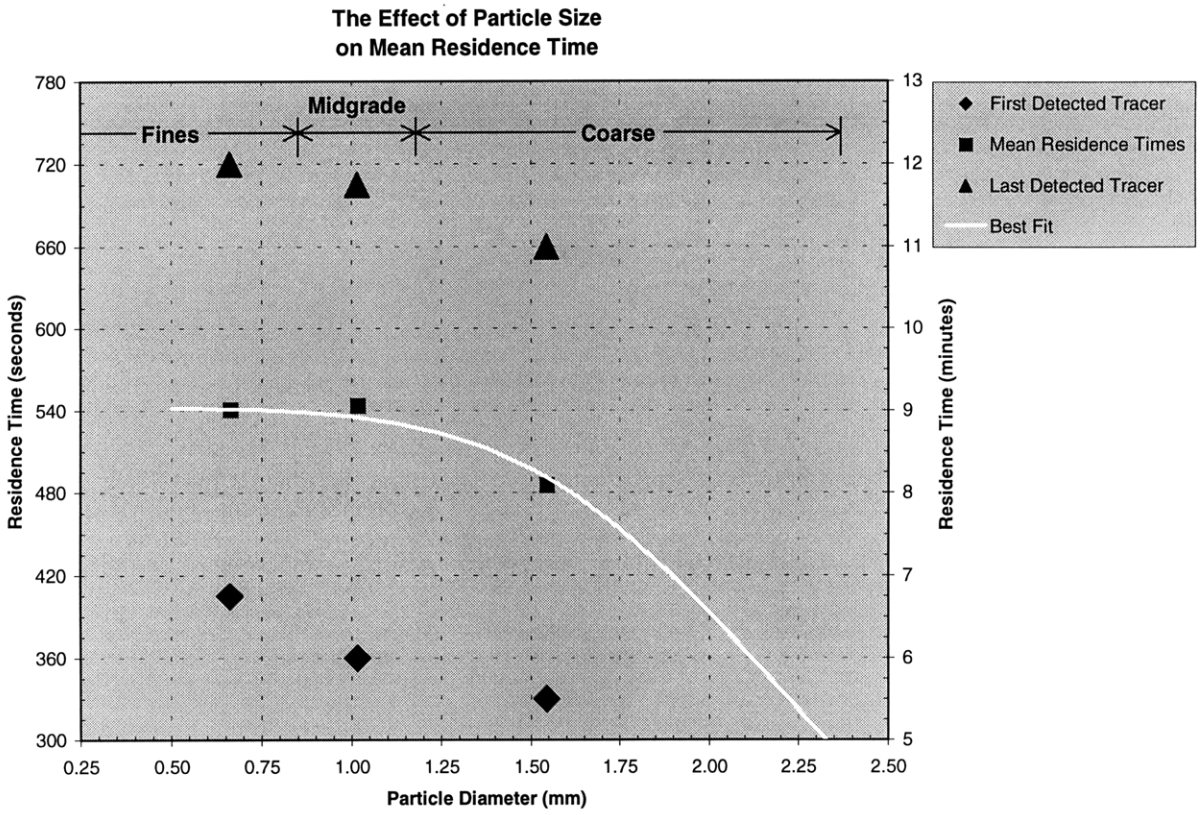

Figure 2.11 Graph of Predicted Mean Residence Time vs. Particle Size

2.2 THE EFFECT OF SLURRY YIELD STRESS ON RESIDENCE TIME DISTRIBUTION

2.2.1 EXPERIMENTAL PROCEDURES

The slurry used in the coating process was a mixture of sodium silicate, water, pigments and clay. The slurries were shear thinning due to the presence of clay.[20] The slurry yield stress could be modified by changing the concentration of clay. Three RTD experiments were conducted in the same manner as before. The first run was completed with a 23.6 weight percent clay slurry, the second with a low yield stress slurry (20.6 wt.% clay), and the third with a high yield stress slurry (26.6 wt.% clay). These numbers were determined by bracketing the medium clay slurry by 3%. The low and medium yield stress slurry runs were completed with coarse grade copper-coated tracer granules. The high yield stress slurry run was conducted with midgrade copper-coated tracer granules due to a shortage of coarse tracer material. From our previous results, it was expected that the midgrade tracer would tend to increase the measured residence time. This did not prevent us, however, from examining the correlation between yield stress and residence time distribution.

The slurry yield stress was measured using a rheometer (Model RMS-800, Rheometrics), with a Plate-and-Cone sensor system. The slurries were mixed for 19 hours using a ball mill. Samples of each slurry were then removed from the milling media, and measured three times using the rheometer. The yield stress was taken to be the stress at the maximum immediately after flow began.

2.2.2 OBSERVATIONS

Table 2.2 provides a summary of the parameters and results of the yield stress experiments. Unfortunately comparisons cannot be made with the particle size RTD experiments detailed in section 2.1 because of differences in the slurry formulations used. Figure 2.12 demonstrates the results of the yield stress measurements on the medium yield stress slurry. All of the yield stress experiments demonstrated this behavior. The RTD results of the three runs are plotted in Figure 2.13. The mean residence time increased with increasing yield stress between the low and medium yield stress slurries, as was expected. The mean residence time was found, however, to decrease with an increase in yield stress above the medium yield stress. These are only preliminary findings, as it was only possible to conduct three experiments. Further experiments

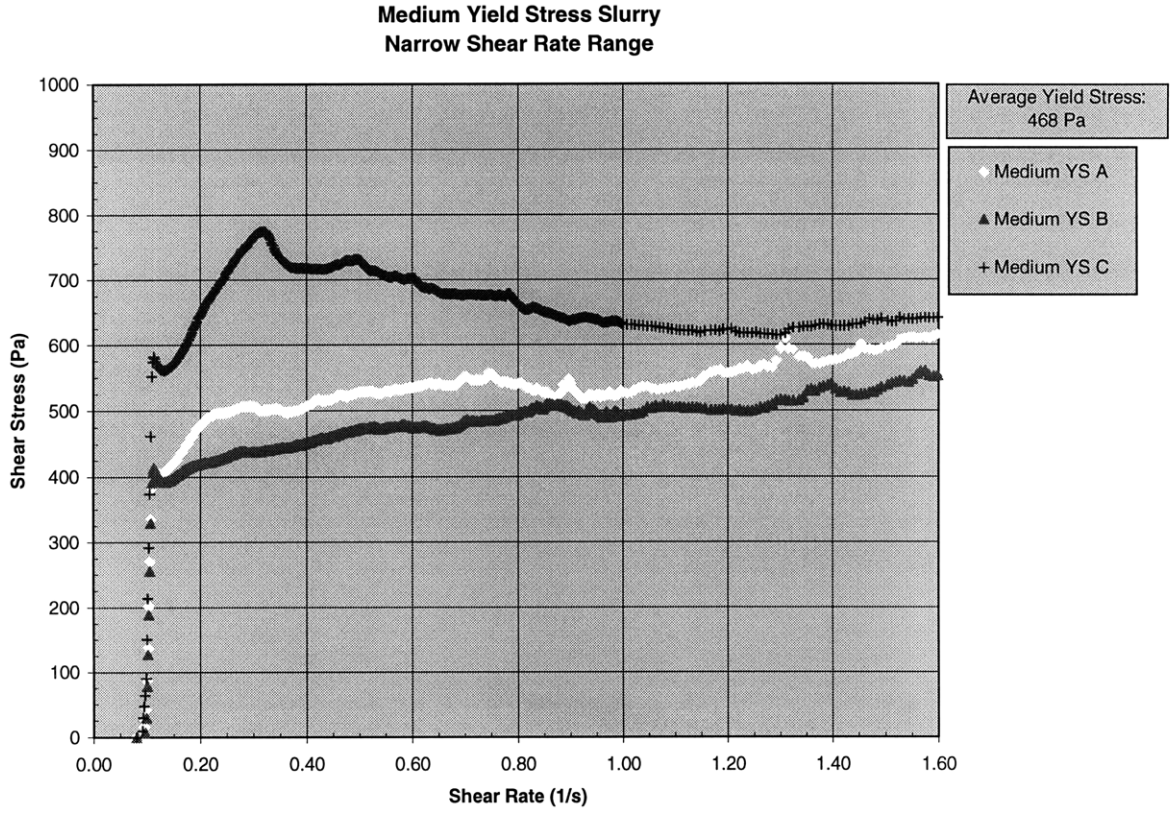

Figure 2.12 Shear Stress Measurements for a 23.6 wt.% Slurry

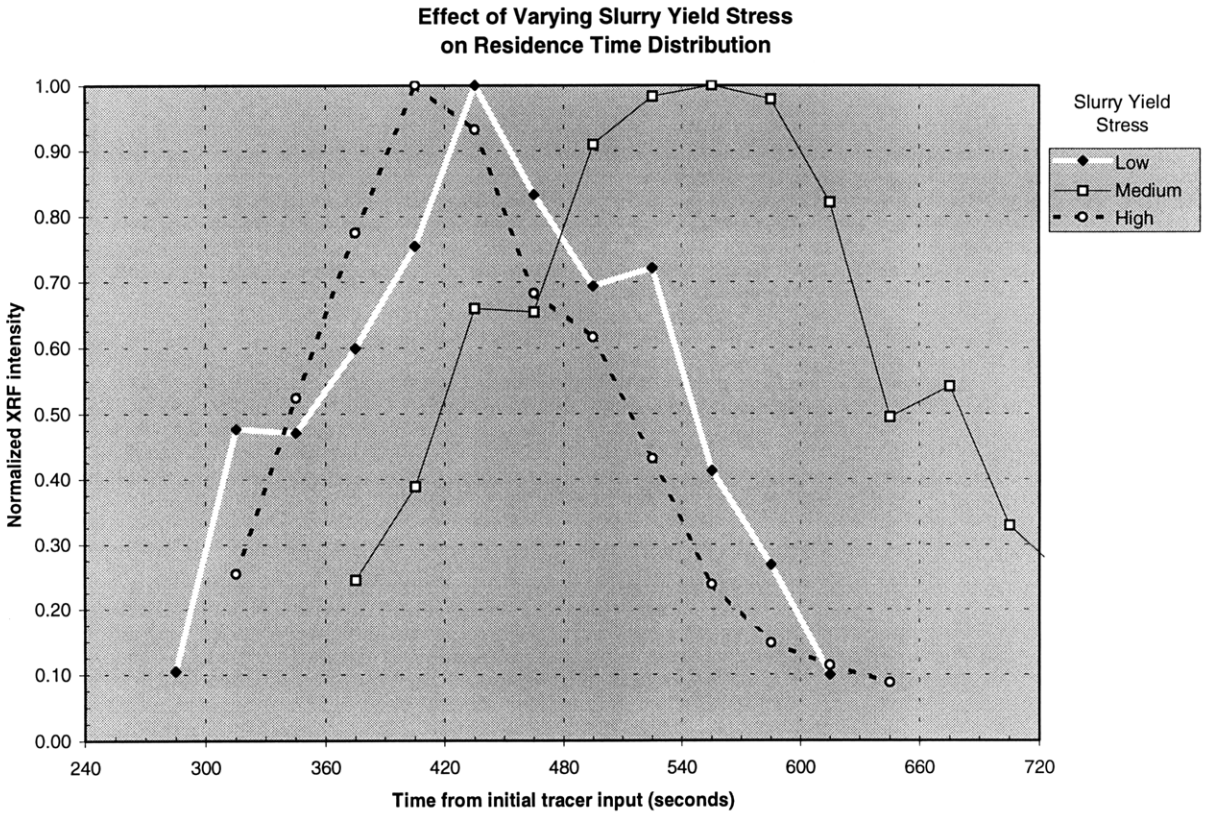

Figure 2.13 RTD for Increasing Slurry Yield Stress

will be necessary to thoroughly define the relationship between slurry yield stress and RTD. The breadth of the residence time distributions for both low and high yield stress slurries was narrower (4:45 and 4:00 minutes respectively) than that of the medium yield stress slurry (6:00 minutes). The breadth was calculated by measuring amount of time between the first normalized XRF count above 0.25 until the XRF count dropped below 0.25.

Table 2.2 Yield Stress RTD Experiment Parameters

Run	Particle size range (mm)	Slurry clay content (wt%)	Yield stress (Pa)	Yield stress standard deviation	Initial tracer observed (seconds)	Peak copper concentration (seconds)	Estimated mean residence time (seconds)
LYS	> 1.18	20.6	320	21 Pa	285	435	435
MYS	> 1.18	23.6	468	81 Pa	375	555	555
HYS	1.18 > x > 0.85	26.6	776	146 Pa	315	405	405

2.2.3 DISCUSSION

The relationship between RT and yield stress appears to involve an inflection around the medium yield stress used in this series of experiments. A prediction of the behavior is illustrated in Figure 2.14. A lower yield stress slurry will clearly result in less cohesive granular mixture, and therefore the wall will have less of an effect on the flow rate. The case of the higher yield stress is more complicated. It is possible that the high yield stress slurry caused severe agglomeration in the mixer, resulting in an increase in effective particle size, and thus increased flow rate. There was not, however, a noticeable change in the flow behavior during this run.

The narrow RTD of the low and high yield stress runs indicate that there is less axial diffusion occurring relative to the case of the standard yield stress slurry. Thus the effectiveness of mixing is partly a function of slurry yield stress.

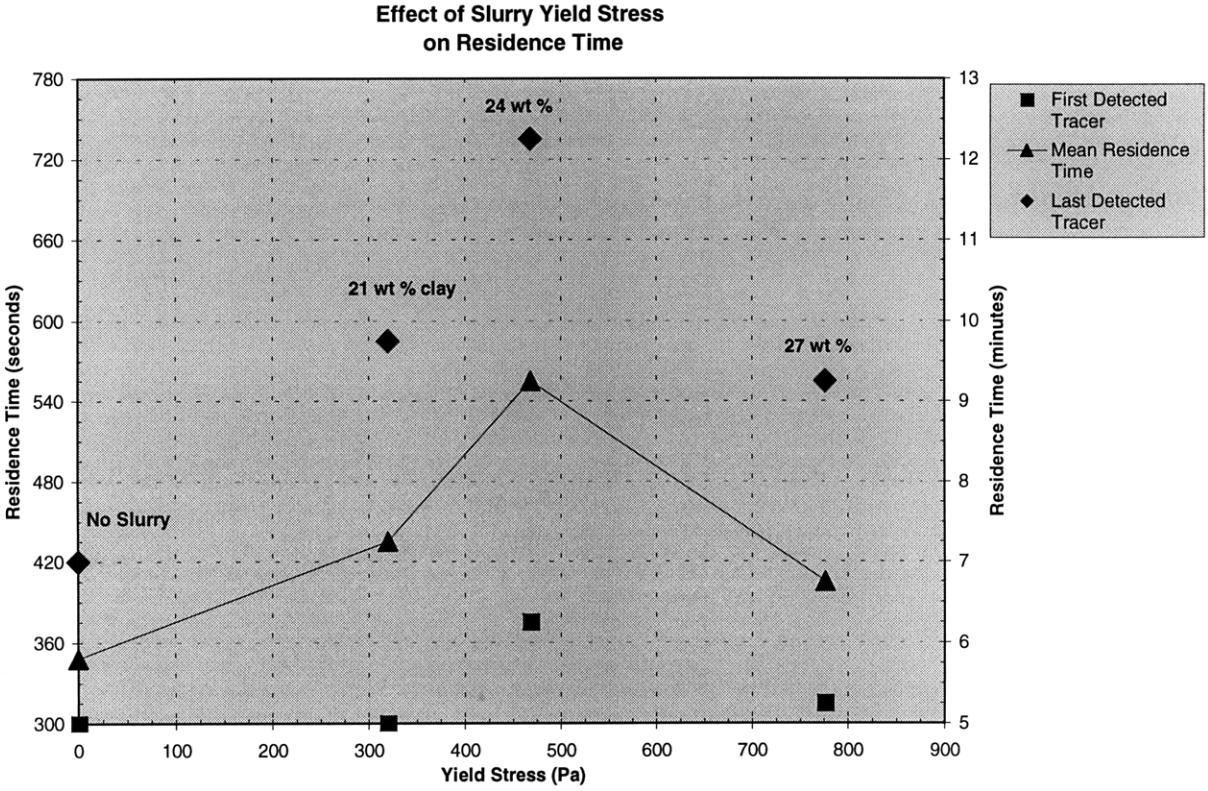

Figure 2.14 Measured RTD for Three Yield Stress Experiments

Note: The 26.6 wt % clay result shown above was found using midgrade tracer, whereas the others were conducted with coarse tracer. Had coarse tracer been used the MRT would have been even lower.

2.3 EFFECT OF INPUT MATERIAL MOISTURE LEVEL ON KILN RTD

2.3.1 EXPERIMENTAL PROCEDURES

The following experiments were conducted on a laboratory scale rotary kiln. The moisture level of the rock added to the kiln was controlled by varying the amount of water added to the material in the rotary mixer. Material from the rotary mixer was then fed to the rotary kiln, as illustrated in Figure 2.15. Three RTD experiments were conducted in the same manner as before. The flow of standard input material was deflected during the 30 second addition of tracer material. The initial run was completed with the water addition rate of 2.5 gallons/hour. The second run was done with the lower water flow rate of 1.5 gallons/hour. Finally the third run had a flow rate of 3.5 gallons/hour. For each run, 15 pounds of unscreened black tracer material, termed *fullgrade*, was used.

Granules are coated in the rotary drum mixer via a two step process: coating transfer between wet granules, followed by spreading of the coating due to contact between wet coated granules and dry granules.[20] This process is examined in more detail in chapter 6. The transfer of slurry between granules does not occur beyond the length of the rotary drum mixer. The tracer material was not coated with slurry during the kiln RTD experiments for this reason. It was thus possible to visually identify the tracer material in the otherwise white output flow. A second RTD measurement technique, visual counting, could then be used for determining the RTD. The visual method also provided a means for validating the XRF measurement technique. Samples were again taken every fifteen seconds after an initial interval of 3:30 - 4:00 minutes. It was necessary to cool the samples in aluminum trays prior to placing them in sample bags, as they were taken directly from the kiln.

The optical counting method involved weighing a portion of each sample, and then separating and counting the black tracer granules contained within each sample. At low tracer levels it was possible to scan through larger amounts of sample, for example 15 grams, so the error in this method was lower. At higher concentration levels, a smaller fraction of material (2.5 grams) was scanned and then the results were normalized for a measurement of a 15 g sample. This was necessary due to the high tracer counts near the tracer peaks.

The run with high moisture was also tested for copper concentration using the aforementioned XRF procedure, in order to provide a comparison with the XRF measurement technique.

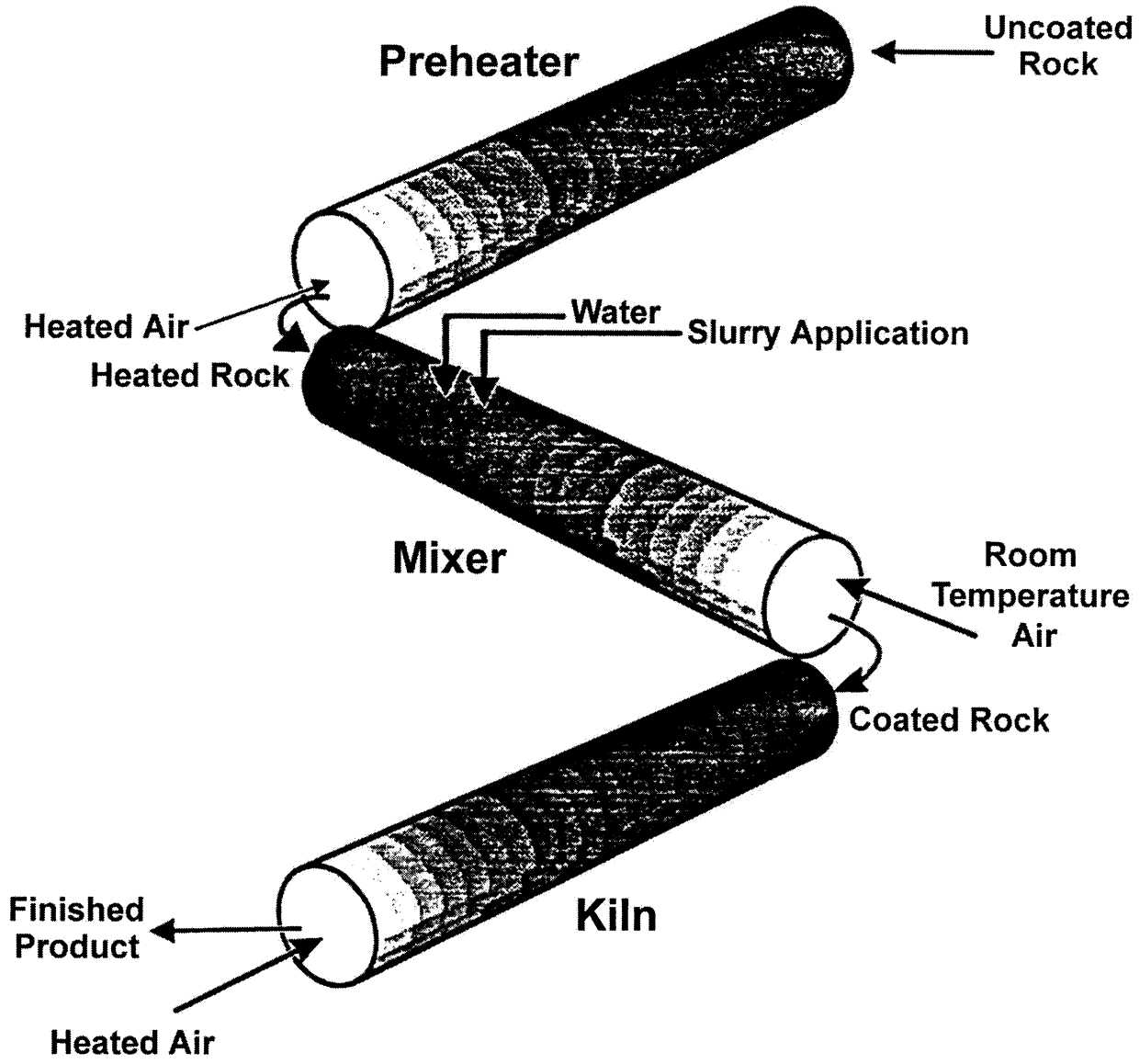

Figure 2.15 Illustration of the Mixer Laboratory Arrangement

Taken from Dr. Rowe's Thesis [20]

2.3.2 OBSERVATIONS

Table 2.3 provides a summary of the parameters and results of the moisture level experiments. The results of the three runs are plotted in Figure 2.16. The mean residence time increased with increasing moisture level, as expected. The magnitude of variation was not as high as expected. These are again only preliminary findings, as it was only possible to conduct three experiments. Further experiments will be necessary to thoroughly define the relationship between input moisture level and RTD.

A concern prior to this series of experiments, and one that we hoped to examine, was whether or not spalling of the coating occurs in the kiln when the moisture level of the input material is decreased. Spalling appeared to occur more frequently, during these experiments, at the lower moisture levels.

Table 2.3 Moisture Level Kiln RTD Experiment Parameters

Run	Particle size range (mm)	Water application rate (L/second)	Initial tracer observed (seconds)	Peak copper Concentration (seconds)	Estimated mean residence Time (seconds)
LM	<2.36	1.58×10^{-3}	390	585	630
MM	<2.36	2.64×10^{-3}	405	615	630
HM	<2.36	3.67×10^{-3}	405	615	660

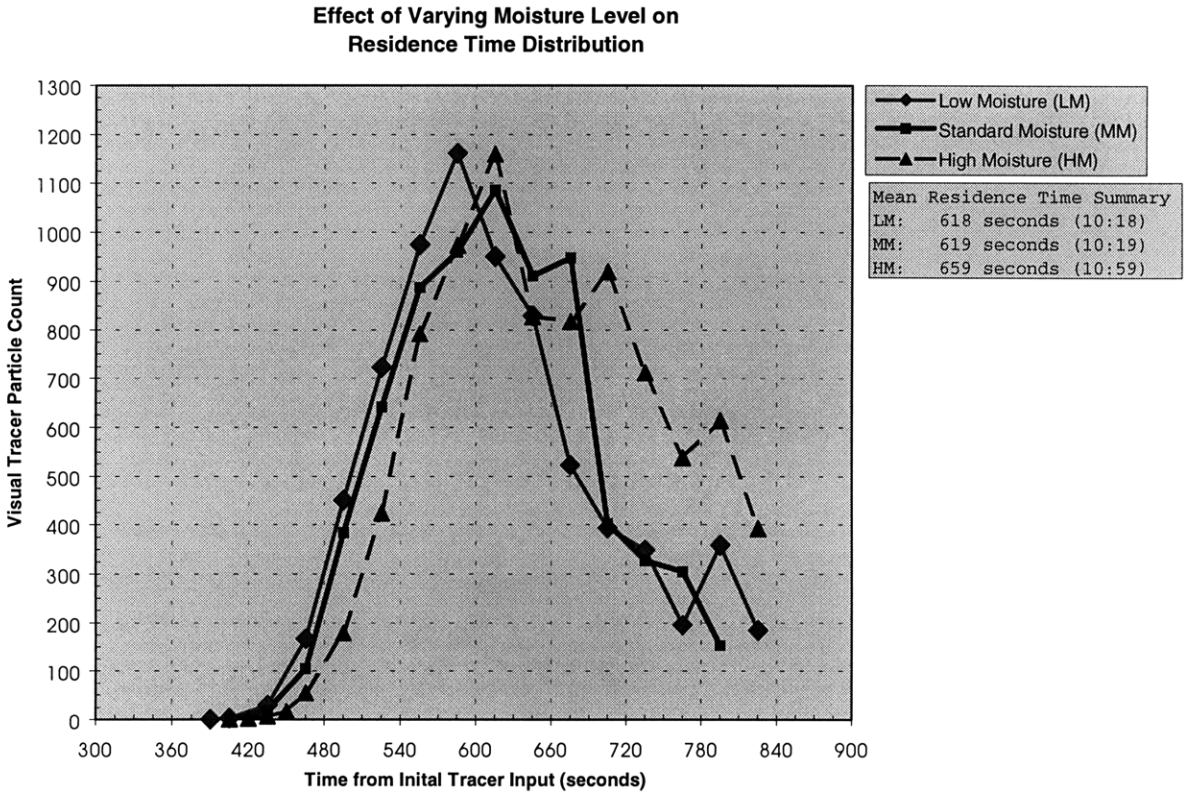

Figure 2.16 RTD for Increasing Granule Bed Moisture

2.3.3 DISCUSSION

We hypothesize that the residence time distribution will be affected by moisture in the manner shown in Figure 2.17. It was expected that there would be an initial regime in which moisture will be adsorbed onto the surface of the granules yet they would retain non-cohesive behavior. In this regime, the increase in RTD with moisture level would be negligible. At some point, the additional moisture would create capillary forces between the particles and the viscosity of the mixture would rapidly increase. The third regime would involve saturation of the granule bed and further moisture added would have little additional effect on the residence time. A more thorough conceptualization of these regimes was explained in a paper by K. Umeya.[36] The behavior of wet agglomerates was also studied by M. Khan and Gabriel Tardos.[35]

It is difficult to judge whether or not the three regimes have been realized from the results of these experiments. It is possible that the three runs all fall into the first regime and thus dramatic changes in RTD were not evident. Further experiments in involving increasing moisture would need to be completed in order to fully test our hypothesis. A smaller scale laboratory mixer might prove more effective for future experiments.

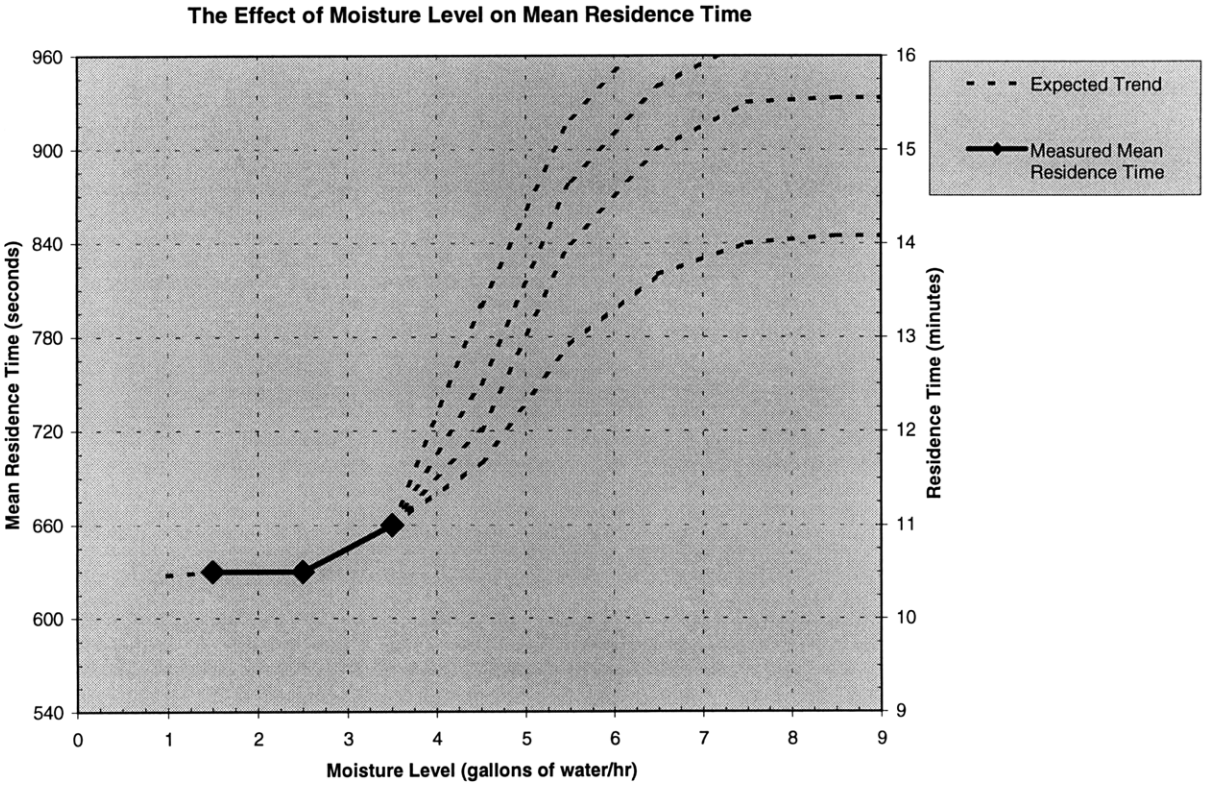

Figure 2.17 Predicted Variation of Mean Residence Time with Increasing Moisture Level

Note: The curve indicates the expected trend not actual predicted values of MRT

CHAPTER 3
INDUSTRIAL SCALE RESIDENCE TIME DISTRIBUTION EXPERIMENTS

A series of RTD experiments were conducted at a production site in order to provide a mechanism for comparison between laboratory and industrial scale mixers. A facility with a production line of the same general layout as in Figure 2.15 was used for these experiments. The object of this study was to examine whether the flow behavior of granular media remains the same at vastly scaled proportions. The resulting RTD data should allow for the laboratory mixer rotational speed to be scaled more accurately to that of the production mixer.

3.1 INDUSTRIAL SCALE MIXER RESIDENCE TIME DISTRIBUTION

3.1.1 EXPERIMENTAL PROCEDURES

Additional limitations were imposed upon the production plant residence time distribution experiments, due to the high rate at which material flowed through the industrial mixer. It was not possible to divert the flow of heated base rock flowing into the mixer. The tracer material was instead added to the mixer in addition to the standard material flow. This resulted in a temporary surge in the amount of material flowing through the mixer. The minimum amount of tracer material necessary for detection in the output flow was added, in order to reduce the effect of this additional material. The tracer was added over a period of 15 seconds and constituted 13 weight percent of the total input flow. The total rate at which material was added to the mixer during this period was increased by 15%, due to the addition of tracer material.

The maximum concentration of tracer in the output flow, given these input parameters, was expected to be between 0.5 and 1.3 percent by weight. This was calculated based upon the tracer-peak spreading behavior observed in the laboratory mixer experiments. The input concentration was 100% for the midgrade MS run and the output contained approximately 6% copper tracer by weight, as noted before. The output concentration was, thus, approximately 0.06 times that of the input concentration. The production plant tracer will make up 13 percent of the material input into the mixer, so the resulting output should contain approximately 0.8 percent tracer. This approximation was only used to obtain an order of magnitude estimate of the output tracer concentration.

The effective detection limit of copper tracer using the XRF technique was found by studying the relationship between measured XRF intensity and copper tracer concentration followed by an error analysis (see Section 2.1.2). The minimum concentration accurately detected by XRF was 3 weight percent copper tracer. An alternative method was required for obtaining tracer concentration data for the production facility runs, as the expected output tracer concentration would be less than 3 percent. Two methods were studied as means for obtaining the RTD information. The first involved an ultraviolet (UV) fluorescent tracer, consisting of granules coated with fluorescent paint. The second utilized the copper tracer mentioned previously and an Inductively Coupled Plasma Spectroscopy measurement technique.

The fluorescent tracer technique involved coating standard granules with a water-based fluorescent paint (Wildfire brilliant yellow, Wildfire Inc., Los Angeles). The paint was diluted at the ratio of 1 part paint to 2 parts water. The granules were then painted with the diluted paint at a ratio of 3-1/3 parts granules to 1 part paint. These ratios were chosen to minimize paint usage while still providing visible fluorescence under UV light. The fluorescent granules were then heated to 170°C to determine if the fluorescent coating would survive the temperature of the preheated granules. The coatings remained fluorescent after heating. Samples of decreasing tracer weight fraction were then examined to determine the minimum level for adequate detection. The minimum detection limit was thus found to be on the order of 0.5 weight percent.

The intended mechanism for measuring the fluorescent tracer concentration was to be the following. (1) Sample material would be spread evenly in a tray. (2a) An UV lamp would be used to irradiate the sample. (2b) At the same time a photograph of the sample would be taken. (3) The photograph would then be scanned into a computer. (4) Finally, the number of tracer particles in the image would then be counted using image analysis software. An advantage of this method was that it allowed a large volume of material to be rapidly examined. It was determined that the lamp emitted light in the visible range, when the initial photographs were found to have been overexposed. A special filter with a bandpass between 250 and 280 nm was added to the lamp, in order to eliminate lamp emission above the fluorescent tracer excitation wavelength of 265 nm. A picture of the lamp is provided in Figure 3.1. A photograph of the tray and lamp arrangement used for taking the photographs is shown in Figure 3.2. The camera was mounted to a vertical copy stand above the sample tray, and then fitted with an UV filter.

Each exposure was made over a period of time, with the room lights off, by indexing the lamp beam around the sample tray, in order to fully illuminate the granules.

Two RTD experiments using the tracer measurement technique described above, but with fluorescent granules replacing copper ones, were conducted in the laboratory rotary drum mixer. The fluorescent tracer was found to be visible in the output flow under UV light. Large amounts of fluorescent tracer were then generated by hand and shipped to the production facility. The fluorescent tracer burns off leaving no detectable residue when baked in the kiln, thus providing an additional benefit of the fluorescent tracer RTD measurement method.

Three runs were completed with fluorescent tracer at the production facility, one in each of three separate mixers. Samples of the output flow were taken every fifteen seconds after an initial two-minute interval. The material was then allowed to dry before being shipped to MIT.

An additional study provided the emission and absorption spectra of the fluorescent paint. A scanning spectrofluorometer (QM-1 Luminescence Spectrometer, Photon Technology International, Monmouth, NJ), made available by the Chemical Engineering Department at MIT, was used for this purpose.

The second method for measuring RTD at the production facility involved the same copper tracer as described in chapter two, used in the same manner as the fluorescent tracer described above, but with a new concentration measurement method. Copper tracer was added to two of the production mixers as described above, and samples were again taken every 15 seconds. The samples were then allowed to dry, and later every second sample was shipped to MIT. The samples were separately ground to a powder using a disc mill made available through the Department of Earth, Atmospheric and Planetary Sciences. A 20-gram fraction of each powdered sample was then taken and sent to the Recra LabNet laboratory in University Park, Illinois.

The Recra lab provided facilities for conducting Trace Inductively Coupled Plasma Atomic Emission Spectroscopy (ICPAES) measurements on copper concentration. The detection limit provided by ICP was 1.0 ppm. A calculation of peak copper concentration for a production run predicted a value on the order of 3 ppm. The ICAP procedure is as follows: each sample was first digested using the following procedure: (1) 2 grams of sample were measured out and (2) 10 mL of 1:1 nitric acid was added. (3) This was then heated to 95°C and refluxed for 15

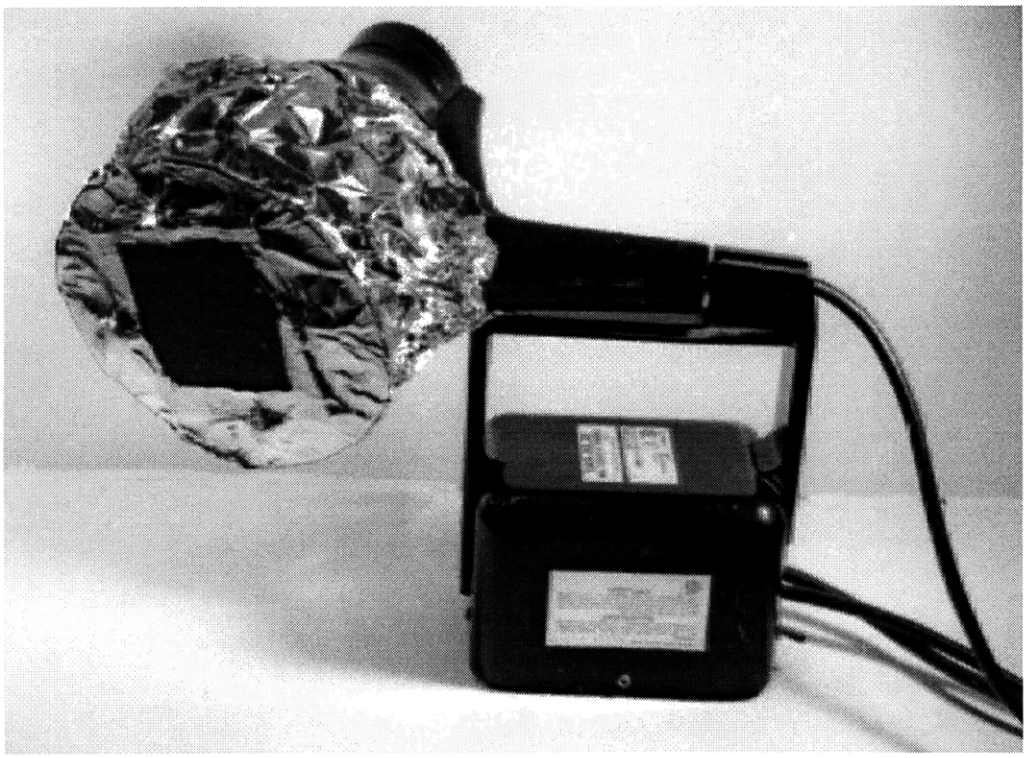

Figure 3.1 Fluorescent Lamp and UV Filter

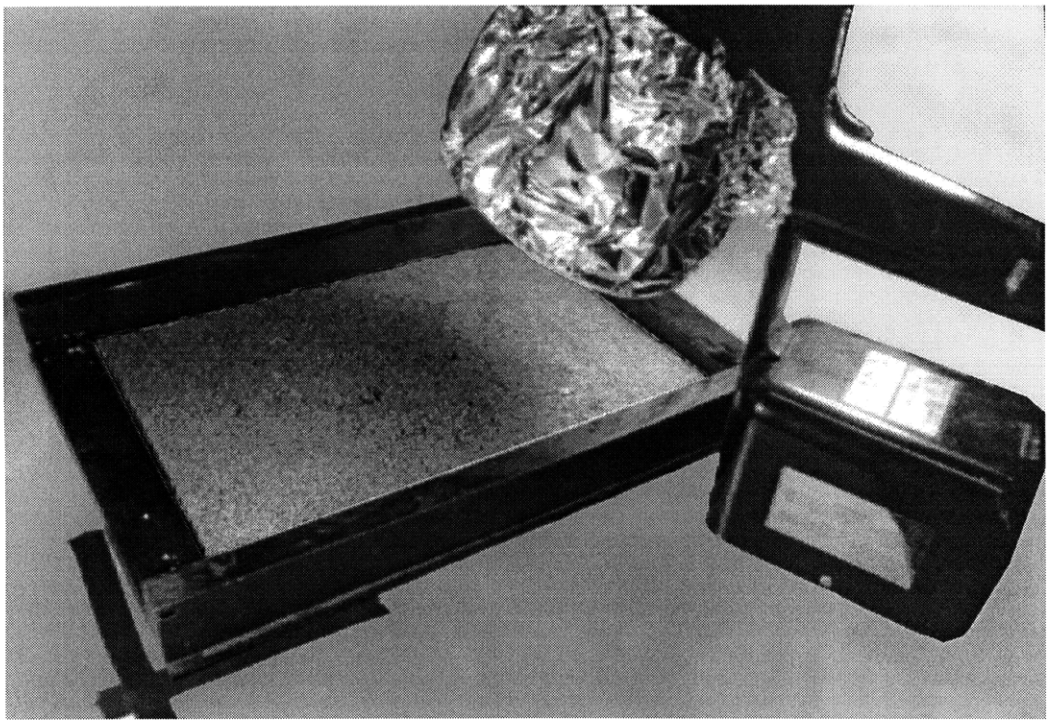

Figure 3.2 Fluorescent Tracer Photography Setup

minutes. (4) The sample was cooled, and then (5) 5 mL of concentrated nitric acid was added. (6) This was allowed to reflux for 30 minutes. (7) Steps 4, 5, and 6 were repeated, and the liquid was allowed to evaporate to 5 mL. (8) The sample was cooled and (9) 2 mL of water and 3 mL of 30% H_2O_2 were added. (10) The sample was heated and further H_2O_2 (up to a maximum of 10 mL) was added until the effervescence stopped. (11) 5 mL of concentrated HCL and 10 mL of water were added and the samples were allowed to reflux for 15 minutes. (12) the samples were cooled, diluted to 100 mL with water and filtered to remove the remaining particulates.

The ICP analysis device was calibrated using 3 mixed calibration standard solutions prior to testing the samples. The system was flushed using a calibration blank after each test. Thirty-seven samples were analyzed in this manner.

3.1.2 OBSERVATIONS

Initial laboratory results of the fluorescent tracer technique, in which fluorescent tracer granules were coated with slurry manually, seemed promising. It was later found that the coatings produced in the laboratory and production mixers were significantly better then those produced with the manual coating technique employed in the laboratory. The manual coating technique involved adding a measured amount of coating slurry to a measured amount of granules in a bowl, and then mixing with a spoon for a period of 5 minutes. The improved coatings in the laboratory and production mixers made it difficult to visually distinguish between the tracer and bulk material under UV light. The resulting photographs did not have much contrast between the tracer and the bulk material. The computer analysis software could not make the distinction, and therefore could not be used to count the tracer granules. Multiple exposures were made at different apertures and shutter speeds in order to determine the optimal exposure parameters. None of the exposures had enough contrast to make the UV fluorescent tracer a viable measurement technique. An example scan is shown in Figure 3.3. The lack of contrast was partially due to the presence of titanium dioxide in the coating material, which also fluoresced under UV light. A diagram of a system that would allow improved distinction between the tracer and the background granule bed, is shown in Figure 3.4. A second filter, which would only allow the wavelengths specific to the fluorescent paint to reach the film, would have been placed on the camera lens. The emission spectra of the fluorescent tracer, measured with a spectrofluorometer, is shown in Figure 3.5.

An additional complication with the fluorescent tracer tests, which was not apparent until samples were made, was that the base rock used at the production facility had mineral constituents which also fluoresced under UV light. Only the copper-ICP RTD technique was used for measuring flow behavior for the production scale mixers, due to the many complications involved with the fluorescent tracer RTD method.

The ICP analysis method was very successful for measuring the residence time of copper tracer throughout the production plant mixers. A background reading of copper was approximately 1-3 ppm. The peaks had values of over 1000 ppm copper, and were thus easily distinguished.

Mixers A and B had different flight arrangements. The slurry in mixer A had a significantly higher concentration of sodium silicate and therefore the granule-slurry mass had a higher viscosity. Figure 3.6 is a comparison of the tracer RTD measurements for mixers A and B. The mean residence time was 30 percent greater in mixer A than in mixer B. Future viscosity measurements of the mixer A and B slurries would allow these results to be compared with the yield stress and RTD experiments discussed in chapter 2.

The parameters used for the production RTD experiments and the key results are listed in Table 3.1.

Table 3.1 Parameters and Results for Production Facility RTD Experiments

Run	Particle Size Range (mm)*	Initial Tracer Observed (seconds)	Peak Copper Concentration (seconds)	Estimated Mean Residence Time (seconds)	Estimated Mean Flow Rate (m/s)
P1	Fullgrade	270	330	344	2.30×10^{-2}
P3	Fullgrade	195	255	263	3.01×10^{-2}
FGS	Fullgrade	330	510	529	5.56×10^{-3}

* Fullgrade description is provided in Figure 2.3.

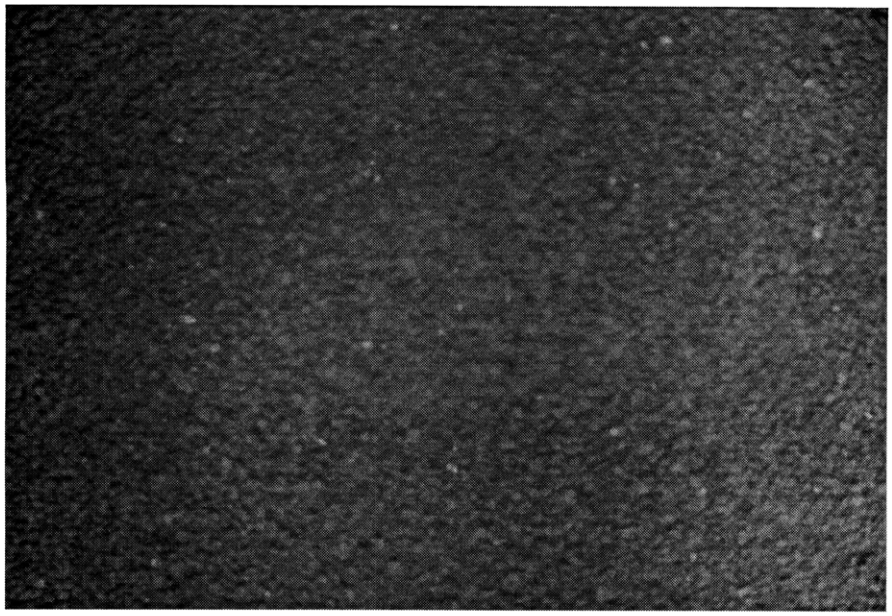

Figure 3.3 Scan of a Fluorescent Tracer Run Sample Photograph. Fluorescent Granules are Shown as Light Spots

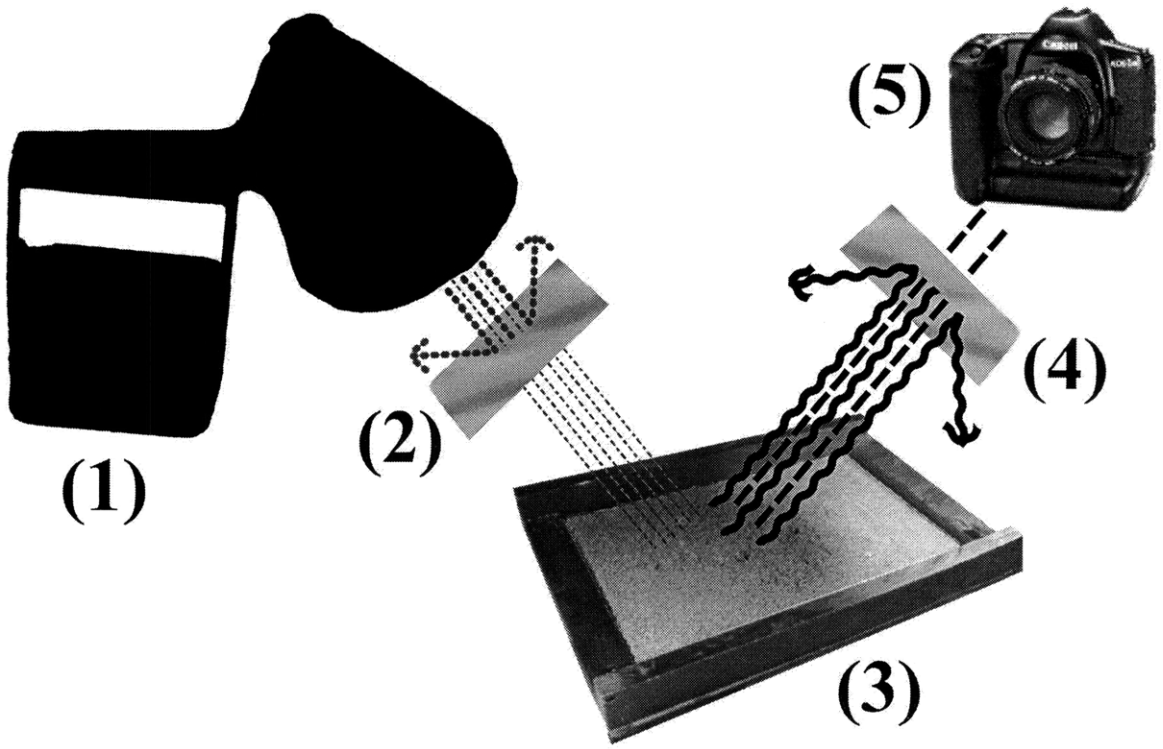

Figure 3.4 Diagram of an Improved Filter Arrangement

(1) UV lamp, (2) UV Bandpass filter, (3) Sample Tray, (4) Bandpass filter centered around fluorescent tracer emission wavelength (655 nm), (5) Camera

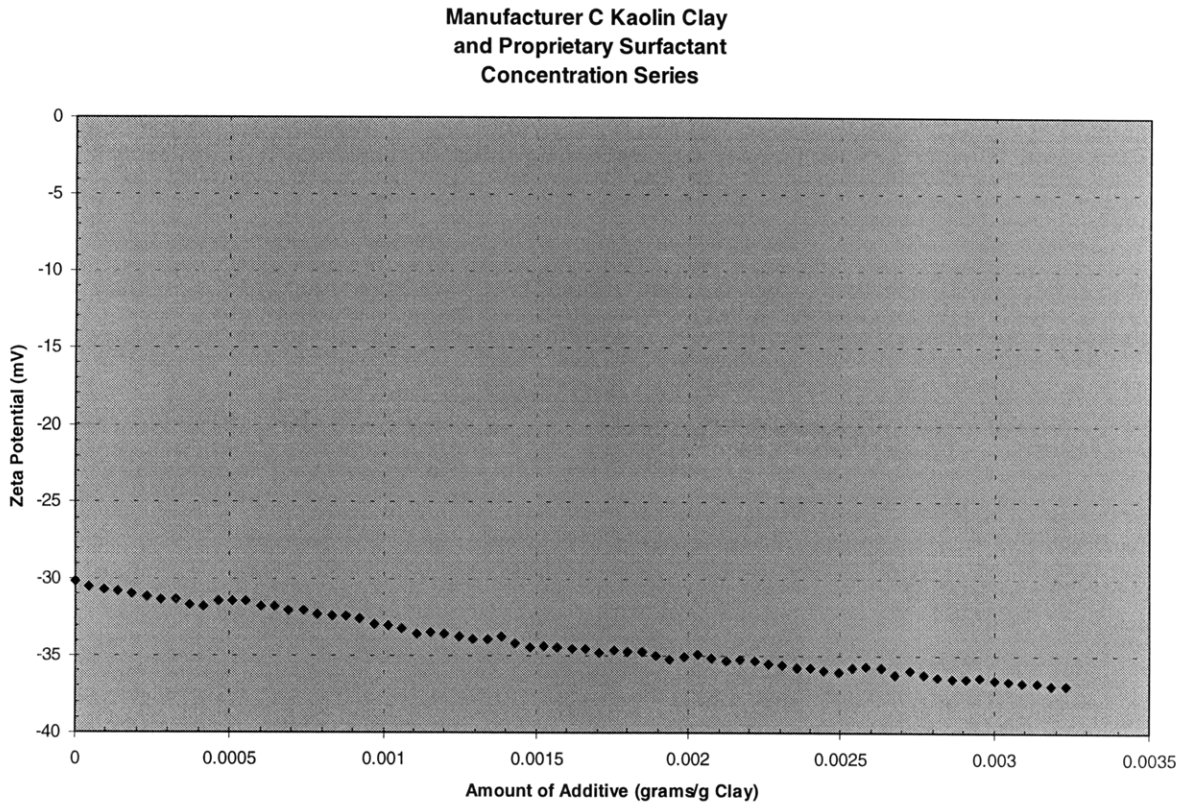

Figure 3.5 Fluorescent Tracer Emission Spectra

The slurry used in mixer A was similar to that used in the laboratory mixer RTD experiments CS, MS, and FS. The latter experiments were conducted with a slightly thinned slurry to aid visual identification. The laboratory experiments were completed with separate coarse, midgrade and fine tracers whereas the production experiments utilized a fullgrade tracer. The results of the three separate laboratory mixer runs have been combined in the following manner, in order to generate a composite RTD curve, which will approximate the results of a laboratory RTD experiment with fullgrade tracer. The results for each laboratory RTD experiment were normalized to their respective peak values, the three respective measurements for each corresponding unit of time were summed, and the resulting curve was normalized to the peak value. The combination of the three runs, which was labeled FGS, is illustrated in Figure 3.7. The FGS peak had a mean residence time of approximately 529 seconds. Had the slurry not been thinned, the resulting peak in the laboratory mixer would have occurred even later.

Figure 3.8 provides a comparison of the composite laboratory fullgrade RTD and the RTD results for production mixer A. The laboratory mixer MRT is 54% later than that of the production mixer.

The tracer residence time distributions were significantly more narrow in the production plant than in the pilot mixer. The breadth of the residence time distribution for production mixer A was 165 seconds, measured between the initial normalized copper concentration of 0.25 and the final concentration of 0.25. The same range gives a breadth of 330 seconds in the laboratory mixer. Thus material flows through the production mixer with much less intermixing then in the laboratory mixer.

3.1.3 DISCUSSION

The flight designs incorporated into the production mixers are different then that of the laboratory mixer, making direct comparison between the residence times less significant. Other characteristics including material flow rate, mixer diameter, mixer angle, and input flow behavior may be different between the mixers. The calculated flow rates of the production and pilot mixers are listed in Table 3.1. Currently material flows through the production mixer at a rate four times faster than in the pilot plant. Material spends less time in the mixing zone of the production mixer. The rotational speed of the pilot mixer needs to be decreased and the inclination of the mixer increased in order to obtain mixing times equivalent to that in the

production mixers. A series of RTD experiments on the laboratory mixer, over varying rotational speeds, would be necessary to determine the proper rotational speed. Ideally the flow rate and volumetric holdup would be proportionately scaled between the laboratory mixer and the production facility.

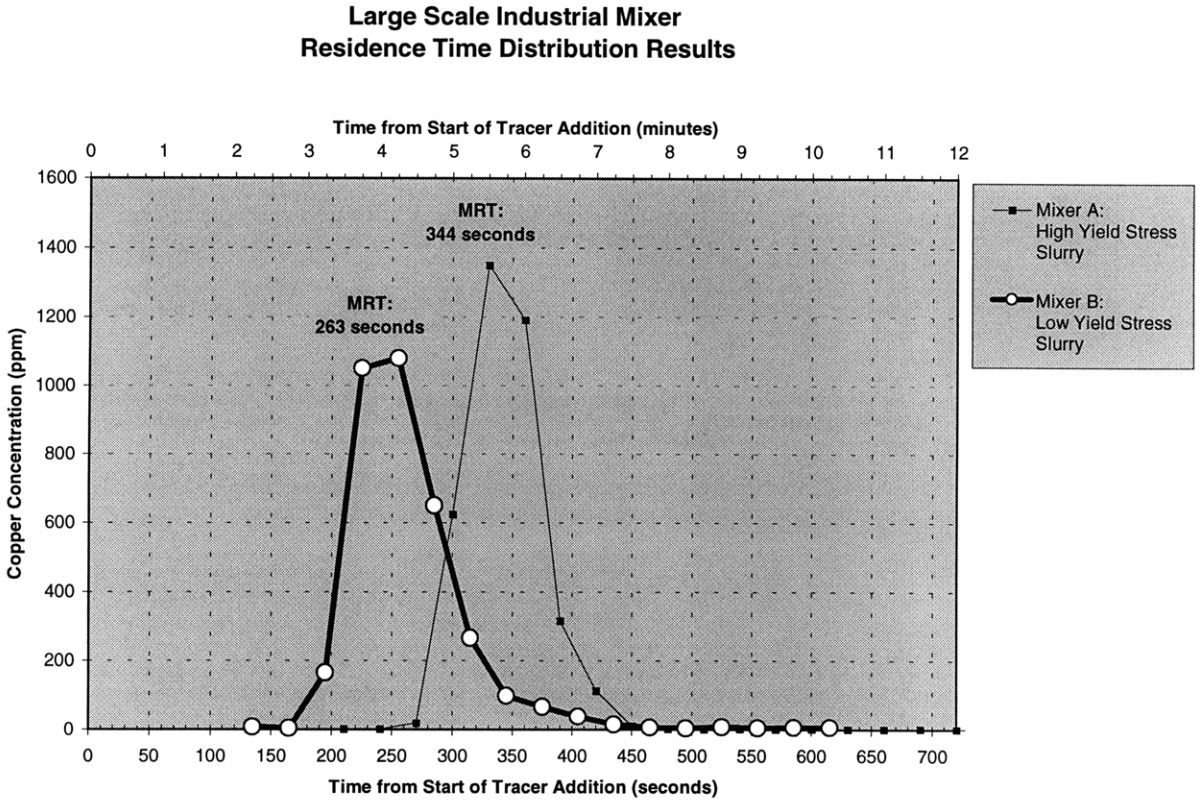

Figure 3.6 Production Mixer Residence Time Distributions

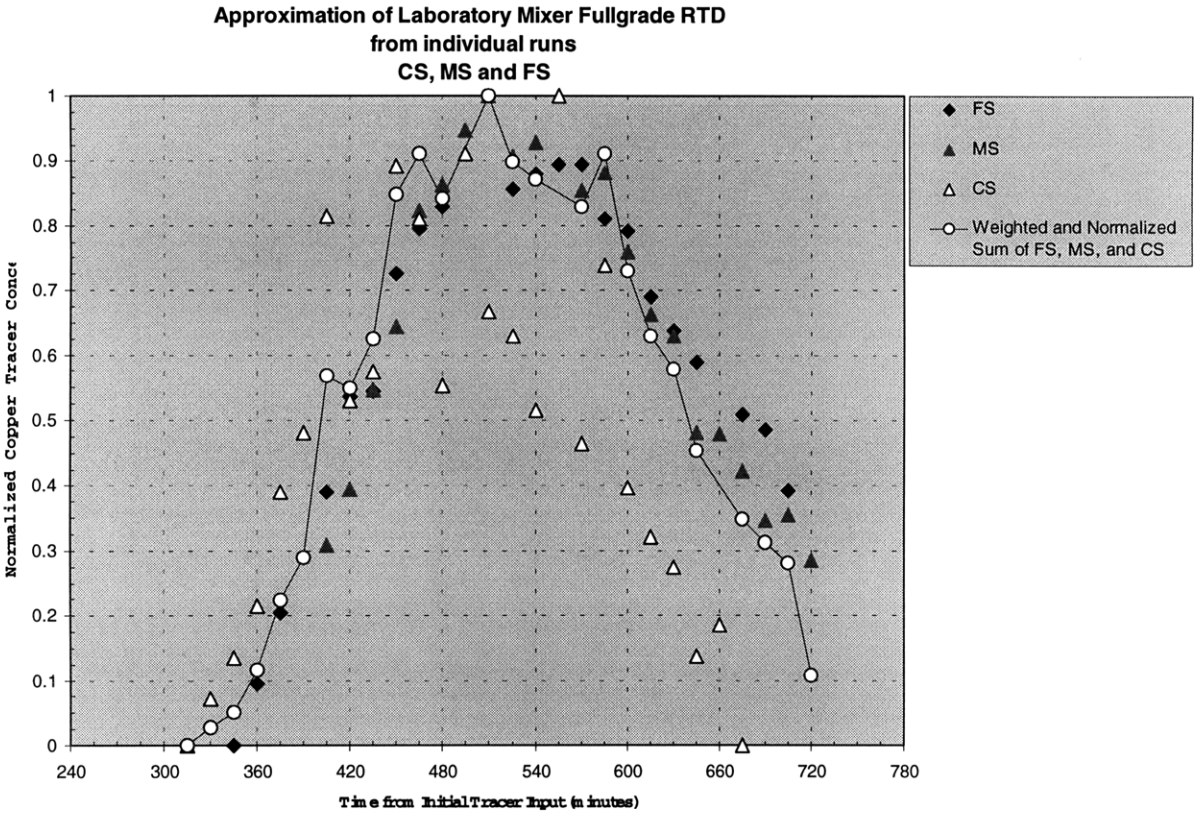

Figure 3.7 Approximation of a Fullgrade Laboratory RTD for Comparison with Production Scale RTD

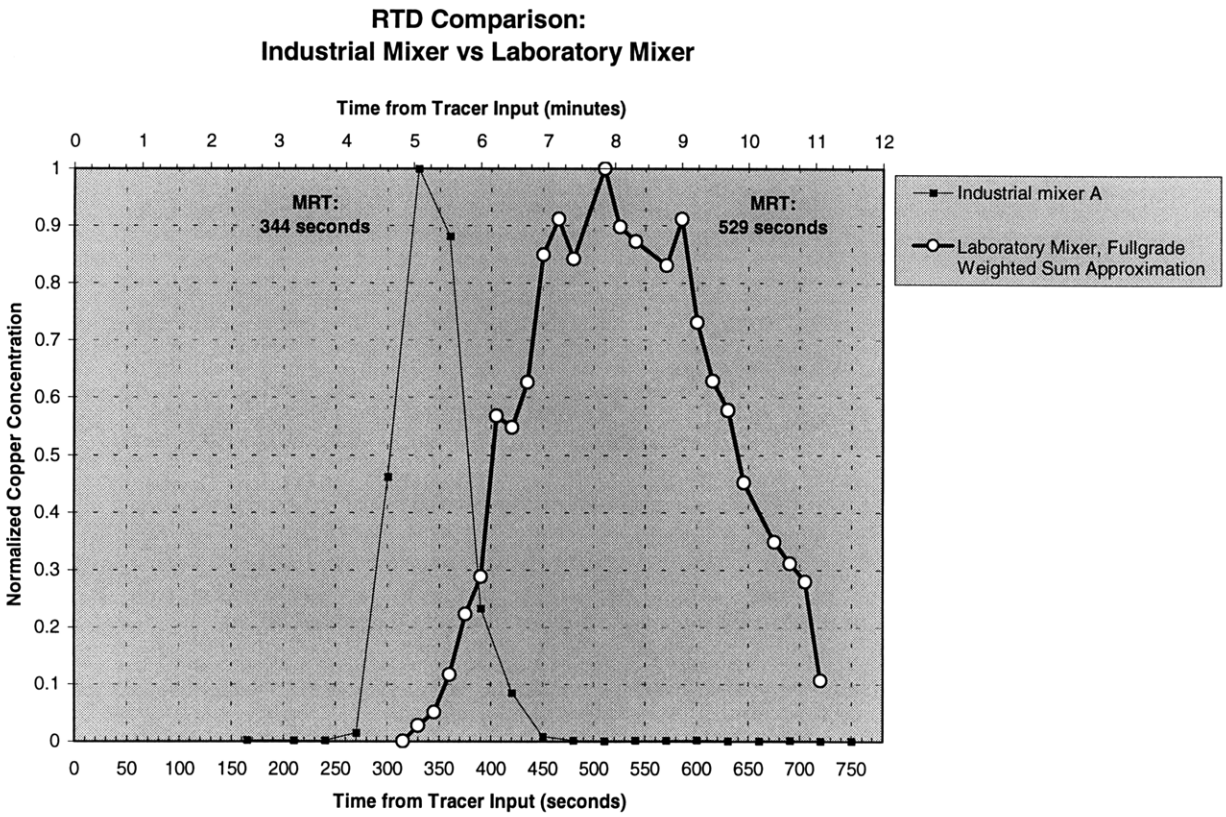

Figure 3.8 Comparison between Laboratory and Production Fullgrade RTD

CHAPTER 4
COATING CHARACTERIZATION AND DISPERSION OF PIGMENTS/EXTENDERS

It was immediately apparent that this industrial coating process does not produce uniform coatings, when examined using an optical microscope. A series of experiments were conducted in order to characterize the granule coatings and pigment dispersion techniques. These experiments included an examination of the surface coating, and particle size and zeta potential analysis of the pigments and extenders used in the coating process. The intent of these experiments was to provide a baseline for judging future coating process improvements and also a means for optimizing coating spreading and pigment utilization through improved pigment dispersion.

4.1 COATING EXAMINATION

4.1.1 EXPERIMENTAL PROCEDURES

Samples of granules coated in an industrial facility were screened in order to separate granules by particle size. The size ranges obtained in this manner included: >1.18 mm, between 1.18 and 0.85 mm, and less then 0.85 mm. The granules were then mounted in epoxy and cross-sectioned. The cross-sectioned samples were examined under an optical microscope and coating thickness measurements were obtained for a number of particles using a ruled eyepiece.

Samples of the same granules were placed on sample stages and sputter coated with gold. Pigment particles contained within the surface coating, found using the SEM, were analyzed in situ with an Oxford energy dispersive spectroscopy (EDS) system. It was not possible to distinguish between those areas of the granule surface coated with slurry and those left uncoated using the SEM.

4.1.2 OBSERVATIONS

Initial observations of the granule coating under an optical microscope revealed highly non-uniform coating coverage. A picture of a coated granule is shown in Figure 4.1. Numerous agglomerated particles were found on the surface of the granules. Using EDS it was found that these agglomerates consisted of clay and titanium dioxide. An example of a titanium dioxide agglomerate is shown in Figure 4.2. The corresponding EDS scan result is provided in Figure 4.3. A SEM photograph of a clay agglomerate is shown in Figure 4.4. The corresponding EDS scan is shown in Figure 4.5.

4.1.3 DISCUSSION

The non-uniform surface coating is a function of both the coating process and the quality of the pigment dispersion. The existence of agglomerated particles in the coating slurry proves that the pigments are not well dispersed, and therefore pigment utilization has not been optimized. Further experiments characterizing pigment-dispersing agents will be conducted in the following sections. An additional benefit of improving the dispersion of slurry constituents would be a small decrease in slurry viscosity. A decrease in slurry viscosity is accompanied by an increase in granule bed penetration and granule coating coverage.[20] Improving the dispersion of pigments should thus provide significant improvement in coating uniformity and coverage.

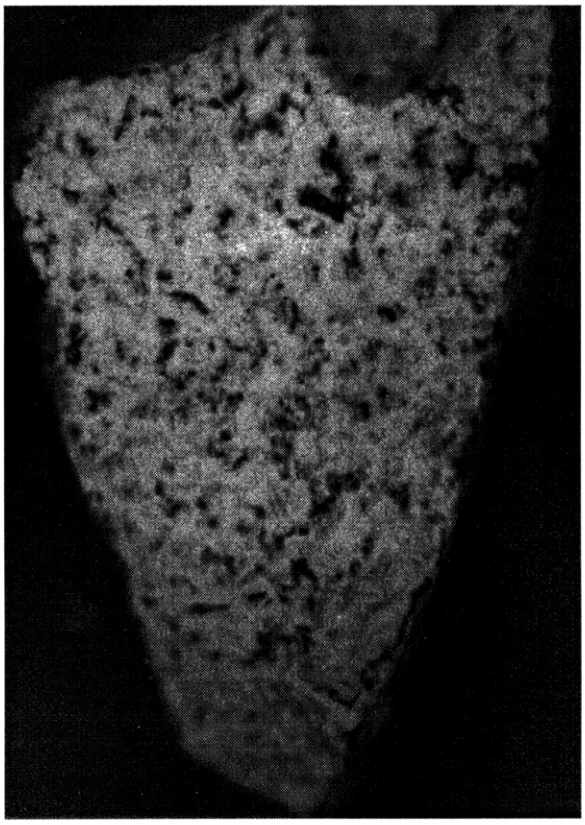

Figure 4.1 Optical Micrograph of a Coated Granule

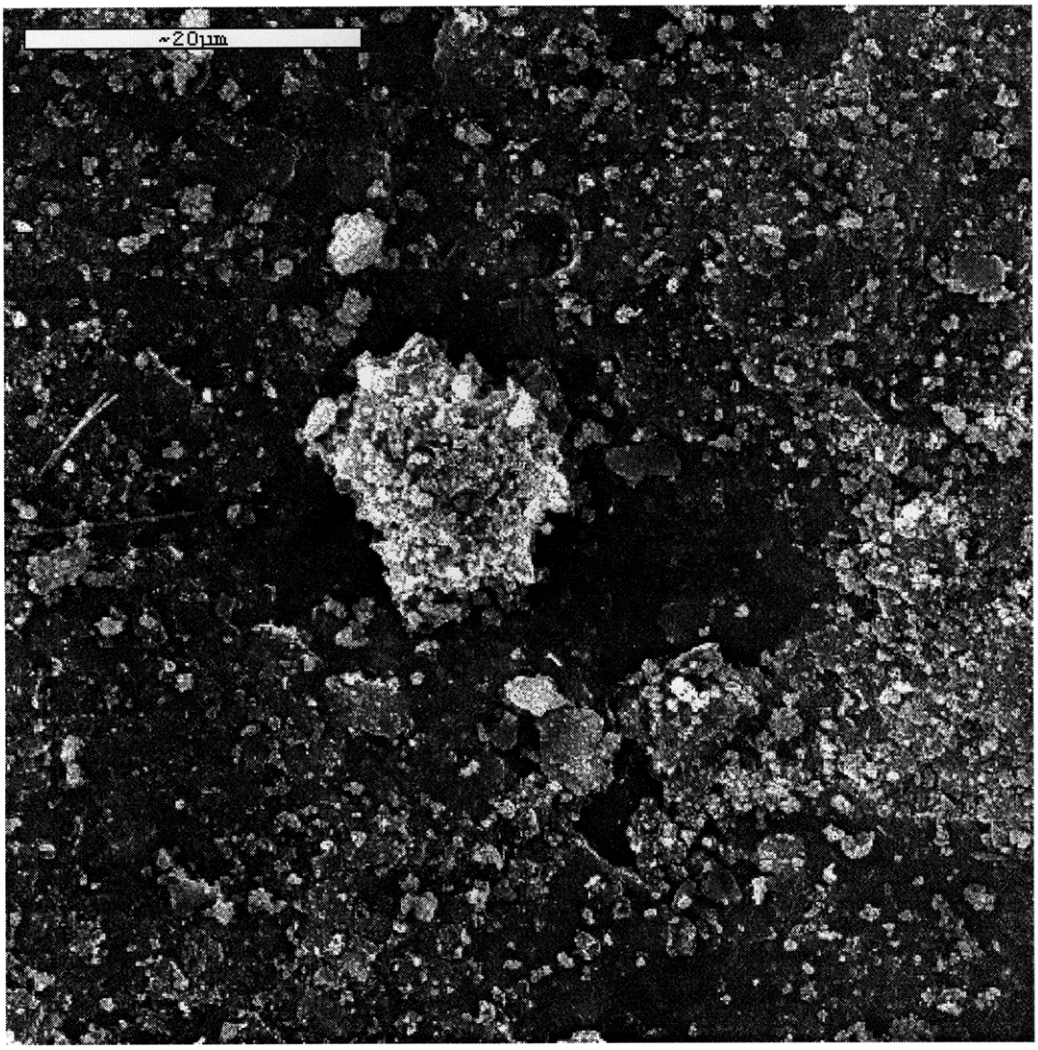

Figure 4.2 SEM Photograph of Titanium Dioxide Agglomerate

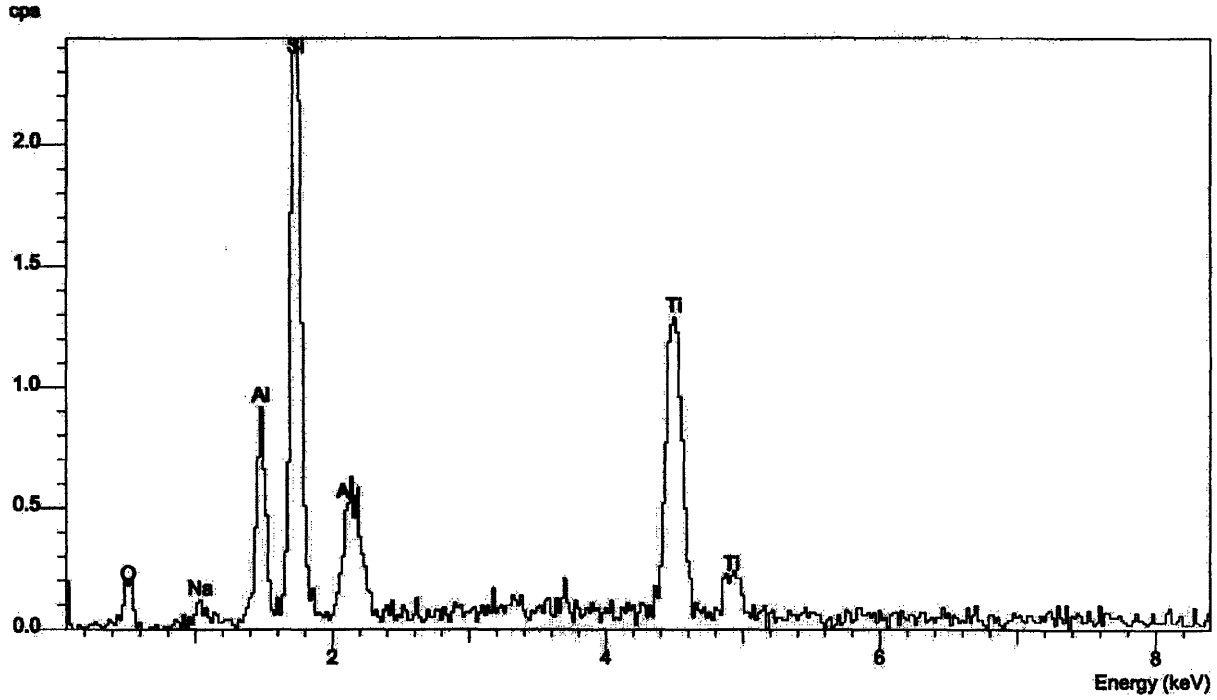

Figure 4.3 EDS Scan of Titanium Dioxide Agglomerate

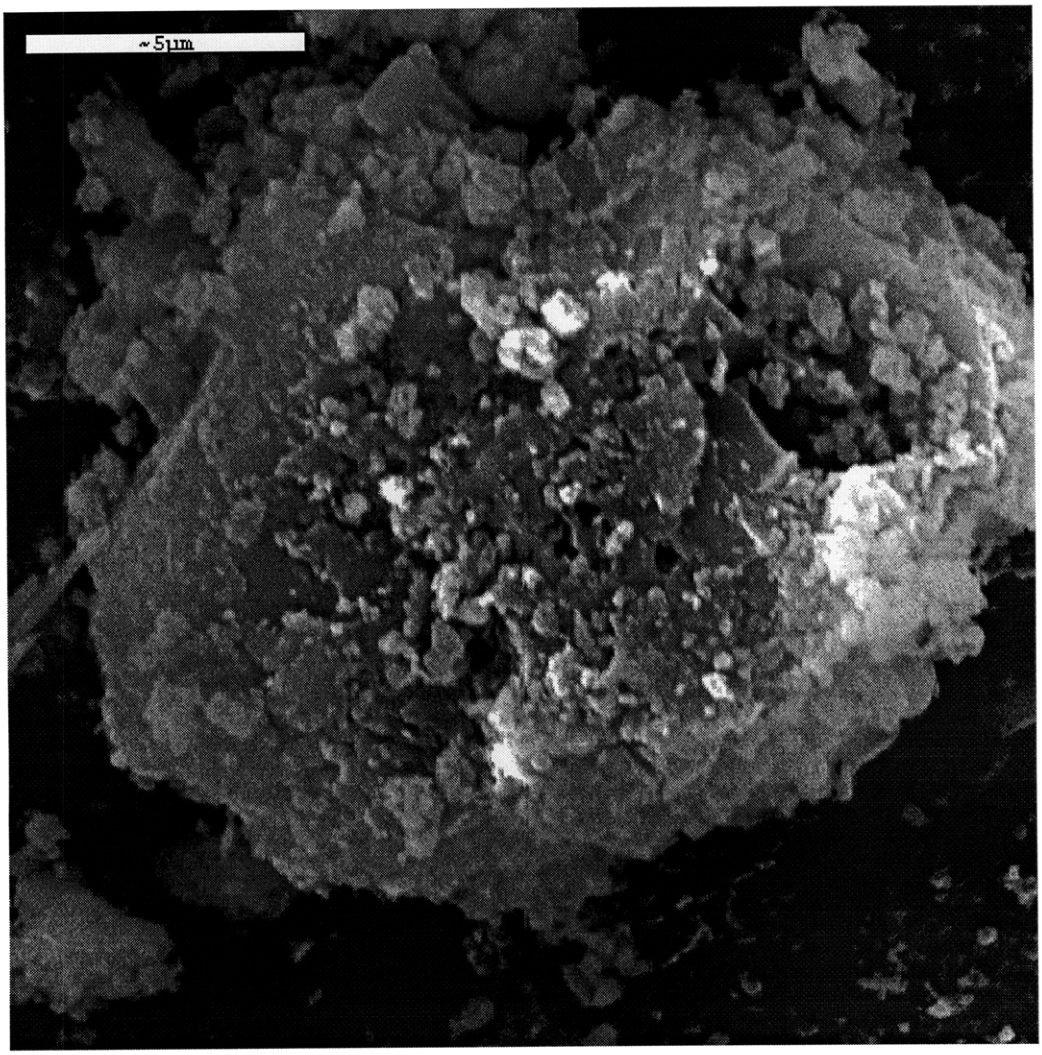

Figure 4.4 SEM Photograph of Clay Agglomerate

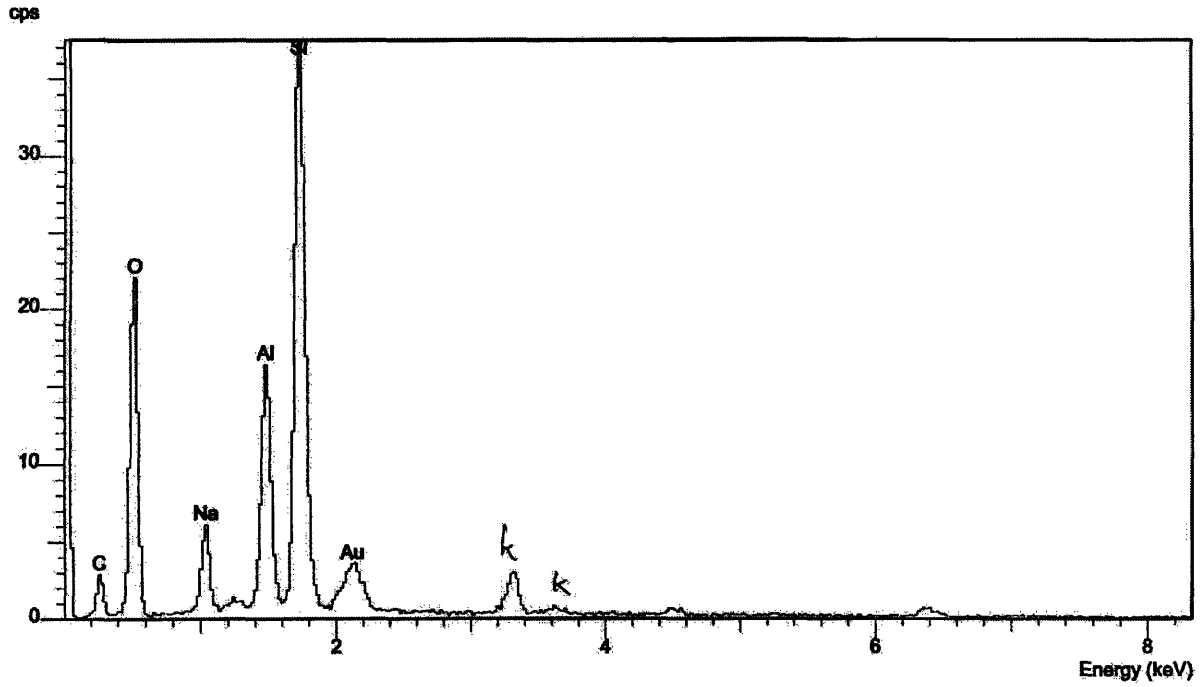

Figure 4.5 EDS Scan of Clay Agglomerate

4.2 PIGMENT/EXTENDER PARTICLE SIZE MEASUREMENTS

4.2.1 EXPERIMENTAL PROCEDURES

Experiments were conducted to determine the particle size distribution and mean particle size (Horiba CAPA particle analyzer, Irvine, CA). Tests were run on titanium dioxide produced by two manufacturers, which I will call A and B, and a kaolin clay, from mnaufacturer C. For each test the material manufacturer's published specific gravity was used to determine the material density. The powders were dispersed in deionized water. The viscosity of the water was calculated using the temperature measured at the time of the run. The formulation used for each run is provided in Table 4.1.

Table 4.1 Particle Size Analysis Parameters

Run	Deionized Water (g)	Acumer 9400 Dispersant (5% solution) (g)	Dispersed Particles (g)
Titanium Dioxide A#1	44.8	0.2	5.0
Titanium Dioxide A#2	45.0	0.2	5.0
Kaolin Clay C#1	45.0	0.2	5.0
Kaolin Clay C#2	45.0	0.2	5.0
Titanium Dioxide B#1	45.0	0.2	5.0
Titanium Dioxide B#2	45.0	0.2	5.0

The formulations were generated in the following manner: (1) Rohm and Haas Acumer 9400 dispersant was added to the deionized water, (2) The solution was mixed for 1 minute with a stirring rod prior to (3) adding the particulate material. The dispersions were then (4) thoroughly mixed for one minute using a Heat Systems-Ultrasonics Inc. Sonicator-Cell Disruptor (model w-220F with a 1-cm diameter ultrasonic head).

A single drop of the particulate solution was added with a pipet to the 10 mm sample holders in order to produce a pigment concentration appropriate for the Horiba detector. The sample holders were then filled completely with deionized water. Two reference cells of deionized water were used as blanks for calibration prior to running the particulate samples. The parameters used for each run are included in Table 4.2.

Table 4.2 List of Horiba Parameters

Run	Dispersant Viscosity (cP)	Dispersant Density (g/cc)	Sample Density (g/cc)	rpm	Time (minutes: seconds)
Titanium Dioxide A#1	0.94	1.0	4.0	3000	12:42
Titanium Dioxide A#2	0.94	1.0	4.0	7000	9:15
Kaolin Clay C#1	0.90	1.0	2.6	700	4:11
Kaolin Clay C#2	0.90	1.0	2.6	3000	5:41
Titanium Dioxide B#1	0.90	1.0	4.2	3000	11:23
Titanium Dioxide B#2	0.90	1.0	4.2	3000	11:23

4.2.2 OBSERVATIONS

Runs Titanium Dioxide A#1 and Kaolin Clay C#1 were broad scans of particle size used to determine the approximate range of diameters for those materials. These initial tests did not, however, provide a reliable measure of the median particle diameter. Their results will not be included. The results of the subsequent experiments are shown in Figures 4.6 – 4.8. The median particle diameters are listed in Table 4.3.

Table 4.3 Median Particle Size Results

Run	Median Particle Size (μm)
Titanium Dioxide A#2	0.27
Kaolin Clay C#2	0.34
Titanium Dioxide B#1	0.22
Titanium Dioxide B#2	0.19

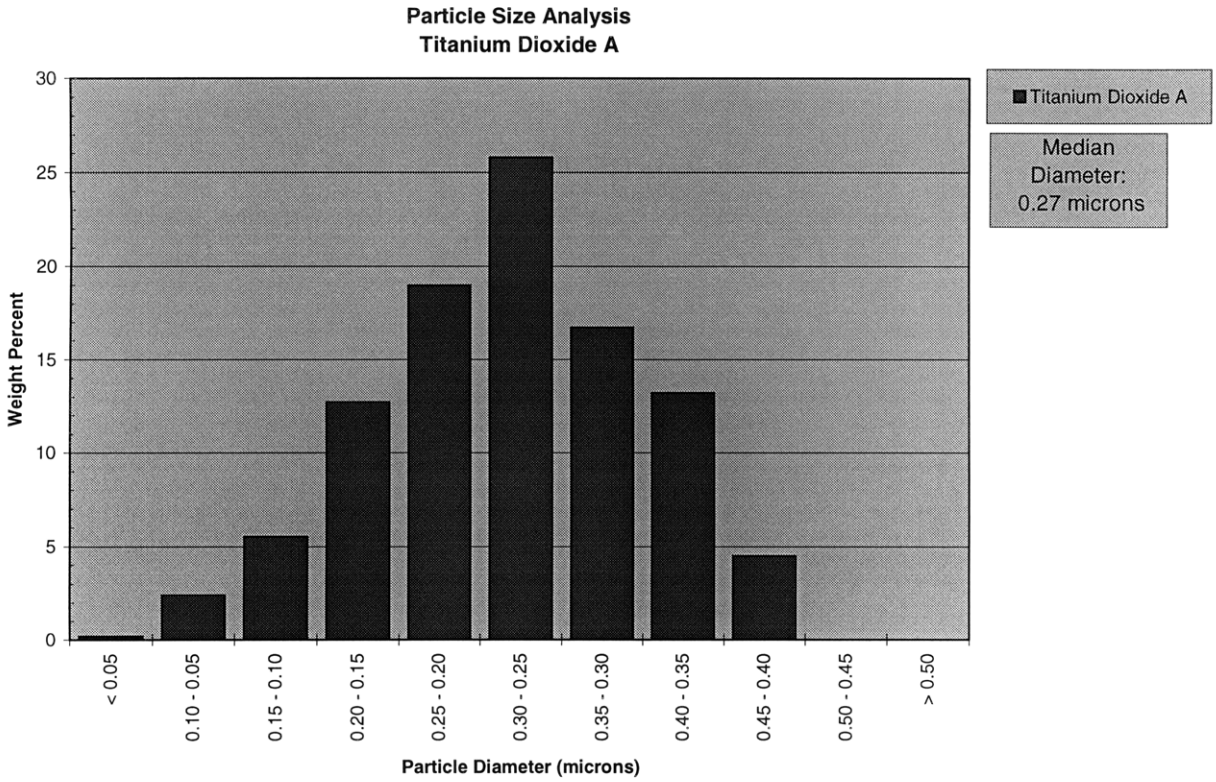

Figure 4.6 Manufacturer A Titanium Dioxide Particle Size Distribution

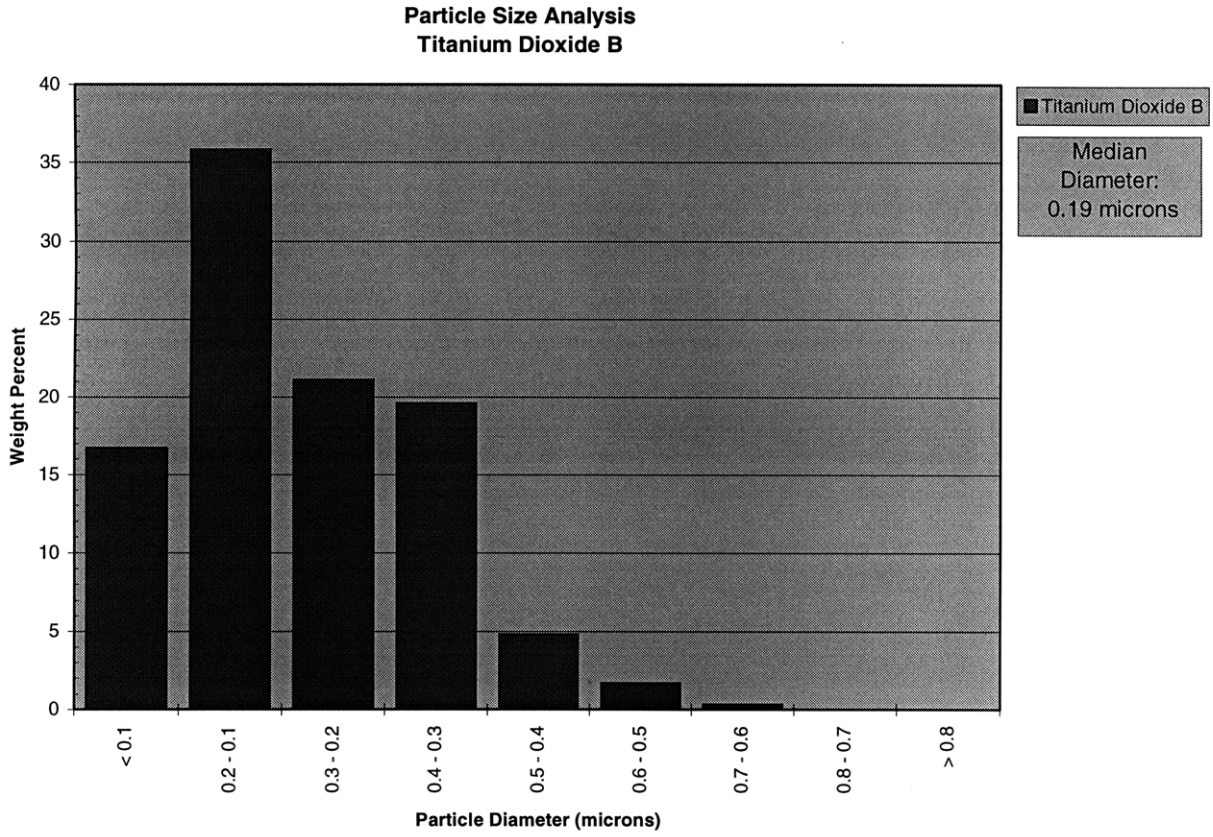

Figure 4.7 Manufacturer B Titanium Dioxide Particle Size Distribution

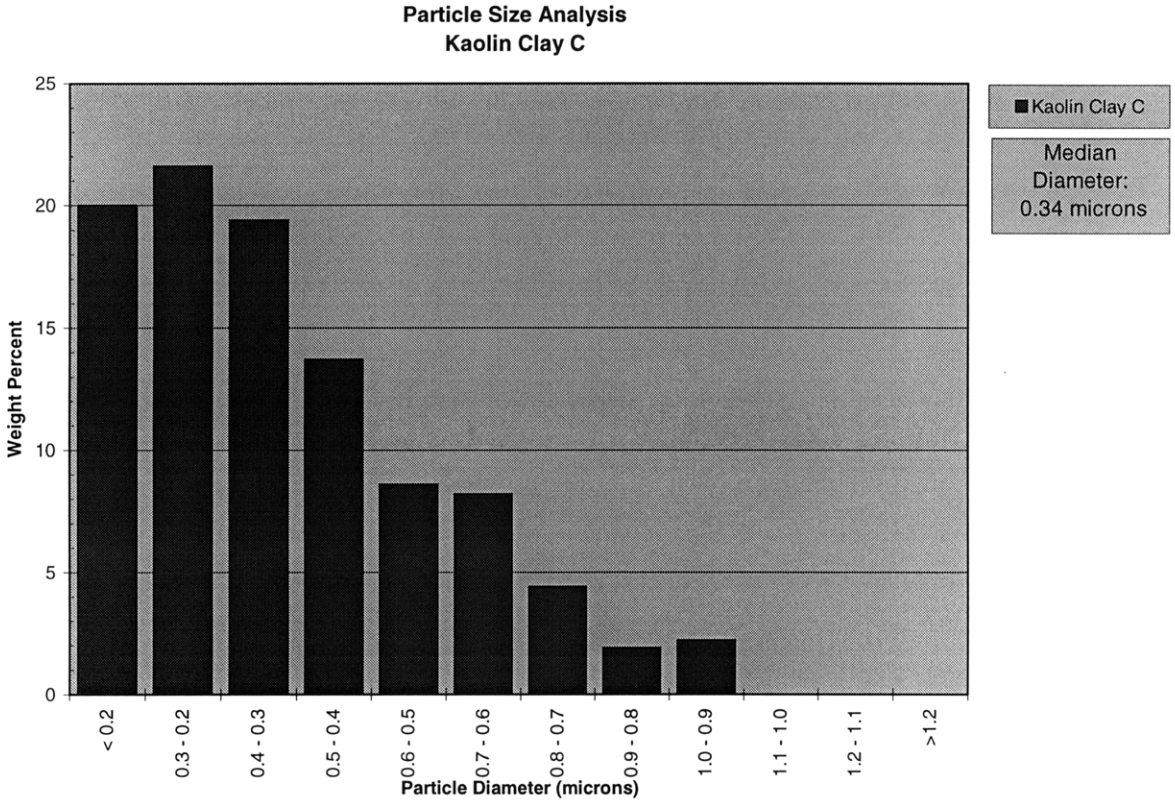

Figure 4.8 Manufacturer C Clay Particle Size Distribution

4.2.3 DISCUSSION

The particle size measurements were a required step for measuring the surface properties of the dispersed particulates. The results are comparable to other reported data.[37] These subsequent experiments will be examined in the following section.

4.3 ZETA POTENTIAL MEASUREMENTS

An Electrokinetic Sonic Amplitude (ESA) measurement system (Matec ESA-8000, Matec Applied Sciences, Northborough, MA) was used to conduct a series of measurements on a variety of dispersions relevant to the granule coating process. The goal of these experiments was to examine how the zeta potentials of the coating slurry constituents were modified in the presence of varying levels of dispersants and surfactants.[38] The appropriate concentration of dispersing agent required for dispersion of each pigment could be identified through this technique. Aggregates of pigment particles will remain in the solution without proper dispersion. A coating made with slurry containing agglomerated pigment particles will exhibit variation in pigment concentration, and therefore non-uniform color. A thicker coating would be required with such a slurry in order to produce uniformly colored coatings. An uniformly dispersed slurry, with no agglomeration of pigments, will produce consistently colored coatings with significantly less coating thickness. The uniformity of the pigment dispersion is a function both of the mixing device used and the dispersing agents. It was intended that with these experiments, an optimal concentration of dispersing agent would be found, which would improve pigment dispersion and thereby coating uniformity.

4.3.1 EXPERIMENTAL PROCEDURES

A Matec Applied Sciences ESA-8000 ESA system was used to measure zeta potential. Titanium dioxide from manufacturer B, and kaolin clay, from manufacturer C were studied. The dispersants tested included a proprietary surfactant from Manufacturer D, Blancol N from Rhône-Poulenc, and Acumer 9400 from Rohm and Haas.

Initial potentiometric-titration experiments studied the effect of increasing pH on zeta potential. Approximately 1 g of 0.1 M nitric acid was added to the ESA-8000 test cell, in each experiment. Deionized water was then added to generate a total of 198 g of solution. The 2 ml of pigment was then added to the cell and mixed with a stirring rod. The nitric acid was added in

order to produce an initial pH of approximately 4.0. The dispersion was then thoroughly mixed with an ultrasonic mixing system (Heat Systems-Ultrasonics Inc. Sonicator-Cell Disrupter (model w-220F) with a 1-cm diameter ultrasonic head) for 5 minutes. The test cell was then mounted in the ESA-8000 and continued to mix with an electric mixer. Finally, the dispersion was cooled for 15 minutes with a water jacket to 25°C. An initial reading of the pH, temperature, zeta potential, and phase angle was measured prior to conducting the potentiometric-titration. Each titration was run between pH 4 and pH 10 using 0.1 molar nitric acid and 0.1 M potassium hydroxide. The pH of a standard white coating slurry was also measured at this time using the pH electrode and reference electrode from the ESA-8000 system. The pH was found to be 12.66

The potentiometric-titration runs were followed by a sequence of concentration-series measurements. In each case, 250 mL of dilute dispersing agent was generated. The formulations for each dispersing agent are listed in Table 4.4.

Table 4.4 Concentration Series Dispersing Agent Formulations

Dispersing Agent	Deionized water (ml)	Dispersing agent (g)
Surfactant D	349.43	0.42 (14 wt. % solution)
Blancol N	348.30	1.12
Acumer 9400	349.26	0.99

A buffer solution with a pH of approximately 11.7 pH was generated by adding 12.0 g of Tetra-n-butyl ammonium hydroxide to 1188 mL of deionized water, prior to running the concentration series experiments. For each experiment, 198 ml of buffer solution was added to the ESA-8000 test cell. 2 ml of pigment was added to the buffer solution, and then the solution was mixed with a stirring rod. The suspension was then thoroughly mixed for 5 minutes with an ultrasonic mixing system. The test cell was then mounted in the ESA-8000 and the electric mixer was turned on. Finally, the dispersion was cooled for approximately 15 minutes with a water jacket. Initial readings of pH, temperature, zeta potential and phase angle were taken prior to conducting the concentration series experiment. The parameters for each concentration series experiment are provided in Table 4.5. In each case the diluted dispersant was added in discrete amounts

(described in the table below) and the suspension was allowed to equilibrate for 25 seconds prior to measurement of the zeta potential.

Table 4.5 Concentration Series Parameters

Pigment	Dispersant	Dispersant addition rate (g/25 seconds)	Maximum dispersant concentration (g)
TiO_2 B	Surfactant D	0.00024	0.0168
TiO_2 B	Acumer 9400	0.0012	0.084
TiO_2 B	Blancol N	0.0032	0.224
Kaolin Clay C	Surfactant D	0.00024	0.0168
Kaolin Clay C	Acumer 9400	0.0012	0.084
Kaolin Clay C	Blancol N	0.0032	0.224

4.4.2 OBSERVATIONS

Figure 4.9 is a graph of the potentiometric titration of titanium dioxide B. The PZC occurred at a pH of approximately 6.9, which is comparable with other published results. [39]

The results of the Kaolin clay potentiometric titration are shown in Figure 4.10. Over the range of pH from 4 to 10, there is no PZC. The zeta potential is decreasing with increasing pH.

Figure 4.11 shows the results of the concentration series experiment with titanium dioxide B and Surfactant D. The initial zeta potential at zero polymer concentration and pH 11.7 was –44 mV. A zeta potential of approximately –90 mV would seem appropriate for this combination of material and pH when extrapolated from the potentiometric titration results. The zeta potential was reduced due to the high electrolyte concentration necessary to create a pH of 11.7. Tetra-n-butyl ammonium hydroxide was chosen in order to minimize the electrolyte concentration necessary to achieve this pH.[40] The zeta potential decreased slowly with increasing concentration of Surfactant D. Figures 4.12-16 show the results of the concentration series experiments with titanium dioxide B and kaolin clay C using Surfactant D, Rhodocal N, and Acumer 9400 additives. In all cases the absolute values of the zeta potentials were diminished due to the concentration of electrolyte. The zeta potentials all decreased slowly with increasing concentration of additive.

These results are not conclusive as to the benefit provided by these surfactants/dispersants. Further experiments measuring the change in slurry viscosity with increasing surfactant concentration would be necessary to determine if there is indeed a benefit to their addition. A significant decrease in viscosity would result if the surfactants were effective.

4.4.3 DISCUSSION

Flocculation is the term given for the aggregation of particles in colloidal suspensions. Flocculation of colloidal particles is caused when their repulsive forces are minimized, due to surface charge, hydration effects, electrolyte concentration, or other surface modifiers thereby increasing the likelihood of particle collisions.[22] Flocculation occurs rapidly when the zeta potentials of the constituent particles are near the point of zero charge. It is crucial to have all of the colloidal particles share the same polarity and to maximize their repulsive forces, in order to improve dispersion and reduce the rate of flocculation. The intention of each concentration series experiment was to determine the dispersant concentration at which the absolute value of the zeta potential was maximized. From these experiments it is apparent that none of the tested dispersants/surfactants caused dramatic increases in the absolute value of the zeta potential.

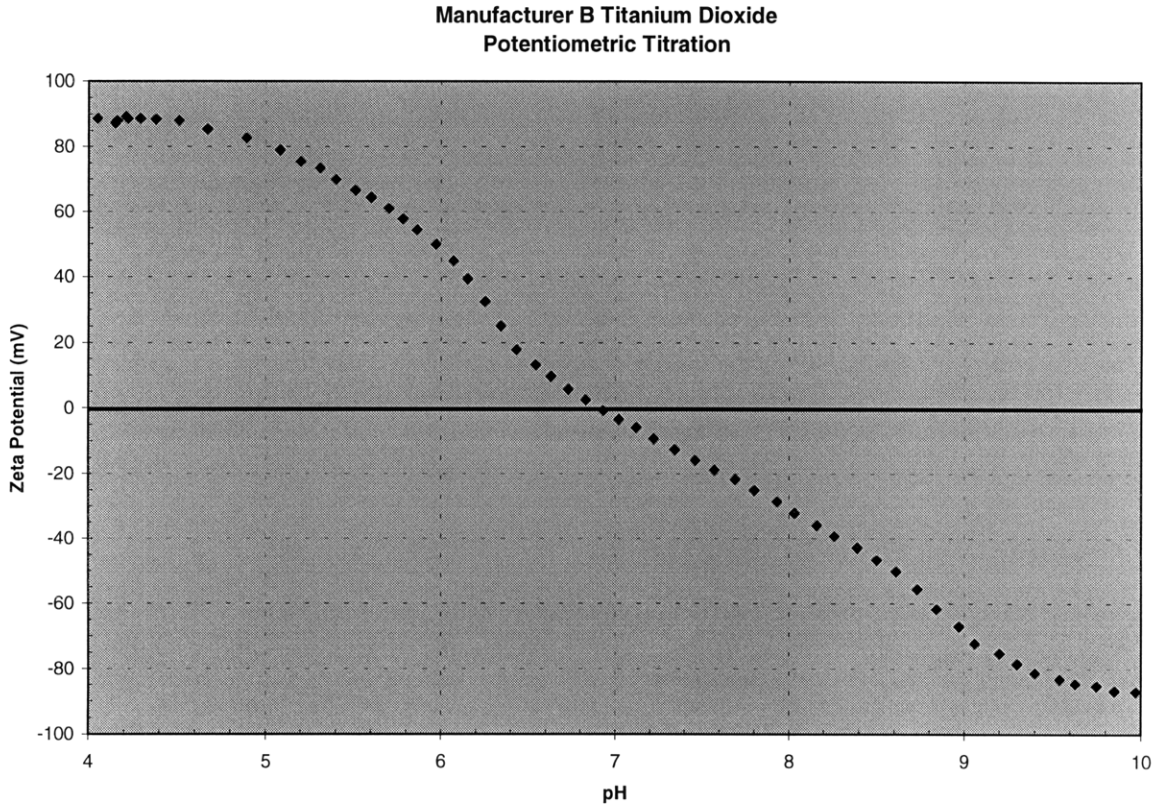

Figure 4.9 Potentiometric Titration of Manufacturer B Titanium Dioxide

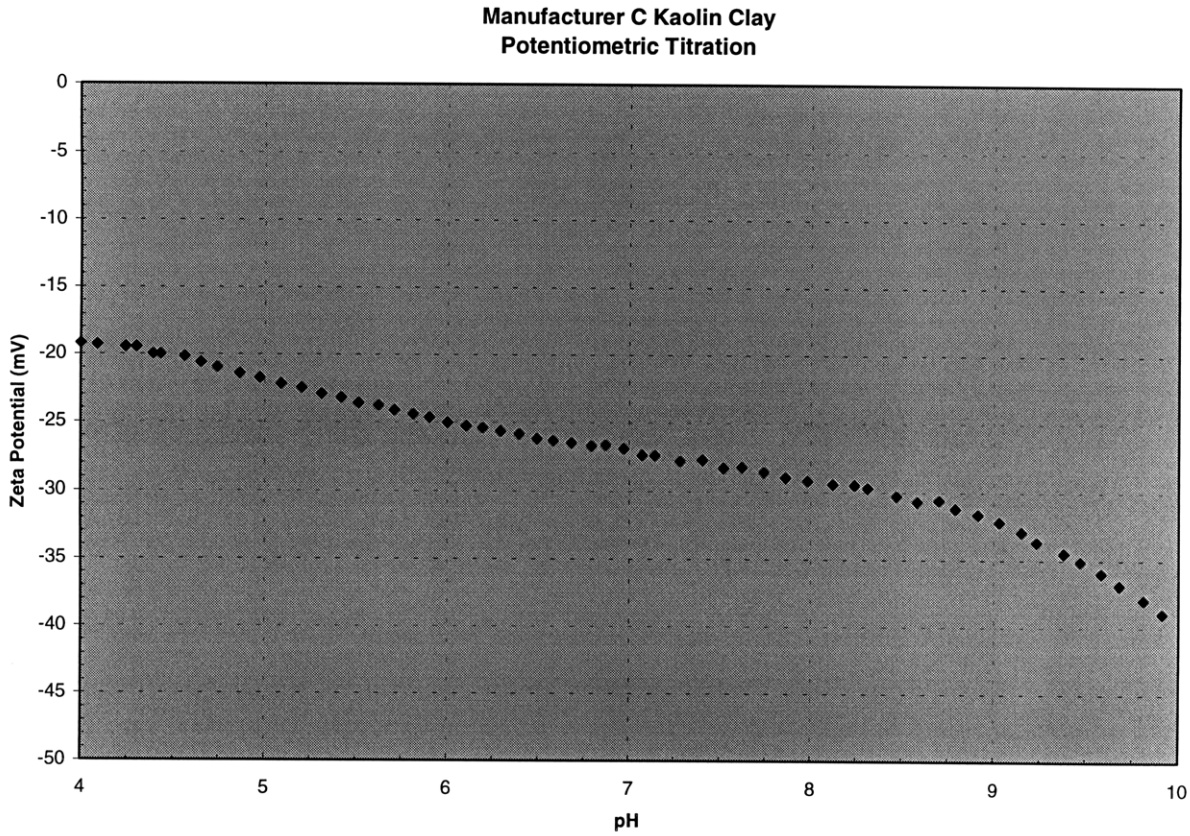

Figure 4.10 Potentiometric Titration of Manufacturer C Kaolin Clay

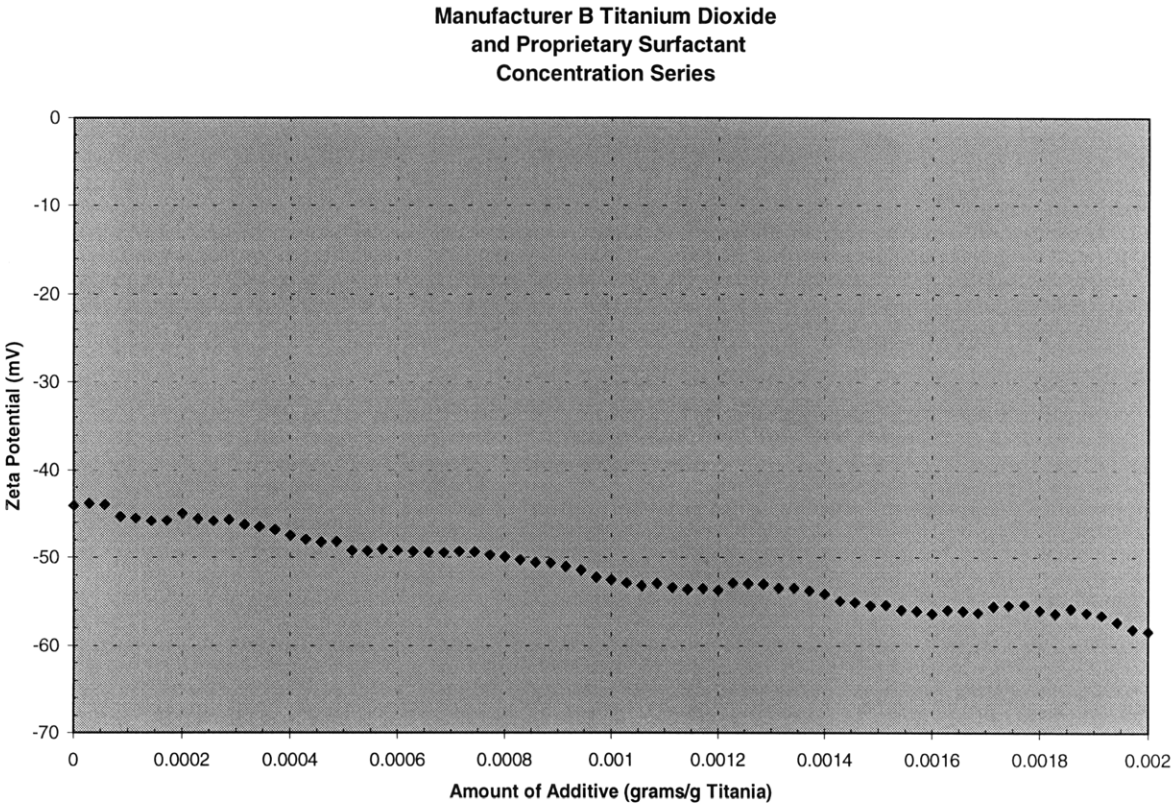

Figure 4.11 Concentration Series with Manufacturer B Titanium Dioxide and Proprietary Surfactant

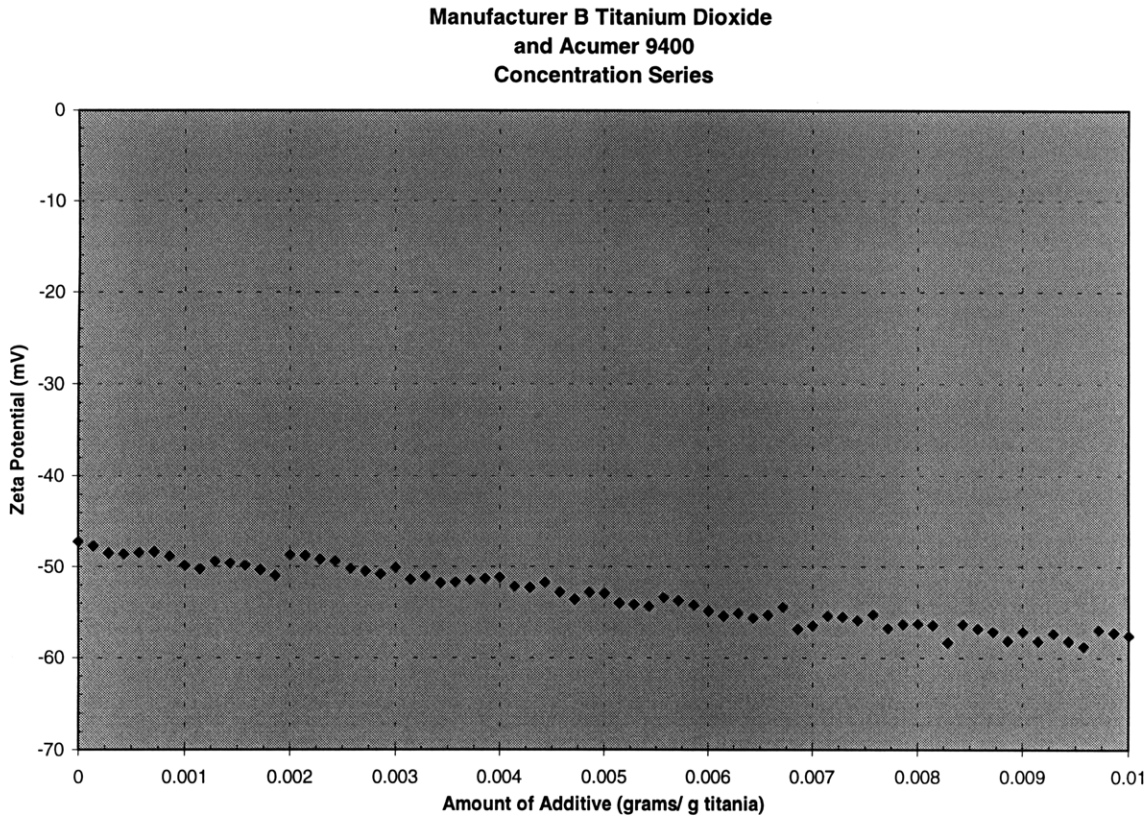

Figure 4.12 Concentration Series with Manufacturer B Titanium Dioxide and Acumer 9400

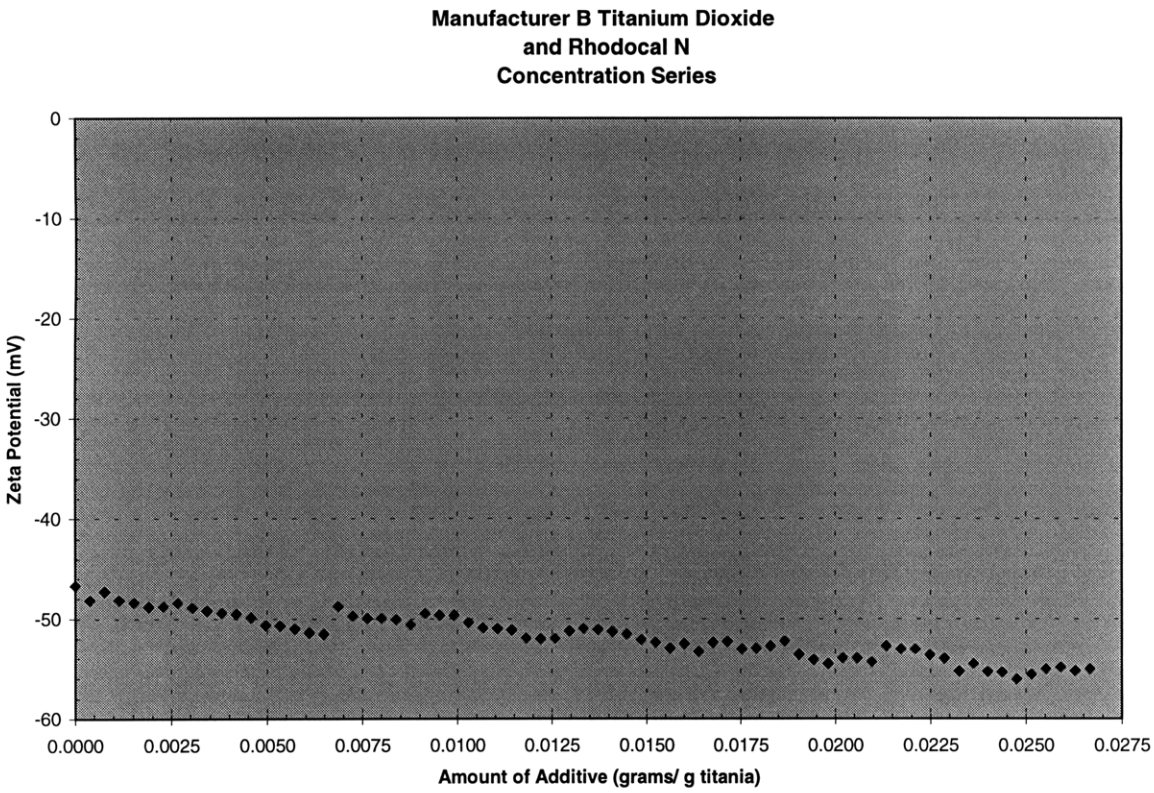

Figure 4.13 Concentration Series with Manufacturer B Titanium Dioxide and Rhodocal N

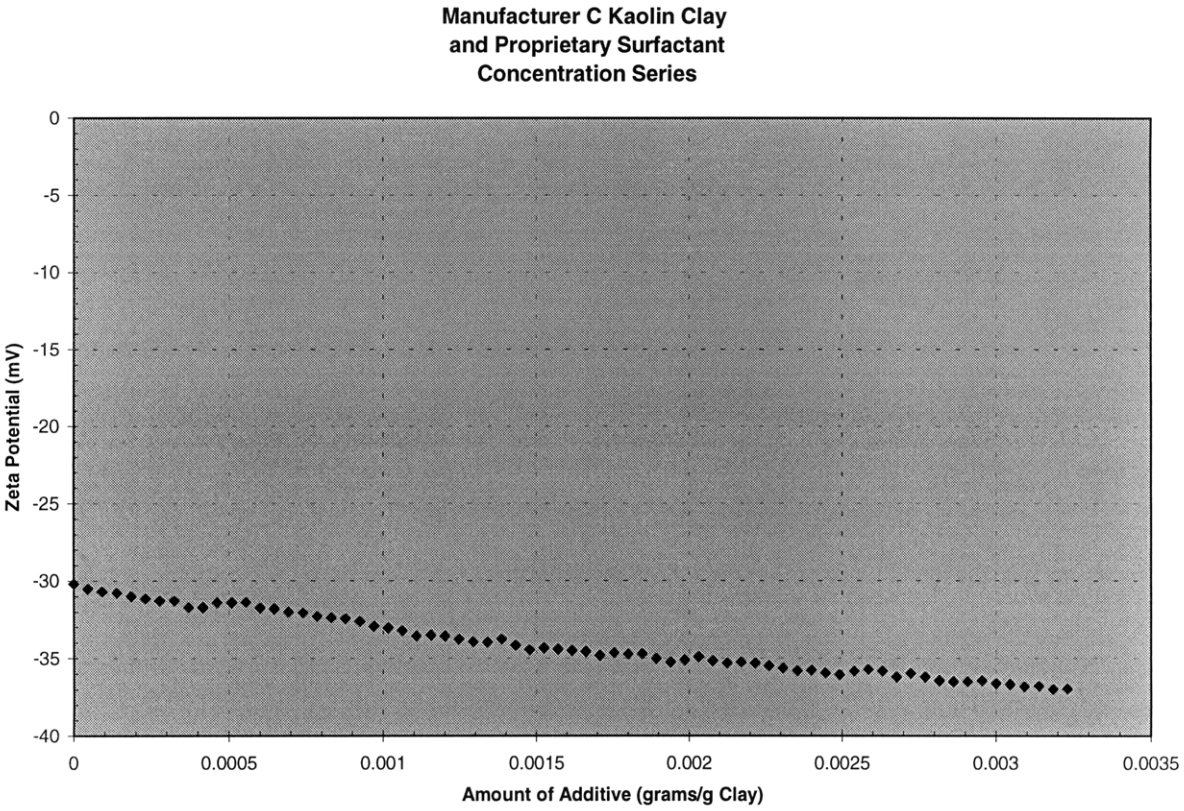

Figure 4.14 Concentration Series with Manufacturer C Clay and Proprietary Surfactant

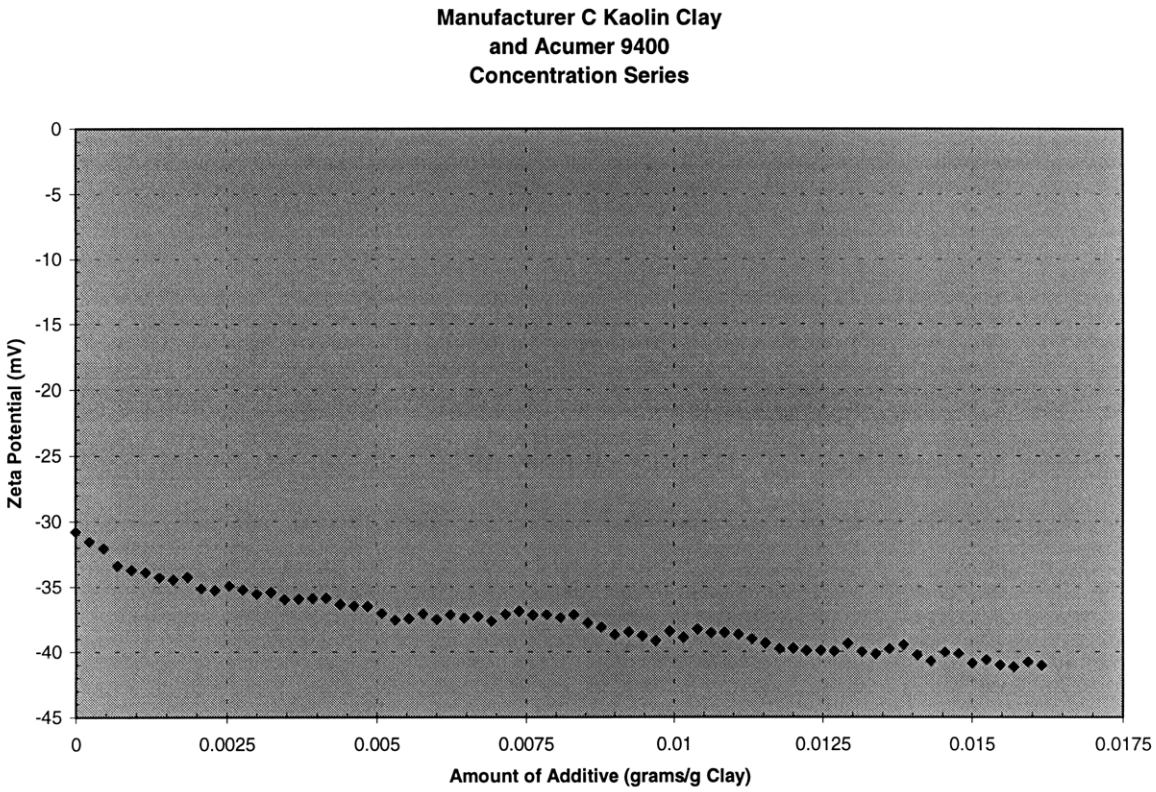

Figure 4.15 Concentration Series with Manufacturer C Clay and Acumer 9400

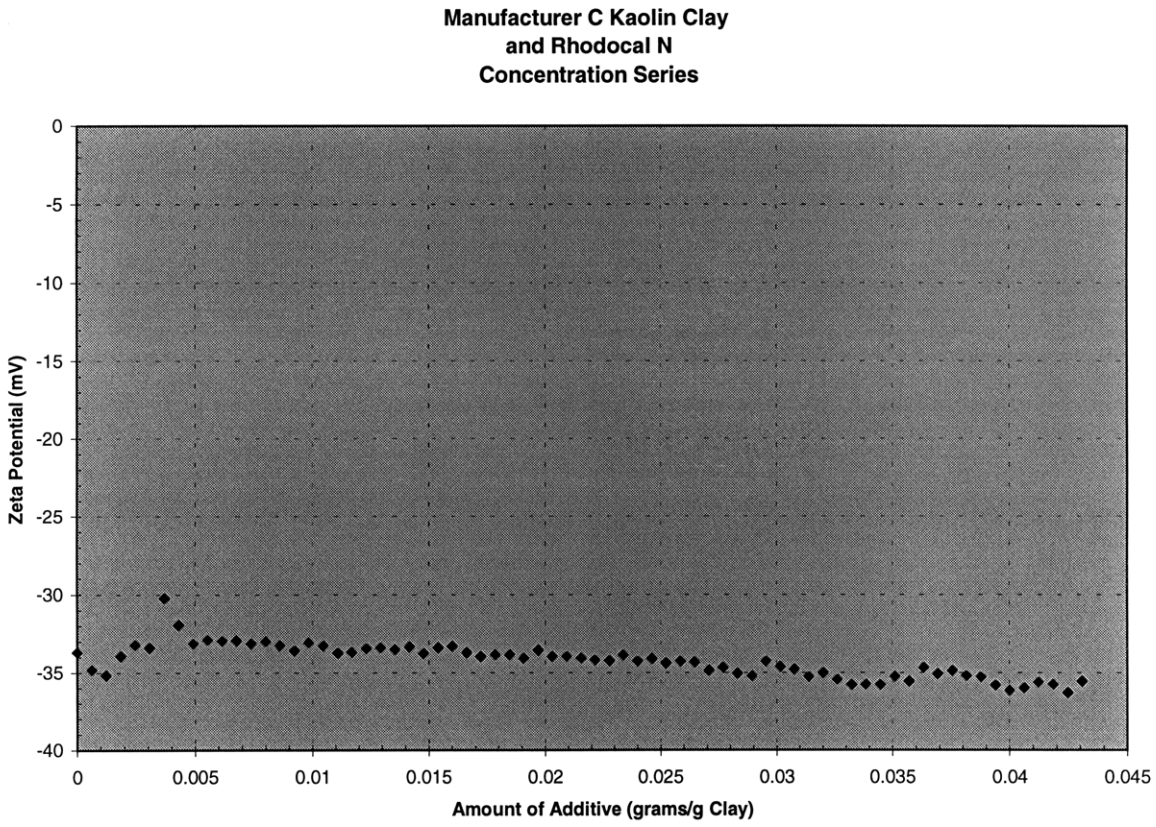

Figure 4.16 Concentration Series with Manufacturer C Clay and Rhodocal N

CHAPTER 5
ROTARY DRUM MIXER DRYING

Dr. William Rowe developed a computer-modeling tool in his Doctoral Thesis to characterize and predict the drying behavior of a rock and slurry system in a rotary drum mixer.[20] Dr. Rowe represented the drum mixer by a series of continuous flow stirred tank reactors (CSTR). The CSTR model presumes that the contents of the mixer are perfectly mixed and that the composition of the output material is identical to that of the material inside the mixer.[41] The aforementioned experiments on particle size segregation make it clear that these assumptions do not necessarily match the actual mixer behavior.

The rotary mixer under examination has two types of flights, as described in chapter 2. Dr. Rowe found that the velocity of particles traveling through the mixer was significantly slower in the spiral flight region. The particles thus spend the majority of their residence time in the spiral flights. Dr. Rowe's model disregarded the effects of the coating region and lifting flights, and only took into consideration the drying behavior in the region of the spiral flights.

Using the following input parameters:

Slurry application rate
Water application rate and Temperature
Rock flow rate and Preheat temperature
Air temperature and Velocity
Heat transfer coefficient
Mass transfer coefficient

The mixer model predicts the distribution of air temperature, rock temperature, humidity, and percent moisture throughout the length of the mixer. For a complete description of the mixer model please refer to Dr. Rowe's Thesis.[20] An experiment measuring the air temperature distribution through the length of the laboratory mixer was conducted in order to provide a test of the computer model. The experimental results could then be compared with the temperature distribution predicted by the model.

5.1 TEMPERATURE EXPERIMENTS

5.1.1 EXPERIMENTAL PROCEDURES

A system durable enough to survive the abrasive environment of the mixer had to be developed in order to measure air temperature along the length of the mixer. A suitable arrangement utilized the following: a metal wire strung through the mixer to which was attached a series of five PVC tubes fitted with a total of 6 thermocouples. The thermocouple wires were run through the PVC tubes to protect them from falling granules. A diagram of the arrangement is shown in Figure 5.1. A list of the thermocouple positions, given in centimeters from the slurry application point is shown in Table 5.1. Details of the mixer design are included in Table 5.2 for comparison. The thermocouples were read incrementally by switching channels on the thermometer (Model HH21 Microprocessor Thermometer with Multiprobe switchbox, Omega Engineering, Stamford, CT).

Initial readings were taken as the preheated rock began to flow through the mixer. Readings were then taken every few minutes as the series of experiments proceeded. The mixer operators changed the water application rate or the slurry application rate, after the system reached a steady state. The process conditions studied are listed in Table 5.3.

Dr. Rowe's computer model was built using Labview software from National Instruments. The modeling software was modified such that the results could be output directly to Microsoft Excel. A second program was developed in Excel to organize and graph the resulting output. This software allowed for rapid trend analysis, such as examining the effect of decreasing mass transfer coefficient on the model's predicted behavior.

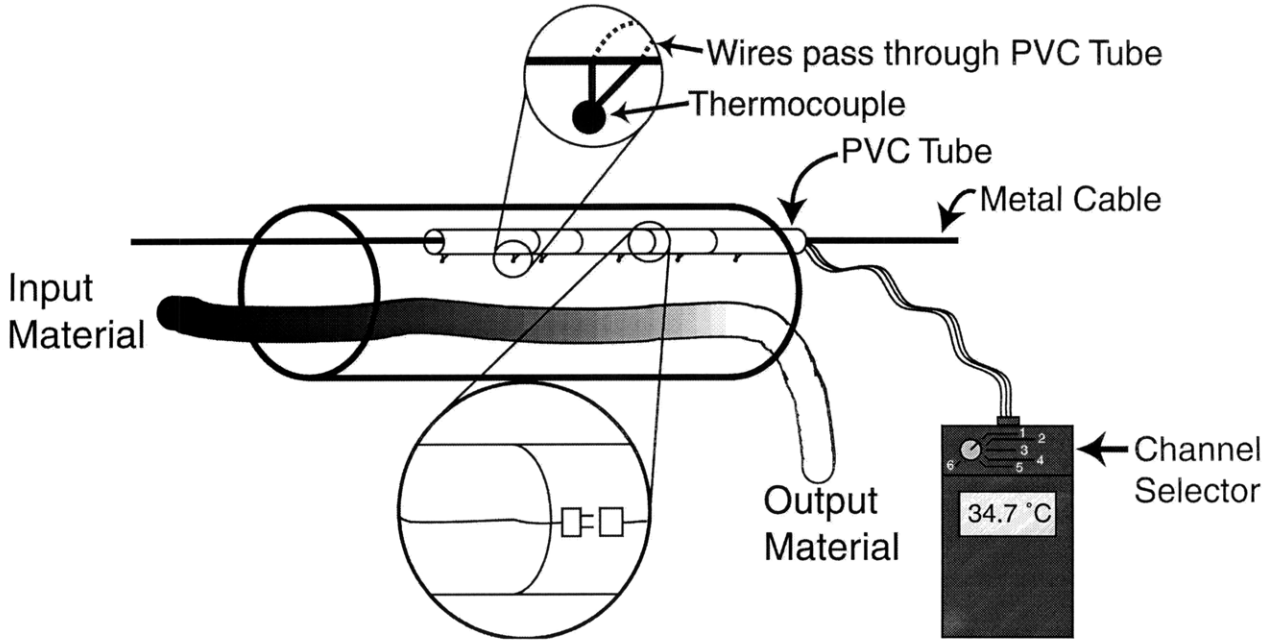

Figure 5.1 Diagram of Temperature Measurement Device

Table 5.1 Thermocouple Positions

Thermocouple	Distance from Slurry Application Point (cm)
1	17.1
2	70.5
3	92.1
4	153.0
5	198.1
6	242.6

Table 5.2 Mixer Specifications

Mixer Feature	Distance from Slurry Application Point (cm)
Water Application	-20.3
End of 1" Wear Bars/Start of Spirals	58.4
End of Spiral Flights/Start of Lifters	165.1
End of Mixer	243.8

Table 5.3 Process Conditions

Initial Conditions

Ambient Air Temperature	23.7°C
Preheat Rock Temperature	93.3°C
Slurry Application Rate	2.12 lb/min (16 g/s)
Water Prewet Rate	2 gallons/hr (2.64×10^{-3} L/s)

Variations of Conditions

Preheat Rock Temperature	112.8°C
Slurry Application Rate	1.75-2.5 lb/min (13.3-18.9 g/s)
Water Prewet Rate	0-3 gallons/hr (0-3.2×10^{-3} L/s)

5.1.2 OBSERVATIONS

Once the temperature probe was in position it was apparent that thermocouples #2 and #3 were not functioning properly. The readings from these thermocouples rapidly fluctuated (±3 degrees). It was not possible to fix the probe at that time, due to the constraints of the system. Readings from these thermocouples were averaged over a period of 5 seconds and the average values were included for the following discussion. The validity of those numbers are, however, suspect.

Figure 5.2 provides a compilation of results from three different sets of process parameters. Included are graphs of the following process conditions: (1) initial preheated rock, (2) preheated rock with 2.12 lb/min slurry and 3.0 gallons/min water application, and (3) preheated rock with

1.75 lb/min slurry and no water application. The temperatures were found to decrease with increasing water or slurry application rate, as expected. The experimental results also show that the air temperatures decreased through the length of the mixer.

The mixer was returned to 2.12 lb/min slurry and 3.0 gallons/min water application and the temperature distribution was measured, after examining the other process conditions. Figure 5.3 provides a comparison of the initial and final measurements for these process conditions. The results were found to compare well except for thermocouple #2, which as mentioned previously, was not functioning properly.

The initial 2.12 lb/min slurry and 3.0 gallons/hour water experimental results were used to compare the actual mixer air temperature behavior with that predicted by the model. A curve was fit to the experimental results and is shown in Figure 5.4. The experimental results best fit is plotted with the temperature distribution curve predicted by the mixer model for the same process conditions in Figure 5.5. The additional parameters used for the model's calculations are shown in Table 5.4. These parameters were for the most part determined by Dr. Rowe during his development of the mixer model. While the predicted values are in close agreement with the experimental results, it was not possible to determine a set of input parameters in which the curvature of the temperature distribution predicted by the model matched that of the experimental results.

Table 5.4 Additional Mixer Model Parameters

Slurry Application Rate	0.01604 kg/s
Water Application Rate	0.00316 kg/s
Water Temperature	23.06°C
Rock Flow Rate	0.25253 kg/s
Preheat Temperature	110°C
Air Temperature	24.17°C
Air Velocity	0.13 kg/s
Heat Transfer Coefficient	850 $Js^{-1}m^{-2}K^{-1}$
Mass Transfer Coefficient	0.0049 ms^{-1}

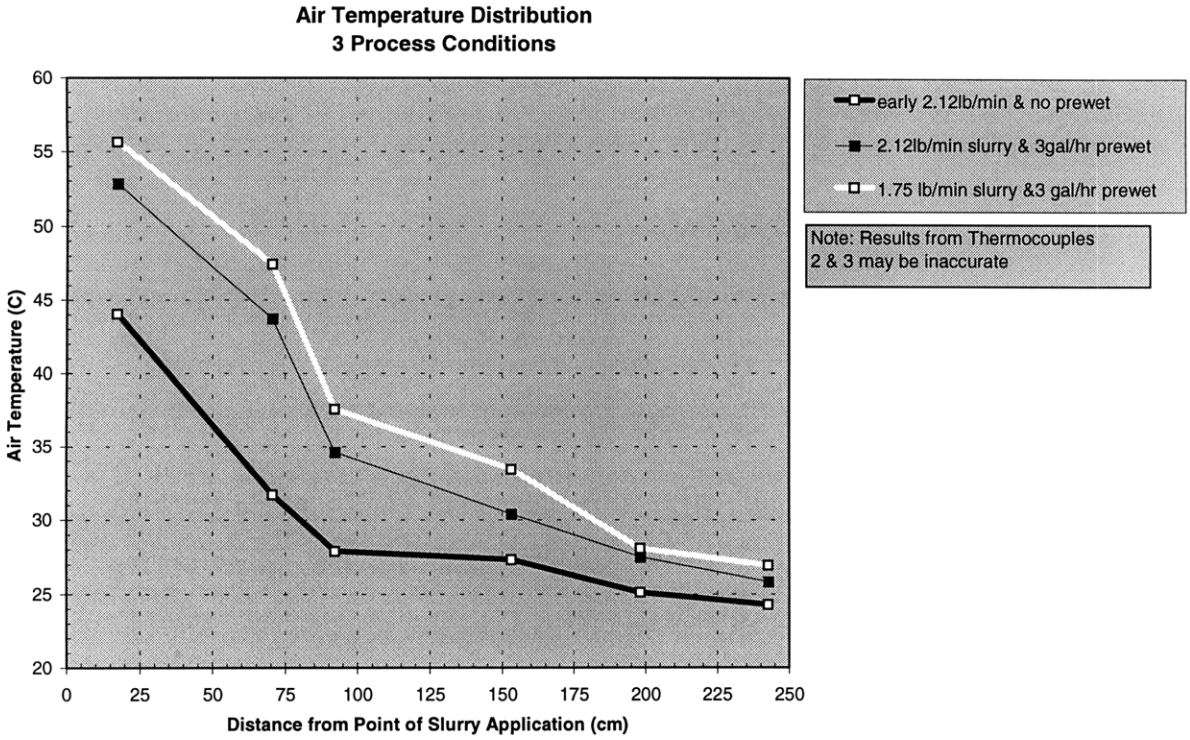

Figure 5.2 Air Temperature Distributions for 3 Process Conditions

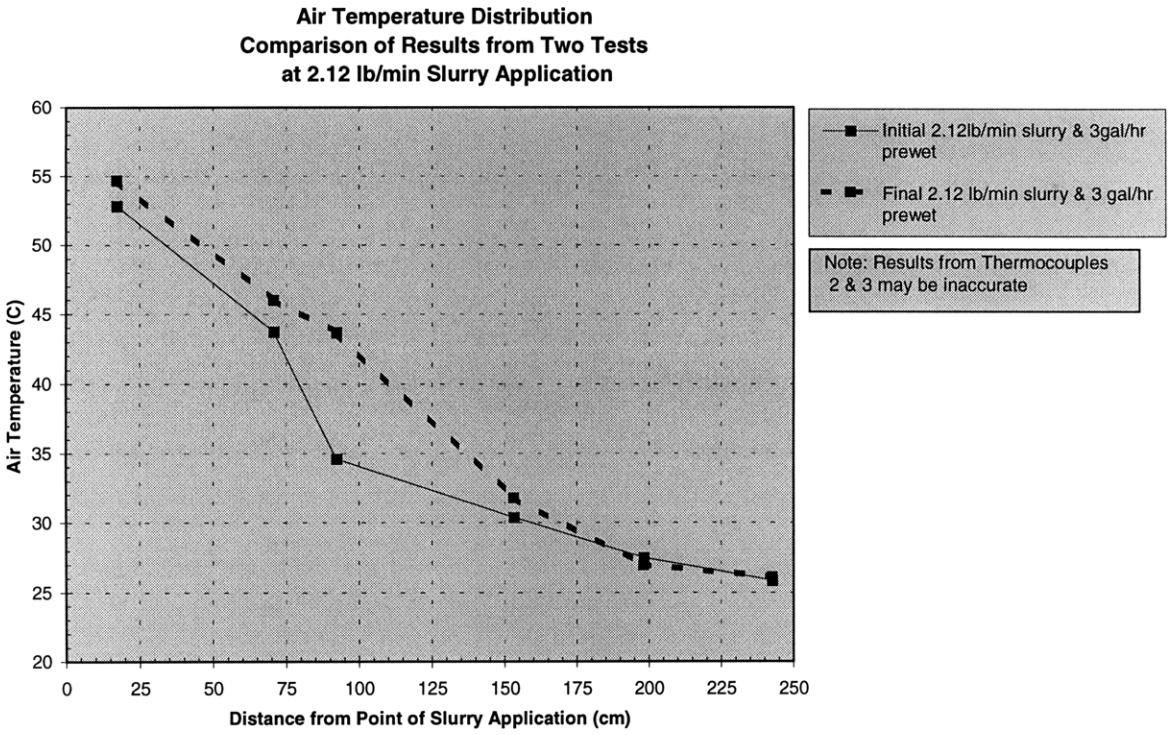

Figure 5.3 Air Temperature Distribution for Initial and Final Experiments at 2.12 lb/min Slurry Application

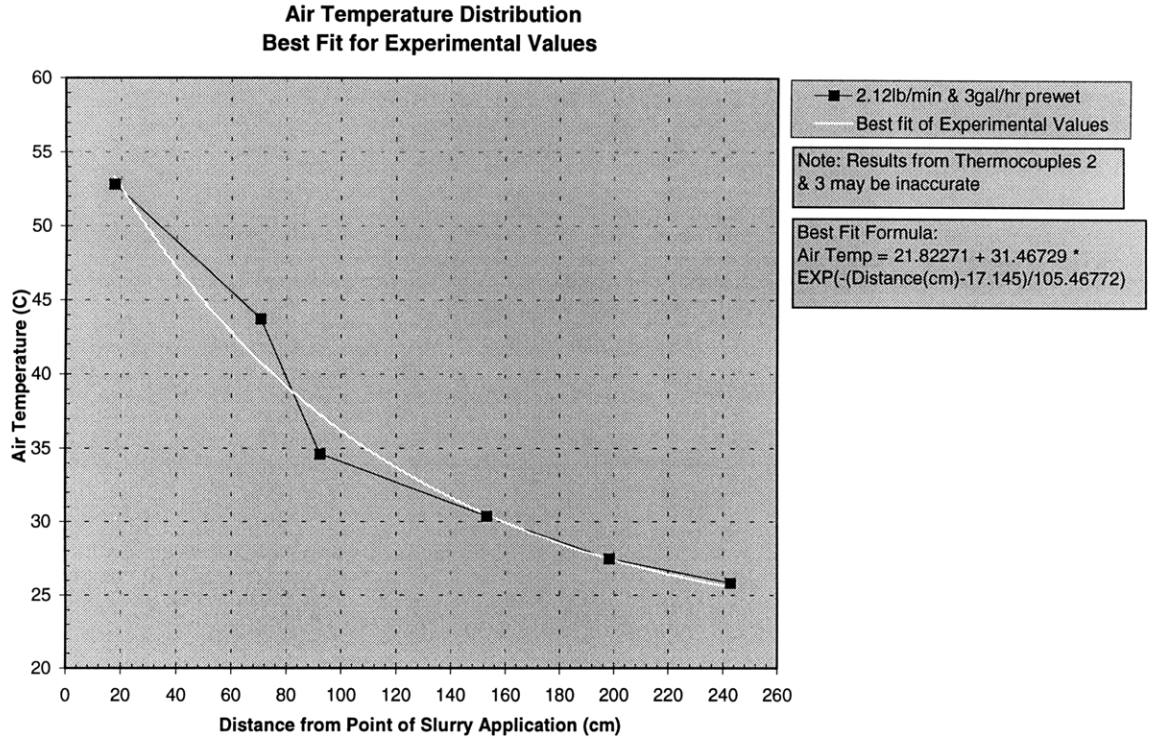

Figure 5.4 Calculated Best Fit for Air Temperature Distribution at 2.12 lb/min Slurry Application

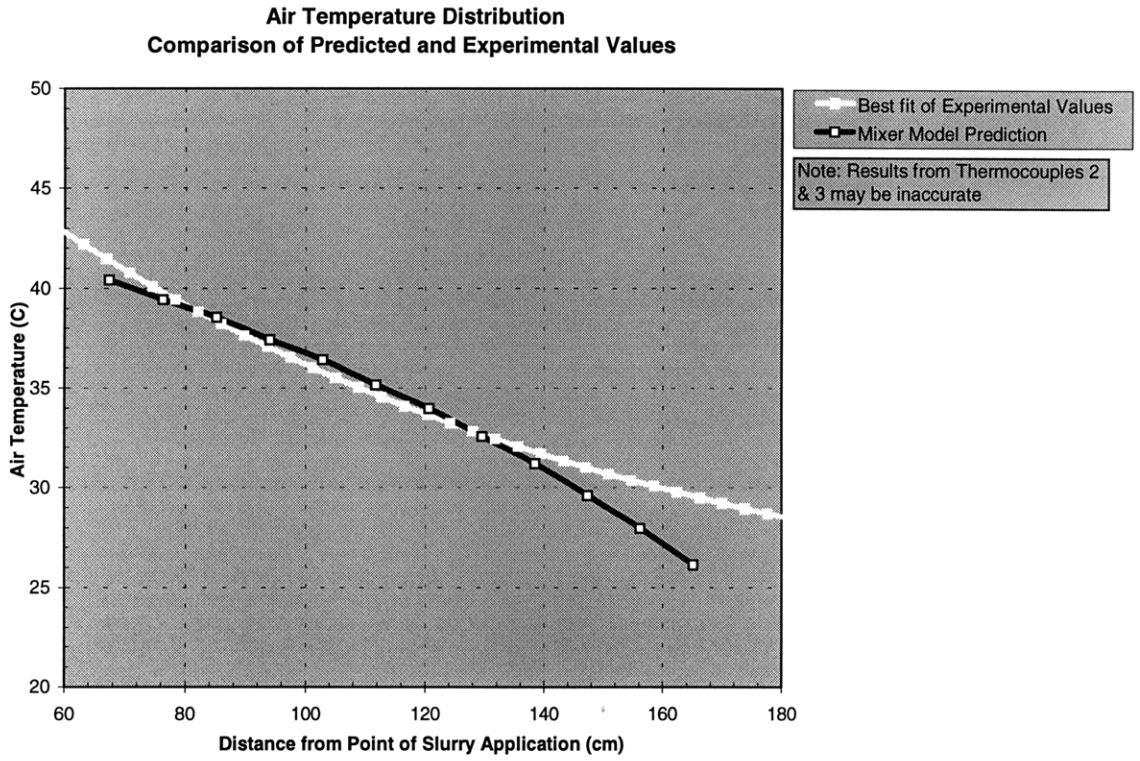

Figure 5.5 Experimental and Predicted Air Temperature Distribution for 2.12 lb/min Slurry in the Spiral Flight Region

5.1.3 DISCUSSION

The slope of the temperature distribution predicted by the mixer model becomes increasingly negative further away from the slurry application point, as shown in Figure 5.5. A peak actually occurs in the middle of the screw flights when using other model parameters. The curvature of the distribution was attributed to the rapid evaporation of the majority of the moisture content near the rock-input end of the mixer. The mixer model does not predict the air temperature before the screw flight region. The experimental results show that the temperature profile rapidly decreases early in the mixer, and then more slowly through the screw flights. This disagreement may be attributed to assumptions built into the model.

The model ignores evaporation of water prior to the screw flights. As will be demonstrated in Chapter 6, a significant amount of moisture evaporation occurs in what is termed the coating region of the mixer, prior to the screw flights. Heating of the air from the rock bed will also occur through the coating region of the mixer and was not included into the model's calculation of the temperature profile. This heating may reduce the significance of cooling due to evaporation.

The model assumes uniform mixing and flow behavior through the spiral flight region. Mixing due to the flight arrangements and particle motion will not produce a uniform mixture, as noted in Chapter 2. The larger granules travel through the mixer at a faster rate than the smaller granules. This may have some effect, albeit a small one, on the transfer of heat from the granules to the air. The smaller granules inherently trap less heat, and as they have larger surface to volume ratios, they will lose heat more rapidly than larger ones. Without taking into consideration the affects of particle size on heat transfer, relevant information may have been left out of the mixer model.

.

5.1.4 CONCLUSIONS

The computer model is a useful tool for visualizing trends caused by changing process parameters, such as increasing airflow rate. It is currently not able, however, to accurately reproduce the true mixer behavior, at least with respect to the air temperature profile. It is most probable that the other output parameters predicted by the model, including rock temperature, humidity, and percent moisture are similarly affected. By means of the comparison conducted above, it appears that the effects of the coating region of the mixer cannot be ignored when developing such a modeling tool. Further refinements of the model will be required to accurately predict the behavior of the drum mixer.

CHAPTER 6
SLURRY TRANSFER IN ROTARY DRUM MIXERS

The transfer of coating slurry from granule to granule was examined by Dr. Rowe through a wetting angle study and experiments in a small batch mixer arrangement. Dr. Rowe found that the majority of the coating transfer occurred within the first 30 seconds of slurry application. Slurry transfer preferentially occurred between granules coated with wet slurry and wet granules (those coated with a layer of water). The transfer of slurry between particles was examined, in the following study, for material in the laboratory rotary mixer. It was expected that the results of this study would correlate well with Dr. Rowe's previous work. The goal of the experiment was to develop a more complete understanding of the rates of slurry transfer and drying.

6.1 SLURRY TRANSFER EXPERIMENTS

6.1.1 EXPERIMENTAL PROCEDURES

Tracer granules were added at various locations along the axis of the rotary mixer, in order to examine the transfer of coating slurry between granules. It was expected that the coating coverage would decrease as the tracer material was dropped farther from the slurry application point. A device was designed to allow granules to be dropped into the rotary mixer at various locations. The device consisted of a metal can with hinged doors, which could be opened remotely by pulling on a string. The can was mounted on a wire strung through the mixer and could be pulled to specific locations in the mixer. The device is illustrated in Figure 6.1. For the experiments, the mixer was brought to a steady state using the standard process parameters.[31] Experiments were conducted in the following manner: First, approximately 1 kg of black granules was added to the can. The can was then pulled to a specific location in the mixer (±8 cm). The material was dropped into the mixer by pulling on a string attached to the hinged door brace. Finally, samples were taken of the output material. The series of experiments were conducted by dropping tracer material at 6-inch intervals. The locations at which tracer material was dropped are included in Table 6.1. In future experiments less material might be added in order to reduce any non-standard mixing behavior induced by the extra material. The tracer material was neither preheated nor pre-wet with water, which may have altered the coating behavior.

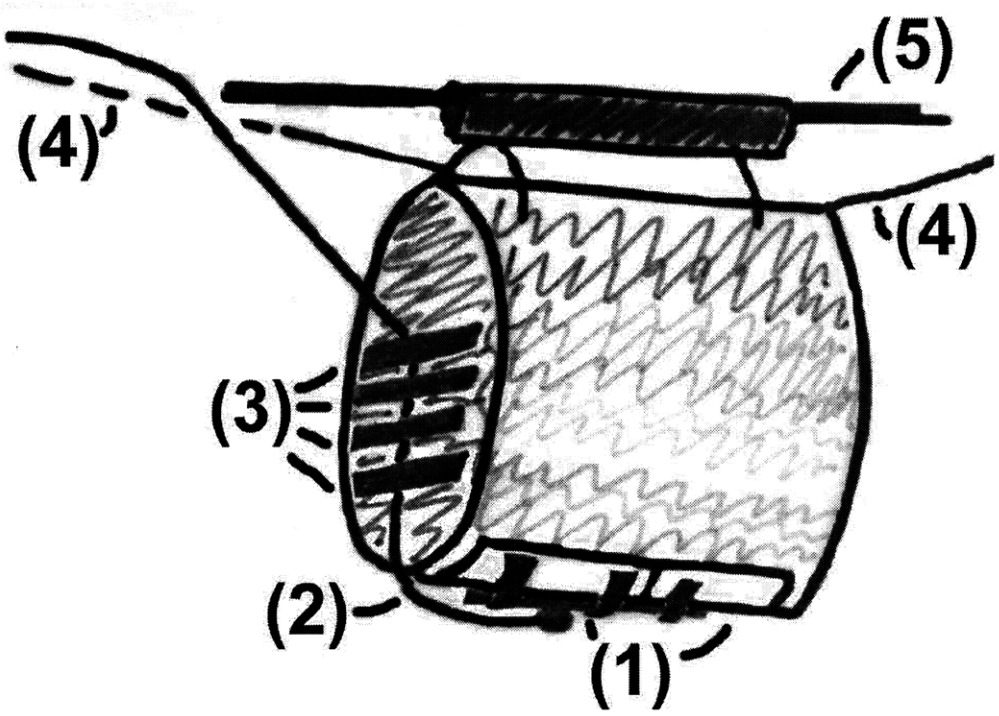

Figure 6.1 Tracer Granule Drop Mechanism

(1) Hinged Doors, (2) Wire for Opening Door, (3) Tape, (4) Wires for Adjusting Position in Mixer, (5) Cable Strung through Mixer

Table 6.1 Locations of Tracer Addition

Distance from Slurry Application Point (cm)
23
38
46
53
69
84

Table 6.2 Mixer Specifications

Mixer Feature	Distance from Slurry Application Point (cm)
Water Application	-20.3
End of 1" Wear Bars/Start of Spirals	58.4
End of Spiral Flights/Start of Lifters	165.1
End of Mixer	243.8

The tracer material was then obtained from the sampled material by visual sorting. The tracer granules were examined under an optical microscope and a few from each drop location were chosen for analysis. The granules chosen were large (~2mm) and had at least one flat surface. These characteristics were chosen in order to maximize the surface area in focus under a microscope. A photograph was then taken of each particle at 37.5 times magnification, and the photographs were scanned into a computer.

Histograms of the scanned images were generated using UTHSCSA ImageTool image analysis software. The histogram of each particle was broken down into four quartiles based on luminosity. This process was described by Dr. Rowe in his doctoral thesis [20]. The formula used to determine the boundary of each quartile was as follows:

$$b_n = low + n\left(\frac{high - low}{4}\right)$$

n was a number between 0 and 4, *low* was the lowest measured pixel luminosity, and *high* was the highest measured pixel luminosity. The quartiles were labeled *Darkest*, *Lower Middle*, *Upper Middle*, and *Lightest*, corresponding to increasing luminosity values. The number of pixels in each quartile could then be used as a measure of coating coverage and uniformity. Using the total number of pixels for an image, the percentage of total pixels contained in each quartile was calculated. A higher percentage of pixels in the "Lightest" quartile would correspond to a well-coated granule with a thick layer of slurry. A higher percentage of pixels in the "Darkest" quartile would indicate a poorly coated granule.

6.1.2 OBSERVATIONS

Included in Figure 6.2 is a series of photographs taken of tracer granules dropped into the mixer at four different locations. The distance from the slurry application point is increasing from left to right. It is readily apparent that the coating coverage is decreasing as the distance from the slurry application point increases. Black tracer granules added to the standard granule input flow could not be recognized in the output flow. While some color difference might exist between a black granule and a standard granule coated in this manner, it was not distinct enough to be apparent to the unaided eye.

Figure 6.3 provides an example of a histogram taken from one of the granule photographs. For an uncoated granule all of the pixels would have a value near 0, whereas a granule with an ideal coating would have all of the pixel values near 255.

The results of the computer analysis are shown in Figure 6.4. The percentages of pixels in each quartile are plotted for each drop location. The lines connect the results for the same quartiles between each location. The vertical axis is percentage of total pixels and the horizontal axis is distance from the slurry application point. Two additional data series were added to the graph, one for standard granules added in the standard mixer input flow, and another for uncoated black granules.

6.1.3 DISCUSSION

These results confirm Dr. Rowe's findings that the majority of the coatings are produced in the initial 30 seconds after slurry application. The coatings examined here are far from ideal, as noted by Dr. Rowe. Coating coverage is incomplete and in most areas not thick enough to mask the underlying darkness of the base material. From Figure 6.4 it can be concluded that the majority of coating transfer occurs in the initial coating zone. Some amount of coating transfer does occur in the spiral flights, but the effects are minimal. The coating process is a function of two actions. At first coating slurry is transferred from wet slurry coated granule to wet uncoated granule. The reduction of coating transfer with increasing distance from the slurry application point is a function of coating drying, slurry viscosity, the pitted nature of the granules, and pre-wet moisture. As the coating dries it will become more viscous. A higher viscosity slurry will be more cohesive and therefore less likely to transfer between granules. Coating transfer is most likely to occur on the hills rather than the valleys of the granule surfaces. A low viscosity slurry

is a necessity, in order to coat the surface valleys. Finally, as the initial pre-wet evaporates, wetting of new surface area becomes less likely, thus reducing the probability of coating transfer. It is clear that very rapid and effective mixing is of crucial importance in the coating zone. Increasing the number of collisions between granules in this region will result in increased coating transfer between granules before drying eliminates slurry transfer. A reduction of the granule preheat temperature would reduce the evaporation rate, thereby extending the coating zone. Extending the coating zone would result in improved coating uniformity and improved slurry utilization.

The second action involved in the coating process is the spreading of wet slurry on the granule surface through collisions with dry granules. Slurry transfer theoretically does not occur during these collisions due to preferential wetting of wet granules over dry ones.[20] A further study is necessary to determine the true effect of coating spreading by dry granules. In such an experiment, granules coated in a batch process would be compared with granules from a batch mixer run in which dry granules were added to the mixture after some period of initial drying. The latter granules should have improved coating uniformity, if coating spreading does occur due to the presence of dry granules in the mixture. The poor coating uniformity seen on these granules indicates that the amount of back mixing of dry granules into the wet slurry bed is insufficient for adequate slurry spreading, provided coating spreading does occur in this manner. The rapidity of the drying process may also limit effective slurry spreading. The amount of dried granules mixing with the wet slurry coated granules would increase by extending the spiral flights further into the coating region. The coating spreading should increase as a result, and thereby improve coating uniformity.

6.1.4 CONCLUSIONS

Slurry transfer and spreading in the coating zone currently does not achieve the desired coating uniformity and thickness. Adjustments to the input parameters: increased water application rate, decreased rock preheat temperature, and decreased slurry viscosity will improve coating coverage and uniformity. Mixer design modifications should be investigated in order to increase the mixing of granules and slurry transfer in the coating zone. A series of experiments examining slurry spreading due to back mixed dry granules should be conducted, in order to determine if increased back mixing would also improve coating spreading in the coating zone.

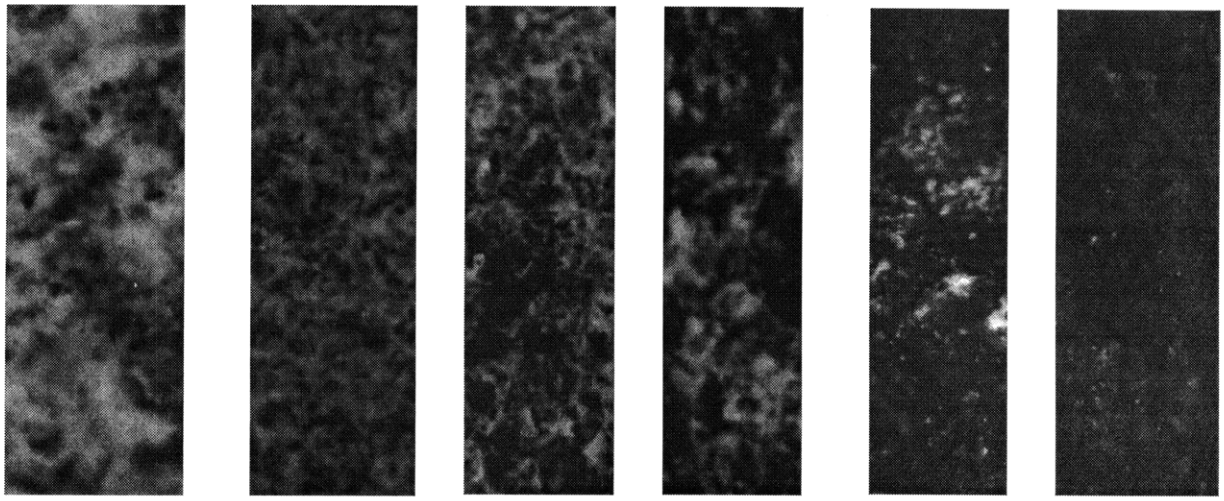

Standard Laboratory Mixer Granule | 38.1 cm | 53.3 cm | 68.6 cm | 83.8 cm | No Slurry

Figure 6.2 Photographs Taken of Tracer Granule Surfaces (37.5x magnification)

Numbers Indicate Distance of Drop Location from Point of Slurry Application

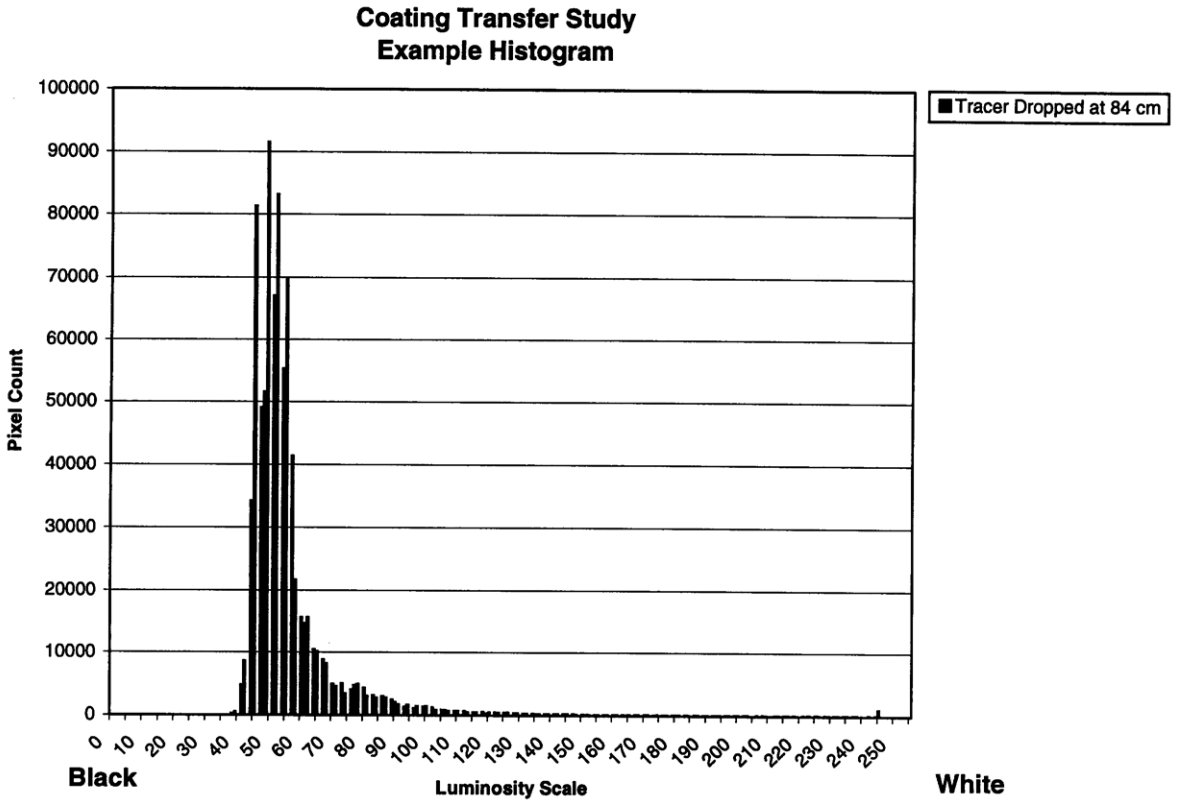

Figure 6.3 Example Histogram

(Material Dropped 83.82 cm From Slurry Application Point)

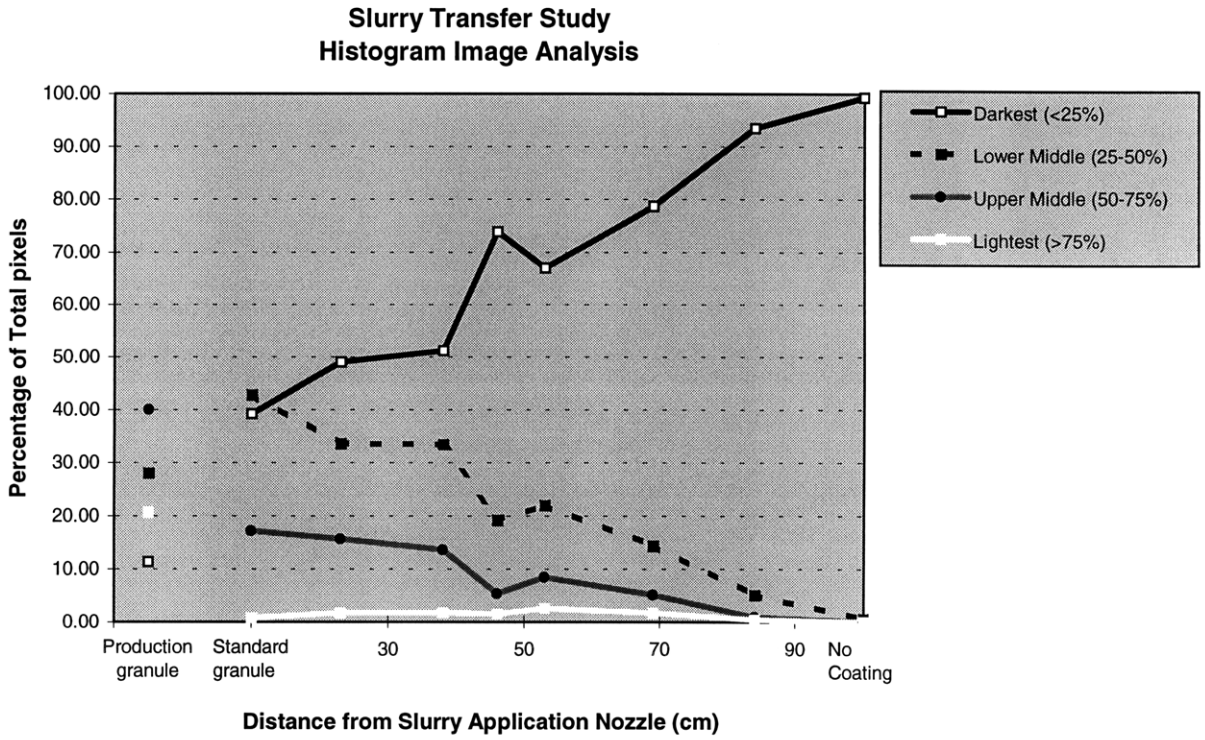

Figure 6.4 Slurry Transfer Histogram Analysis Results

CHAPTER 7
CONCLUSIONS AND FUTURE WORK

7.1 CONCLUSIONS

The purpose of this thesis was to augment the research conducted by Dr. William Rowe, providing further understanding of the process parameters involved in bulk coatings utilizing sodium silicate slurries, and a basic understanding of the behavior of granular materials in rotary drum mixers. The specific conclusions drawn from this work are as follows:

(1) X-ray Fluorescence Spectroscopy and copper tracer granules were used to show that the residence time distribution of granules in a rotary drum mixer is inversely related to granule particle size. The mean residence time decreases with increasing particle size. The time spent in the coating zone will thus be greater for granules of smaller particle size.

(2) X-ray Fluorescence Spectroscopy and copper tracer granules were used to show that two regimes exist when the viscosity of the applied slurry increases. In the first regime mean residence time (MRT) increases with increasing viscosity. At some viscosity the MRT peaks, and then in the second regime, decreases with further increases in slurry viscosity.

(3) Visual analysis of copper tracer granules in rotary kiln output flow was used to make a few predictions about the effect of moisture on flow behavior. We predict the existence of three separate behavioral regimes. In the first regime a layer of water is adsorbed on to the surface of the granules, but has little effect on the bulk flow properties. In the second regime additional moisture has a large effect on the flow properties as capillary action rapidly increases the cohesiveness of the water-granule mass. In the third regime water permeates the granule bed, and additional water will have little effect on the bulk flow properties.

(4) Inductively Coupled Plasma Atomic Emission Spectroscopy and copper tracer granules were used to examine the bulk flow behavior of two industrial scale mixers. The RTD is significantly more narrow and the MRT is 54 % less in the industrial mixers than in the laboratory mixer.

(5) Optical and SEM examination of coated granules showed that the slurry coating was non-uniform and the pigments were not well dispersed in the coated areas. Further ESA experiments proved that the surfactants currently used in the slurry formulation have little to no effect on the surface properties of titanium dioxide or kaolin clay. Addition of an effective dispersant and improvement in slurry mixing process through the use of a high shear mixer would improve pigment utilization.

(6) The mixer behavior predicted by Dr. Rowe's computer model, was found to not quite agree with that of the actual laboratory mixer. A variety of elements which were not included in the model, and assumptions made during its creation were discussed as causes for this discrepancy.

(7) A Coating transfer study corroborated Dr. Rowe's conclusion that the majority of slurry coating occurs very quickly after slurry application. Extending the length of the slurry transfer region by reducing rock input temperature, decreasing slurry viscosity, and increasing mixing effectiveness would improve coating uniformity.

7.2 SUGGESTIONS FOR FUTURE WORK

From the coating transfer study it was apparent that coating uniformity has not been optimized. Dr. Rowe predicted that back-mixing of dry granules causes increased coating spreading on wet granules. In order to corroborate Dr. Rowe's prediction, a series of studies investigating the effect of the addition of dry granules to batch mixer coating runs should be conducted. An improvement in coating uniformity could be measured using the histogram analysis described in Chapter 6.

The ESA analysis of the effect of various dispersants on titanium dioxide and kaolin clay proved that the current surfactants have little effect on dispersion. A search should be conducted for appropriate dispersants and similar studies should be conducted. Candidates which provide improved dispersion should then be tested in a batch mixer to determine what effect if any the dispersant has on color after kiln burnout.

While it was expected that a fluorescent tracer technique would provide a means for online RTD measurement, it was found not to provide the required contrast from the base material flow. As Dr. Rowe stated, an online RTD measurement technique would provide a useful tool for measuring process conditions. Further study is necessary to develop an online RTD measurement technique, which provides the low-level detection required and does not significantly effect the color of the output material.

BIBLIOGRAPHY

[1] O. Pouliquen and N. Renaut. "Onset of Granular Flows on an Inclined Rough Surface: Dilatancy Effects" *Journal de Physique II* **6** (1996) p923

[2] É. Clément, J. Duran, and J. Rajchenbach. "Experimental Study of Heaping in a Two-Dimensional 'Sandpile.'" *Physical Review Letters* **69(8)** (1992) p1189

[3] http://www.chem-eng.nwu.edu/mixing/granular/granular.html 3/31/1998

[4] S. Edwards and A. Mehta. "Dislocations in Amorphous Materials." *Journal de Physique* **50** (1989) p.2489

[5] H. Jaeger, C-h. Liu, and S. Nagel. "Relation at the Angle of Repose." *Physical Review Letters* **62(1)** (1989) p40

[6] F. Cantelaube, Y.Limon-Duparcmeur, D. Bideau, and G.H. Ristow. "Geometrical Analysis of Avalanches in a 2D Drum" *Journal de Physique I* **5** (1995) p 581

[7] M. Jaeger, J. Knight, C. Liu, and S. Nagel. "What is Shaking in the Sandbox?" *MRS Bulletin* ***19*** (1994) p25

[8] M. Jaeger, S. Nagel, and R. Behringer. "The Physics of Granular Materials." *Physics Today* (1996) p32

[9] J. McCarthy, T. Shinbrot, G. Metcalfe, J. Wolf, and J. Ottino. "Mixing of Granular Materials in Slowly Rotated Containers." *AIChE Journal* **42(12)** (1996) p 3351

[10] G.A. Kohring. "Studies of Diffusional Mixing in Rotating Drums via Computer Simulations." *Journal de Physique I* **5** (1995) p 1551

[11] H. Henein, J. Brimacombe, and A. Watkinson. "Experimental Study of Transverse Bed Motion in Rotary Kilns." *Metallurgical Transactions B* **14B** (1983) p191

[12] G. Woodle and J. Munro. "Particle Motion and Mixing in a Rotary Kiln." *Powder Technology* **76** (1993) p241

[13] M. Donald and B. Roseman. "Mechanisms in a Horizontal Drum Mixer." *British Chemical Engineering* **7(10)** (1962) p749

[14] R. Jullien and P. Meakin. "Three-Dimensional Model for Particle-Size Segregation by Shaking." *Physical Review Letters* **69(4)** (1992) p641

[15] J.C. Williams. "The Segregation of Particulate Materials. A Review." *Powder Technology* **15** (1976) p245

[16] N. Nityanand, B. Manley, and H. Henein. "An Analysis of Radial Segregation for Different Sized Spherical Solids in Rotary Cylinders." *Metallurgical Transactions B* **17B** (1986) p247

[17] K. Choo, T.C.A. Molteno, and S. Morris. "Traveling Granular Segregation Patterns in a Long Drum Mixer." *Physical Review Letters* **79(16)** (1997) p2975

[18] O. Zik, D. Levine, S.G. Lipson, S. Shtrikman, and J. Stavans. "Rotationally Induced Segregation of Granular Material." *Physical Review Letters* **73(5)** (1994) p644

[19] M. Nakagawa, S. Altobelli, A. Caprihan, E. Fukushima, and E.-K. Jeong. "Non-invasive measurements of granular flows by magnetic resonance imaging." *Experiments in Fluids* **16** (1993) p54

[20] W. Rowe. "Bulk Coating Processes with Sodium Silicate Slurries" *Doctoral Thesis*, Massachusetts Institute of Technology, 1996

[21] R. McKay ed. "Technological Applications of Dispersions." Marcel Dekker Inc. (New York 1994) p15

[22] J. Gregory. "Fundamentals of Flocculation." *Critical Reviews in Environmental Control* **19(3)** (1989) p187

[23] S. Nagel. "Instabilities in a sandpile." *Reviews of Modern Physics* **64(1)** (1992) p321

[24] G. Baxter and R. Behringer. "Pattern Formation in Flowing Sand." *Physical Review Letters* **62(24)** (1989) p2825

[25] G. Metalf, T. Shinbrot, J. McCarthy, and J. Ottino. "Avalanche Mixing of Granular Solids." *Nature* **374** (1995) p39

[26] E. Ehrichs, H. Jaeger, G. Karczmar, J. Knight, V. Kuperman, and S. Nagel. "Granular Convection Observed by Magnetic Resonance Imaging." *Science* **267** (1995) p1632

[27] S. Edwards and A. Mehta. "Dislocations in Amorphous Materials." *Journal de Physique* **50** (1989) p 2489

[28] A. Avidan and J. Yerushalmi. "Solids Mixing in an Expanded Top Fluid Bed." *AIChE Journal* **31(5)** (1985) p835

[29] C. Broadbent, J. Bridgewater, D. Parker, S. Keningly, and P. Knight. "A Phenomenological Study of a Batch Mixer Using a Positron Camera." *Powder Technology* **76** (1993) p317

[30] For a description of X-Ray Fluorescence Spectroscopy see M. Snider. "X-Ray Techniques for Coatings Analysis." *Analysis of Paints and Related Materials* ASTM STP1119 (1992) p82

[31] Private Conversation, D. Jerdet, Industrial Sponsor, 1997

[32] Private Conversation, Dr. D. Reed, Industrial Sponsor, 1997

[33] J. Taylor. *An Introduction to Error Analysis.* University Science Books (1982)

[34] Metorex X-MET 880 Manual v1.0.1 (July 11, 1991) p13

[35] I.M. Khan and G.I. Tardos. "Stability of Wet Agglomerates in Granular Shear Flows." *Journal of Fluid Mechanics* **347** (1997) p347

[36] K. Umeya. "Rheology of Powder Systems." *Advances in the Mechanics and Flow of Granular Materials* **v2** (1983) p719

[37] Conversation with Dr. Jooho Moon, MIT 2/98

[38] R. O'Brien, D. Cannon, and W. Rowlands. "Electroacoustic Determination of Particle Size and Zeta Potential." *Journal of Colloid and Interface Science* **173** (1995) p406

[39] Conversation with Dr. Jooho Moon, MIT 3/98

[40] K. Hirakata, W. Rhine, and M. Cima. "Surface Chemistry of Lead Titanate and its Impact on Binder Removal." *Journal of American Ceramic Society* **79**[4] (1996) p1002

[41] Charles G. Hill, Jr. *An Introduction to Chemical Engineering Kinetics and Reactor Design.* Wiley and Sons, New York, 1977, pp245-304.